EXPLORATORY STUDY OF RFID APPLICATIONS FOR AIR CARGO OPERATIONS

By

MAGALIE LANIEL

A DISSERTATION PRESENTED TO THE GRADUATE SCHOOL
OF THE UNIVERSITY OF FLORIDA IN PARTIAL FULFILLMENT
OF THE REQUIREMENTS FOR THE DEGREE OF
DOCTOR OF PHILOSOPHY

UNIVERSITY OF FLORIDA

2010

To all who guided me throughout my lifetime, making this milestone possible

ACKNOWLEDGMENTS

This work has been carried out under the guidance of my advisor Dr. Jean-Pierre Émond. His brilliant ideas and suggestions more than helped shape this research. I will never be thankful enough for the opportunity and support that he gave me through all my studies. I feel very privileged and fortunate to have him as my advisor and want to thank him for believing in me.

I would also like to thank each of my committee members, Dr. Ray Bucklin, Dr. Tom Burks, Dr. Daniel Engels and Dr. David Mikolaitis for their advice and contribution to my education thus far and in the future. Besides, I would like to express my thankfulness to Ismail Uysal who helped me extensively structure this dissertation and with whom I hope to have the pleasure to work with in the future.

I would like to send a special thank to Trevor Howard and all of Air Canada Cargo for their generous implication and participation to this research. Without their help, many experiments would have simply been impossible to achieve. Moreover, I want to send a warm recognition to everyone at Franwell for helping in any way they could and providing key equipment at critical times. Thank you for your trust and encouragement. I also want to thank Mr. Chris Noel from Sealed Air Corporation for providing temperature sensors in a timely manner and making my last experiment possible.

I would like to extend my gratitude towards my parents for their unconditional love and support regardless of distance and sacrifices. I would also like to thank my other half Martin for his patience, guidance and never ending revisions. Last but not least I would like to thank all my friends and colleagues for their support. Particularly Cecilia, it was such a pleasure to share this path together.

TABLE OF CONTENTS

page

ACKNOWLEDGMENTS 4

LIST OF TABLES 9

LIST OF FIGURES 11

LIST OF ABBREVIATIONS 15

ABSTRACT 16

CHAPTER

1 GENERAL INTRODUCTION 18

2 RFID IN AIR CARGO: A LITTERATURE REVIEW 24

Introduction 24
RFID Technology and Definitions 24
Radio Waves 25
Polarization of electromagnetic waves 26
Electromagnetic waves properties 27
RFID System Overview 30
Readers 30
Antenna 31
Tags 33
Frequencies 36
Air Cargo 38
Aviation History 38
Air Cargo Supply Chain 39
Air cargo warehouse operations 40
Unit load device (ULD) 41
Market 42
Materials in Commercial Aircrafts 43
Composites 43
Metals 44
Electrical Systems in Commercial Aircrafts 45
Temperature Profile in Commercial Aircraft 46
Aircraft Safety 46
Cargo security and monitoring 46
Fire detection 47
Technologies 48
RFID in Aviation 49
ISM Frequency and Aviation RFID Considerations 49

Aviation Applications 51
Passenger baggage sortation 51
Verification / authentication 52
Tracking and locating 53
Cargo 54
Cold chain 56
Wireless Interference 58
Electronic devices 60
RFID interference 60
RFID airworthiness policy 61
Concluding Remarks 62

3 AIR CARGO WAREHOUSE ENVIRONMENT AND RF INTERFERENCE 68

Introduction 68
Materials and Methods 72
Montreal Warehouse 74
Toronto Warehouse 74
Results and Discussion 74
433MHz 75
915MHz 76
2.45GHz 77
Conclusion 78

4 RADIO FREQUENCY PROPAGATION INSIDE THE CARGO HOLD OF A DC-10 AIRCRAFT 86

Introduction 86
Materials and Methods 89
Test 1: Propagation Study 90
Data analysis 90
Statistical analysis 94
Test 2: Validation of Relation between Signal Strength and Tag Reads 95
Data point comparison 96
Results and Discussion 96
Test 1: Propagation Study 96
Attenuation 96
Signal strength 99
Test 2: Validation of Relation between Signal Strength and Tag Reads 100
Conclusion 102

5 RADIO FREQUENCY INTERACTIONS WITH AIR CARGO CONTAINER MATERIALS FOR REAL-TIME MONITORING 115

Introduction 115
Materials and Methods 118
Test 1 120

Test 2 120
Test 3 121
Results and Discussion 122
Test 1 122
433MHz 122
915MHz 123
2.45GHz 123
Test 2 125
Test 3 125
Conclusion 127

6 TEMPERATURE MAPPING INSIDE AIR CARGO CONTAINERS DURING AIRSIDE OPERATIONS 131

Introduction 131
Materials and Methods 134
Results and Discussion 136
During Flight 136
Before and After Flight 138
Conclusion 139

7 GLOBAL TRACKING SYSTEM FOR AIR CARGO SUPPLY CHAIN 145

Introduction 145
Typical Air Cargo Warehouse Operations 146
Typical Air Cargo Ramp Operations 148
Findings from this Study and Recommendations for RFID Tracking System Implementation 149
Passive and Active RFID Tags 150
ULD Materials 152
Frequency 152
Conclusion 154

8 GENERAL CONCLUSION 160

APPENDIX

A DC-10 CARGO HOLD AND CARGO DOOR SPECS 162

B RADIO FREQUENCY ATTENUATION SURFACE PLOTS 164

C STATISTICAL ANALYSIS RESULTS FOR DC-10 RADIO FREQUENCY PROPAGATION 173

D RADIO FREQUENCY SIGNAL STRENGTH PROPAGATION SURFACE PLOTS 179

E UNIT LOAD DEVICES, TEMPERATURE GRAPHS AND POSITIONS 188

LIST OF REFERENCES 194

BIOGRAPHICAL SKETCH 205

LIST OF TABLES

Table		page
2-1	EPCglobal tag class structure	63
2-2	Permissible field strengths for RFID systems in accordance with FCC Part 15 (FCC, 2008).	63
2-3	Aircraft radio systems	63
3-1	Receiving antenna specifications	80
3-2	Minimum and maximum interference readings (in dBm) for six positions and three frequencies at the Montreal warehouse.	81
3-3	Minimum and maximum interference readings (in dBm) for nine positions and three frequencies at the Toronto warehouse.	81
4-1	Specifications of the three RF systems used.	104
4-2	Calculated parameters for the attenuation equation (Eq. 4-5) and maximum allowed output power adjustment.	104
4-3	Averages and standard deviations of attenuation levels for each test.	104
4-4	Statistical analysis results for the effect of antenna location.	105
4-5	Statistical analysis results for the effect of antenna polarization.	105
4-6	Signal strength data for each test, averaged per vertical slice, and total cargo hold (Avg).	105
4-7	Table summarizing the recorded and adjusted power levels and read rates for circular and linear antennas across the 12 cross sectional planes.	106
5-1	Specifications of the six antennas used.	128
5-2	Signal strength measurements (dBm) for control (no sample), test 1. Receiver antenna positions are measured from the emitting antenna.	128
5-3	Signal strength deviation, test 1. Receiver antenna positions are measured from the emitting antenna and sample materials are positioned at λ.	128
5-4	Signal strength measurements, plus signal strength deviation between material samples and control at three frequencies for test 2.	129
5-5	Signal strength measurement, test 3. Receiver antenna positions are measured from the emitting antenna.	129

5-6 Signal strength deviation, test 3. Receiver antenna positions are measured from the emitting antenna and sample materials are positioned at λ..... 129

6-1 Routes, aircraft and ULD specs from Toronto (YYZ). 140

6-2 Temperature comparison between heated and unheated cargo holds inside an Airbus 330. 140

7-1 Current processes as well as proposed RFID solutions for the air cargo supply chain (cargo acceptance part). 155

7-2 Current processes as well as proposed RFID solutions for the air cargo supply chain (cargo build-up part). 156

7-3 Current processes as well as proposed RFID solutions for the air cargo supply chain (cargo to/from the ramp section). 157

7-4 Current processes as well as proposed RFID solutions for the air cargo supply chain (cargo break-down and storage section). 158

7-5 Current processes as well as proposed RFID solutions for the air cargo supply chain (cargo delivery part). 159

C-1 Effects of frequency, antenna location and antenna polarization on attenuation levels of the complete dataset. 173

C-2 Effect of width on attenuation levels for each frequency, antenna location and polarization. 174

C-3 Effect of height on attenuation levels for each frequency, antenna location and polarization. 175

C-4 Effect of depth on attenuation levels for each frequency, antenna location and polarization. 176

LIST OF FIGURES

Figure		page
1-1	Brief overview of the air cargo supply chain.	22
1-2	Some problems associated to the air cargo warehouse and aircraft operations.	22
1-3	Some questions associated with warehouse and aircraft air cargo operations.	23
2-1	Electromagnetic spectrum	64
2-2	Different parts of a wave (Lahiri, 2006)	65
2-3	Example of an RFID system on conveyor belt.	65
2-4	Wave propagation for linear and circular polarization	65
2-5	Cargo warehouse floor plan and activity areas.	66
2-6	International flight temperature profile with both high-temperature excursions (during stopovers) and low-temperature excursions (in flight)	67
2-7	Example of a GSM/GPS capable RFID system for real time data acquisition (Schmoetzer, 2005).	67
3-1	Montreal cargo warehouse facility floor plan and interference reading points (numbered 1 to 6).	82
3-2	Toronto cargo warehouse facility floor plan and interference reading points (numbered 1 to 9).	83
3-3	Noise floor of spectrum analyzer at three different resolution bandwidths.	83
3-4	Worst case scenario for signal interference readings around 433MHz. Span: 10MHz, RBW: 10kHz, attenuation: 0dB, gain: 0dBi.	84
3-5	Worst case scenario for signal interference readings around 915MHz. Span: 50MHz, RBW: 10kHz, attenuation: 0dB, gain: 2.5dBi.	84
3-6	Worst case scenario for signal interference readings around 2450MHz. Span: 50MHz, RBW: 10kHz, attenuation: 0dB, gain: 8dBi.	85
4-1	Section of an aircraft fuselage (Airbus A380)	106
4-2	DC-10-30F from Arrow Cargo.	107

4-3 Typical fuselage section of a DC-10-30F, lower cargo hold circled in blue (Boeing, 2010c) 107

4-4 Cargo hold dimensions and RF emitting antenna positions. 108

4-5 Data point positions in the 3x3 grid. Twelve 3x3 grids are measured long the length of the cargo hold, every meter. 108

4-6 Tag readability test configuration. Tyvek® sheet with 29 RFID tags (circled) covering half of the cargo hold cross section 109

4-7 Attenuation surface plots for each vertical slice of 3x3 data point at 433MHz, circular antenna and top end antenna position. 109

4-8 Attenuation surface plots for each vertical slice of 3x3 data point at 433MHz, circular antenna and center ceiling antenna position. 110

4-9 Attenuation surface plots for each vertical slice of 3x3 data point at 915MHz, circular antenna and top end antenna position. 110

4-10 Attenuation surface plots for each vertical slice of 3x3 data point at 915MHz, linear antenna and top end antenna position. 110

4-11 Attenuation surface plots for each vertical slice of 3x3 data point at 915MHz, circular antenna and center ceiling antenna position. 111

4-12 Attenuation surface plots for each vertical slice of 3x3 data point at 2.45GHz, circular antenna and top end antenna position. 111

4-13 Attenuation surface plots for each vertical slice of 3x3 data point at 2.45GHz, linear antenna and top end antenna position. 111

4-14 Attenuation surface plots for each vertical slice of 3x3 data point at 2.45GHz, circular antenna and center ceiling antenna position. 112

4-15 Distribution (in percentage) of each frequency tested, for circular antenna only and two antenna locations. 113

4-16 Comparison of the change in average power levels and tag read rates for both antennas through linear regression. 114

5-1 Diagram of the anechoic chamber setup for test 1. Four receiver antennas shown for illustrative purposes. One receiver antenna is used at a time. 130

5-2 Anechoic chamber set-up for test 2. A) The sample material is surrounded by foam absorber and placed one wavelength from the emitting antenna. B) The receiver antenna is taped behind the material sample. 130

6-1 ULD types and their respective tag positions. 140

6-2 Temperatures recorded for top and bottom tags during flight (gate to gate). Data is congregated by total flight time and type of aircraft.. 141

6-3 Graph of averaged top and bottom tag temperatures during flight (gate to gate) for both short flights (1-2h) to and from Montreal (YUL). 142

6-4 Graph of averaged top and bottom tag temperatures during flight (gate to gate) for both medium-short flights (4-6h) to and from Vancouver (YVR)..... 142

6-5 Graph of averaged top and bottom tag temperatures during flight (gate to gate) for all 7-8h flights to and from London (LHR) or Frankfurt (FRA)..... 143

6-6 Graph of averaged top and bottom tag temperatures during flight (gate to gate) for the longest flight (>9h) from London (LHR) to Vancouver (YVR). 143

6-7 Temperature profiles of all tags for ULDs AKH 1817 to and from Montreal..... 144

7-1 Overview of the air cargo operations where the circled steps represent suggested RFID reading points. 159

A-1 Standard cargo compartment and containers for model DC-10 series 10, 10CF, 30, 30CF, 40 and 40CF. 162

A-2 Forward cargo loading door, model DC-10 series 10, 10CF, 30, 30CF, 40 and 40CF..... 162

B-1 Attenuation surface plot example – one slice of data (dBm)..... 164

B-2 Attenuation surface plot for 433MHz, top end antenna position and circular polarization. 165

B-3 Attenuation surface plot for 433MHz, center ceiling antenna position and circular polarization..... 166

B-4 Attenuation surface plot for 915MHz, top end antenna position and circular polarization. 167

B-5 Attenuation surface plot for 915MHz, top end antenna position and linear polarization. 168

B-6 Attenuation surface plot for 915MHz, center ceiling antenna position and circular polarization..... 169

B-7 Attenuation surface plot for 2.45GHz, top end antenna position and circular polarization. 170

B-8 Attenuation surface plot for 2.45GHz, top end antenna position and linear polarization. 171

B-9 Attenuation surface plot for 2.45GHz, center ceiling antenna position and circular polarization..... 172

D-1 Signal strength surface plot example – one slice of data (dBm)..... 179

D-2 Signal strength surface plot for 433MHz, top end antenna position and circular polarization..... 180

D-3 Signal strength surface plot for 433MHz, center ceiling antenna position and circular polarization..... 181

D-4 Signal strength surface plot for 915MHz, top end antenna position and circular polarization..... 182

D-5 Signal strength surface plot for 915MHz, top end antenna position and linear polarization. 183

D-6 Signal strength surface plot for 915MHz, center ceiling antenna position and circular polarization..... 184

D-7 Signal strength surface plot for 2.45GHz, top end antenna position and circular polarization..... 185

D-8 Signal strength surface plot for 2.45GHz, top end antenna position and linear polarization. 186

D-9 Signal strength surface plot for 2.45GHz, center ceiling antenna position and circular polarization..... 187

E-1 Temperature profiles of all tags for ULDs (A) AKH 2084 and (B) AKH 9778 to and from Montreal (YUL) 188

E-2 Temperature profiles of all tags for ULDs AKH 1987 to and from Vancouver (YVR)..... 189

E-3 Temperature profiles of all tags for ULDs (A) AKE 03782, (B) AKE 04090, (C) AKE 04969, and (D) AKE 05335 to and from London (LHR)..... 191

E-4 Temperature profiles of all tags for ULDs (A) AKE 03748, (B) AKE 04632, (C) AKE 05168, and (D) AKE 05255 to and from Frankfurt (FRA). 193

LIST OF ABBREVIATIONS

A320	Airbus 320
A321	Airbus 321
A330	Airbus 330
AKE	air cargo container prefix for LD3 without forklift holes
AKH	air cargo container prefix for LD3-45
B777	Boeing 777
dB	decibel
dBi	decibel isotropic – the forward gain of an antenna compared with the hypothetical isotropic antenna, which uniformly distributes energy in all directions
dBm	decibel milliwatt – power ratio in decibels (dB) of the measured power referenced to one milliwatt (mW).
FAA	Federal Aviation Administration
FCC	Federal Communication Commission
FRA	Frankfurt international airport
IC	integrated circuit
LHR	London Heathrow international airport
RBW	resolution bandwidth
RF	radio frequency
RFID	radio frequency identification
SNR	signal to noise ratio
ULD	unit load device
YUL	Montreal-Trudeau international airport
YVR	Vancouver international airport
YYZ	Toronto Pearson international airport

Abstract of Dissertation Presented to the Graduate School
of the University of Florida in Partial Fulfillment of the
Requirements for the Degree of Doctor of Philosophy

EXPLORATORY STUDY OF RFID APPLICATIONS FOR AIR CARGO OPERATIONS

By

Magalie Laniel

August 2010

Chair: Ray A. Bucklin
Major: Agricultural and Biological Engineering

The air cargo system is a complex network that handles a vast amount of freight aboard passenger and all-cargo aircraft. With today's globalization, there is a growing need for fresh products to be delivered year round all over the world, thus, temperature sensitive items are likely to be shipped by air because of their relatively short shelf life. Moreover, increasing demand for just in time delivery; containers being packed by third parties; inspection time being very limited and transportation security being linked to volume, monitoring of goods within containers as well as within the cargo warehouse may contribute to enhanced security, operation efficiency and provide valuable real-time information. New technologies to better track cargo shipments are accountable for maintaining control and tracking along the supply chain. Radio frequency identification (RFID) is seen as an emerging technology for improving the air cargo supply chain.

For RFID technology to be implemented, more research has to be done regarding the environmental compatibility of air cargo warehouses, the regulations involved and the materials encountered in this supply chain. Moreover, the frequency of choice may be critical for system optimization. Therefore, the main objectives of this dissertation are: indentify the multiple RF interferences encountered inside an air cargo warehouse;

evaluate the RF propagation behavior inside the cargo hold of an aircraft at different frequencies; verify the effect of container wall materials on RF propagation; study the temperature distribution of different cargo holds during flight.

The main findings of this research are that interferences are lowest at 915MHz inside the air cargo warehouses studied. Following the same direction, RF propagation inside the cargo hold was found to be best at 915MHz when taking into account federal spectrum regulations. In addition, the container materials experiment showed a very strong effect of aluminum on RF transmission and minimal interaction for all other composite materials. Moreover, there can be a significant temperature gradient between the top and bottom of air cargo containers during ground operations as well as during flights. The global system proposed from this research states that a combination of active and passive tags at 915MHz could create a well suited structure for tracking of the air cargo supply chain. To summarize, the findings of this dissertation suggest that using 915MHz RFID systems for air cargo operations would lead to the most success and system flexibility considering warehouse interference, cargo hold RF propagation, temperature monitoring needs and types of tag technology available today.

CHAPTER 1
GENERAL INTRODUCTION

Automatic identification (Auto ID) of objects enables the organizations that manage global supply chains to operate more efficiently and save cost. Auto ID includes a host of technologies such as bar codes, smart cards, voice recognition, biometric technologies and radio frequency identification (RFID). Bar codes have been the primary means of identifying products since late 1960s. RFID offers many compelling advantages over bar-codes, including non-line-of-sight operation, unique identifier, higher read rate volumes and sensor capabilities, to name a few.

In addition, RFID technology enables computers to collect the unique ID assigned to items. In combination with the Internet and associated infrastructure, RFID also allows companies to track and trace individual items through the supply chain. RFID aims to provide users a near-perfect supply chain visibility. That is, companies would be able to know exactly where every item in their supply chain is at any moment in time.

The air cargo system consists of a large distribution network linking manufacturers and shippers to freight forwarders to airport sorting and cargo handling facilities where shipments are loaded and unloaded from aircraft (Figure 1-1). Business and consumer demand for fast and efficient shipment of goods has fueled the rapid growth of the air cargo industry over the past 25 years. World air cargo traffic is forecasted to expand at an average annual rate of 5.8% for the next two decades, tripling current traffic levels (Boeing, 2008). The air cargo supply chain has been looking at RFID as a solution to increase its safety, operation efficiency and monitoring capability for many years (Figure 1-2). Today's mostly manual processes (accepting, weighing, dimensioning, sorting, storing, building and breaking down shipments, etc.) are not keeping up with the

growing demand for fast and reliable shipping services. In addition, no time stamp is provided each time a shipment is loaded or unloaded from an aircraft, and only manual inspection tells if the shipment is in the right aircraft or not. In air cargo operations, shipments are still being lost and items sometimes travel without their associated documents, which leads to claims that the carrier has to pay. Moreover, real time locating of loose goods as well as unit load devices (ULD) in and out of the air cargo warehouse can provide visibility that not only the shipping company could benefit from; but also customers see value in knowing where their shipments are.

The tracking and rapid locating of baggage, loose freight and containers (especially the associated integrity assurance of those items) is also essential to the overall security of a commercial flight. This tracking / locating of goods is accomplished today, for the most part, only by a very labor-intensive manual process. The introduction of RFID to provide this asset tracking and locating offers the opportunity for: centralized monitoring; continuous surveying; automatic event logging; and, of course, more rapid finding of items when retrieval is mandatory (Cerino and Walsh, 2000).

When time becomes a primary consideration for delivery, air transportation is the mode of choice. According to McCarthy (2003), one of the key drivers for the use of air cargo over other modes is the weight to value ratio of shipped goods. Some specific market segments include: extremely high value products such as jewelry, luxury automobiles, and race horses; just-in-time products such as electronics and auto parts; perishables such as fresh foods, flowers, and seasonal apparel; and time-sensitive products such as medical supplies and pharmaceuticals. Many pharmaceutical and biotech products have a correlated sensitivity to temperature and high value (Wright,

2008) which makes these industries a major customer of the air cargo industry. Moreover, the quality and integrity of pharmaceutical products can be vital to people's lives; therefore, temperature management of such shipment is of prime importance.

With today's globalization, there is a growing need for fresh products to be delivered year round all over the world and with the cold supply chain requiring fast delivery; more and more perishable items are being shipped by air (Vega, 2008). Unfortunately, a faster transit time does not always imply controlled temperature throughout transportation. Of approximately 2.6 million tons of perishables air freighted in 2008, nearly 30% was estimated to be lost due to handling and temperature abuse (Catto-Smith, 2006).

RFID technology can also be combined with many different sensor applications, such as monitoring temperature, humidity, motion, etc. These features, with real-time tracking of unique IDs throughout the air cargo supply chain open numerous valuable opportunities for shippers and customers. In essence, RFID is revolutionizing the way products and goods are tracked and traced in the supply chain.

It has been shown that RFID can significantly improve warehouse operation efficiency and supply chain performance (Chow et al., 2006; Poon et al., 2009; Véronneau and Roy, 2009; Visich et al., 2009; Wang et al., 2010). It has also been shown that RFID can improve the overall quality and shelf life of perishables through the cold supply chain (Émond, 2007; Jedermann et al., 2007, 2009; Ruiz-Garcia et al., 2008; Abad et al., 2009). Although, to implement such technology in the air cargo industry, more research has to be done regarding many compatibility aspects of RFID technology and the air cargo world.

Commercial RFID systems are available under different standards, which work at different frequencies. Choosing the best suitable frequency for an application depends on many factors. For instance, the read range needed, the size of tags preferred and the type of environment surrounding the RFID system (materials and other interferences). In this research, three frequencies will be evaluated: 433MHz, 915MHz and 2.45GHz. Those frequencies are thought to be the most appropriate for the air cargo world today, mostly because of their longer read ranges.

Objectives. The main goal of this work is to evaluate the possibilities of using RFID to improve air cargo operations in general, as well as for perishable transportation. More specifically, some questions associated with air cargo operations will be addressed (Figure 1-3). Therefore, the four main objectives of this dissertation are:

- Measure and evaluate the interference level at 433MHz, 915MHz and 2.45GHz in air cargo warehouses (chapter 3).
- Obtain 3D mapping of RF propagation inside a cargo hold at 433MHz, 915MHz and 2.45GHz and compare with RFID tag readability at 915MHz (chapter 4).
- Evaluate RFID behavior around five air cargo container (ULD) materials at 433MHz, 915MHz and 2.45GHz (chapter 5).
- Study the temperature distribution inside air cargo containers in different cargo holds and aircrafts during flight (chapter 6).

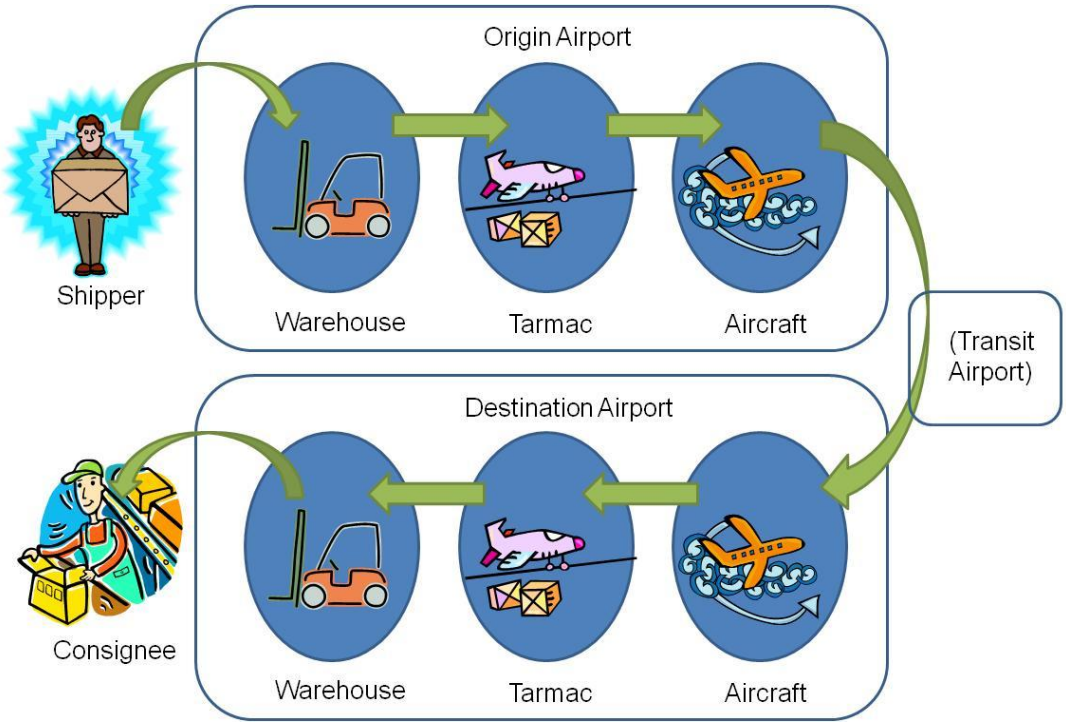

Figure 1-1. Brief overview of the air cargo supply chain.

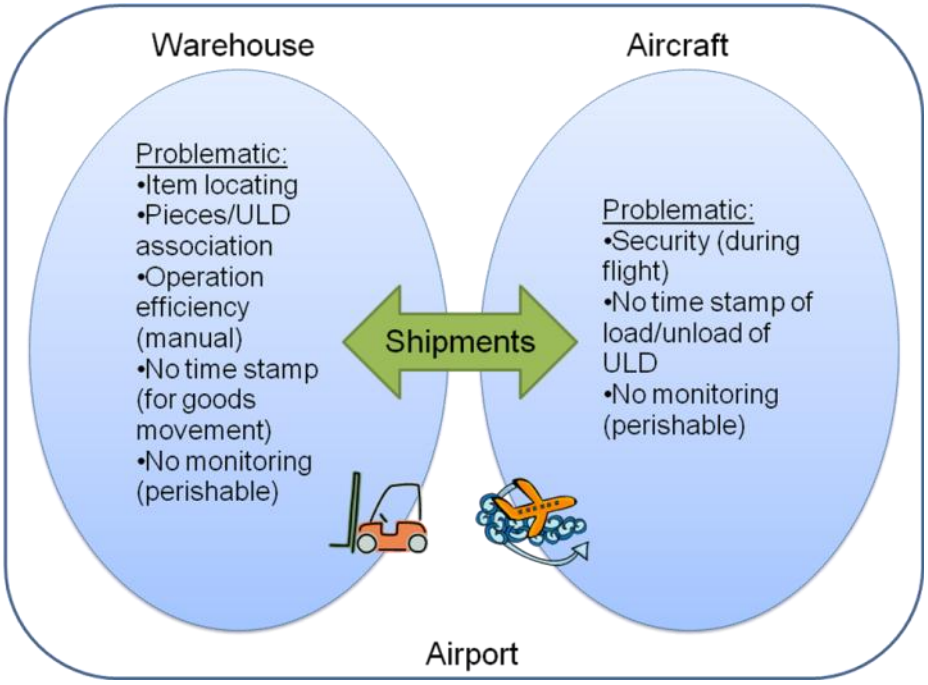

Figure 1-2. Some problems associated to the air cargo warehouse and aircraft operations.

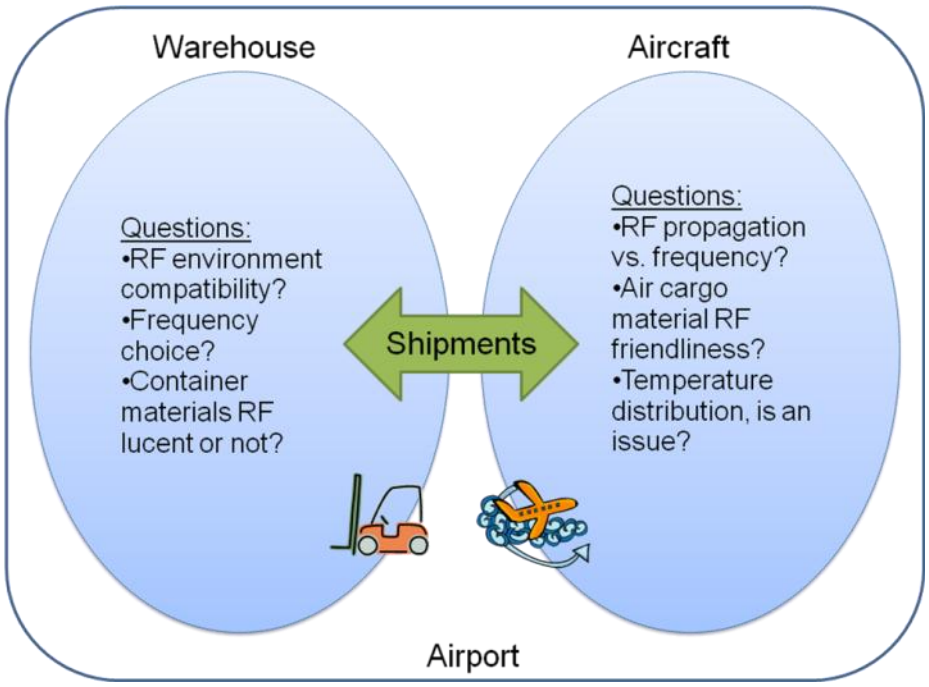

Figure 1-3. Some questions associated with warehouse and aircraft air cargo operations.

CHAPTER 2
RFID IN AIR CARGO: A LITTERATURE REVIEW

Introduction

This review will give a general idea of radio frequency identification (RFID) technology, its definitions and the way systems work. Then will follow an overview of the air cargo world, aviation history, the current market status, plus a brief description of the major parts and their operations. In addition, aircraft construction, systems, avionics and safety issues will be discussed. Subsequently, the subject of RFID in aviation will be described through regulations, applications as well as possible interference of the technology. The concluding remarks comment on the potential of RFID to improve air cargo operations in general.

RFID Technology and Definitions

Radio frequency identification (RFID) is an automatic wireless data collection technology with a long history. The fundamentals of RFID technology are based on electromagnetic energy studies, originating with Michael Faraday's explanation of light and radio waves as forms of electromagnetic energy back in 1846. For the last two decades RFID tags have been used in many applications (e.g. automatic toll roads, smart cards, store theft protection, access control, animal tracking, item tracking, etc.) which supply chain management and item tracking have been the fastest growing areas (Landt, 2005). Improvements in semiconductor technology resulted in reduction in the size of circuitry, reduction in cost of tags, increased functionality, and increased reliability, which sped up the industrial applications of RFID (Landt, 2005).

Radio Waves

Radio waves account for a portion of the electromagnetic spectrum (Figure 2-1). Radio waves at their most basic are considered as wave forms of electrical and magnetic fields and as a result, have amplitude, wavelength (λ), velocity (v) and frequency (f), the relationship of which is expressed as:

$$v = \lambda \cdot f \tag{2-1}$$

Electromagnetic waves are created by electrons in motion and consist of oscillating electric and magnetic fields. These waves can pass through a number of different material types (Lahiri, 2006).

The highest point of a wave is called a *crest*, and the lowest point is called a *trough,* as shown in Figure 2-2. The distance between two consecutive crests or two consecutive troughs is called the *wavelength*. One complete wavelength of oscillation of a wave is called a *cycle*. The time taken by a wave to complete one cycle is called its *period of oscillation*. The number of cycles in a second is called the *frequency* of the wave. The frequency of a wave is measured in *hertz* (abbreviated as Hz) and named in honor of the German physicist Heinrich Rudolf Hertz. If the frequency of a wave is 1Hz, it means that the wave is oscillating at the rate of one cycle per second. It is common to express frequency in KHz (or kilohertz = 1,000Hz), MHz (or megahertz = 1,000,000Hz), or GHz (or gigahertz = 1,000,000,000Hz). *Amplitude* is the height of a crest or the depth of a trough from the undisturbed position (Lahiri, 2006).

Radio waves can be further divided up into groups; Low Frequency (LF), High Frequency (HF), Ultra High Frequency (UHF) and Microwave Frequency (MF) with similar categories applying to RFID systems. Electromagnetic energy has been best

described as a stream of photons each traveling at the speed of light in a wave like pattern. An electromagnetic wave propagates in a direction that is at right angles to the vibrations of both the electrical and magnetic oscillating fields (Winder and Carr, 2002). Radio waves and microwaves are situated towards the lower end of the electromagnetic spectrum (Figure 2-1) meaning that waves situated in the low frequency category posses lower amounts of energy (*E*) compared to microwave frequency waves according to Planck's equation:

$$E = h \cdot f \tag{2-2}$$

Where h is Planck's constant.

Electromagnetic waves can be characterized in terms of frequency, wavelength or energy (as shown using Planck's relation above). Taking the speed of light ($c = 3x10^8$) as the velocity, it is now possible to say (Meyers et al., 2007):

$$c = \lambda \cdot f, \qquad \lambda = \frac{c}{f} \quad \text{or} \quad f = \frac{c}{\lambda} \tag{2-3}$$

Polarization of electromagnetic waves

The polarization of an electromagnetic wave is determined by the direction of the electric field of the wave. There is a difference between linear polarization and circular polarization. In linear polarization the direction of the field lines of the electric field in relation to the surface of the earth provide the distinction between horizontal (the electric field lines running parallel to the surface of the earth) and vertical (the electric field lines running at right angles to the surface of the earth) polarization (Finkenzeller, 2003).

The transmission of energy between two linear polarized antennas is optimal if the two antennas have the same polarization direction. Energy transmission is at its lowest point, on the other hand, when the polarization directions of transmission and receiving antennas are arranged at exactly 90° or 270° in relation to one another (e.g. a horizontal antenna and a vertical antenna). On the other hand, circular polarization occurs when the polarization direction of the electromagnetic field generated rotates through 360° every time the wave front moves forward by a wavelength. The rotation direction of the field can be determined by the arrangement of the delay line. We differentiate between left-handed and right-handed circular polarization (Finkenzeller, 2003).

Electromagnetic waves properties

In free space, all electromagnetic waves obey the inverse-square law which states that the power density of an electromagnetic wave is proportional to the inverse of the square of the distance from the source. In other words, as the separation distance is doubled, the electrostatic force is decreased by a factor of four (Henderson, 2010). As the electromagnetic waves propagate in their environment, they encounter many objects and behave differently around those obstacles, sometimes in a critical way towards the communication link needed for the functioning of an RFID system. It has been reported that environmental factors may decrease the reader range of passive RFID systems by at least 50% (Keskilammi et al., 2003). It is also well established that higher frequencies experience greater attenuation levels than lower frequencies (Keskilammi et al., 2003). Any wave incident upon an object will penetrate the material, a portion may be transmitted and another portion may also be reflected back into the environment. The exact amount of transmission and reflection is also dependant on the angle of incidence, material thickness, and dielectric properties (Blaunstein and

Christodoulou, 2007). Part of the high frequency energy that reaches the object is absorbed by the object and converted into heat; the rest is scattered in many directions with varying intensity (Finkenzeller, 2003).

Radio waves can be affected by the material through which they propagate. A material is called RF-lucent for a certain frequency if it lets radio waves at this frequency pass through it without any substantial loss of energy. A material is called RF-opaque if it blocks, reflects, and scatters RF waves. A material can allow the radio waves to propagate through it but with substantial loss of energy. These types of materials are referred to as RF-absorbent. The RF-absorbent or RF-opaque property of a material is relative, because it depends on the frequency. That is, a material that is RF-opaque at a certain frequency could be RF-lucent at a different frequency (Lahiri, 2006).

The presence of more than one wave in a space may result in interference between the waves, which can be constructive (they reinforce one another), or destructive (cancel each other in whole or in part). There are a number of different ways an electromagnetic wave may interact with materials in its surrounding area as follows (Wu et al., 2006; Domdouzis et al., 2007):

Scattering: This occurs when a wave hits an obstacle smaller than its wavelength. It leads to the formation of scattered waves which are redirected with random phase and amplitude (Blaunstein and Christodoulou, 2007). This can be the result of rough surfaces, small objects or irregularities in the transmission medium.

Refraction: This is the change in direction of a wave due to a change in its speed. This is most commonly observed when a wave passes from one medium (with a certain

refraction index) to another at an angle. Refraction is described by Snell's law, which states that the angle of incidence is related to the angle of refraction (Reed, 2009).

Fading: This is a variation of the signal strength with time (Meyers et al., 2007). It occurs due to time dependent changes in multipath. Fade zones are small areas inside the interrogation zone that lead to periodic attenuation of the received signal. This effect increases with the distance from the emitting antenna. This occurrence is too random to make possible the prediction of signal strength at a particular point in time (Mac Carthy, 2009).

Multipath: This occurs when a radio wave arrives at a particular receiving antenna from more than one propagation route due to its interactions with the surrounding environment (Lahiri, 2006). Multipath, or path loss strongly depends on propagation environment.

Reflection and cancellation: The electromagnetic field emitted by the reader is not only reflected by a transponder, but also by all objects in the vicinity, the spatial dimensions of which are greater than the wavelength of the field (Rappaport, 2002). The reflected fields are superimposed upon the primary field emitted by the reader. This leads alternately to a local damping or even so-called cancellation (anti-phase superposition) and amplification (in-phase superposition) of the field at intervals of λ/2 between the individual minima. The simultaneous occurrence of many individual reflections of varying intensity at different distances from the reader leads to a very erratic path of field strength around the reader, with many local zones of cancellation of the field. Such effects should be expected particularly in an environment containing large metal objects (Finkenzeller, 2003). The importance of these properties cannot be

over emphasized as they are all hugely important in relation to passive UHF RFID systems as they impact on how the electromagnetic wave (essential for coupling) is affected by different objects.

Direct penetration: Little or no reflection occurs when electromagnetic waves penetrate directly through objects such as paper, non conductive plastics or textiles (Penttilä et al., 2006). These materials, including most composites, are non-absorbing and possess low refractive indexes. Such materials are generally referred to as being RF-lucent.

Diffraction: Similarly to light propagation, materials surrounding radio waves can provoke diffraction of the waves, which can lead to RF signal variations. It is described as the apparent bending of waves around small obstacles, the spreading out of waves past small openings or the deviation in the path of a wave that encounters the edge of an obstacle. At high frequencies, diffraction, like reflection, depends on the geometry of the object, as well as the amplitude, phase, and polarization of the incident wave at the point of diffraction (Rappaport, 2002)

RFID System Overview

A basic RFID system consists of a computer with software connected to a reader and one or more reader antennas, which communicate wirelessly with tags (Figure 2-3). The reader transmits an RF signal to the tags via its antenna(s). The tags receive power from the antenna and then send their information back. Following is a description of each component in more detail.

Readers

RFID readers can be portable or fixed, depending on the application. A typical RFID reader has both transmitting and receiving functions for data transfer and

communication with tags (Keskilammi et al., 2003; Poussos and Kostakos, 2009). Most interrogators consist of an RF transceiver module (transmit and receive), a signal processor, a controlling unit and a coupling element (antenna) and data interface to a host system (Lahiri, 2006).

EIRP: The Equivalent Isotropic Radiated Power (EIRP) determines the power of the signal transmitted by the reader in the direction of the tag. Maximum allowed EIRP is limited by national regulations (e.g. in North America it is 4W) (Nikitin and Rao, 2006).

Reader sensitivity: is another important parameter which defines the minimum level of the tag signal which the reader can detect and resolve. The sensitivity is usually defined with respect to a certain signal-to-noise ratio or error probability at the receiver. Factors which can affect reader sensitivity include receiver implementation details, communication protocol specifics, and interference, including signals from other readers and tags. An ideal reader can always detect an RFID tag as long as the tag receives enough power to turn on and backscatter (Nikitin and Rao, 2006).

Antenna

Antennas are essential components of both RFID tags and readers. Their principal function is the facilitation of a dual directional communication link between tag and reader (Dobkin, 2008). At its most basic an antenna is a particular arrangement of conductors designed to transmit an electromagnetic field in response to the application of an alternating electric current. It also has the ability to generate a voltage between terminals when placed in a time varying electromagnetic field (Finkenzeller, 2003). Both RFID tags and reader antennas come in a variety of sizes and shapes which determines their operational characteristics (polarization for example).

Reader antenna: These are used to communicate with the nearby tags. Antennas have emitting and receiving capabilities. The antenna first propagates the RF wave into the environment in order to establish a communication link between the tags and reader to facilitate coupling (Liang et al., 2006). This RF wave creates an interrogation zone which is an area surrounding the antenna where communication will take place provided that a tag is present. Once communication is established, the antenna also receives a resultant signal from the tag which is transferred to the reader for demodulation.

The antenna may be physically incorporated into the reader, which is generally the case for handheld units. Alternatively, the antenna might be individually housed and attached to the reader by appropriate cables (Roussos and Kostakos, 2009). Depending on the desired use, readers can support connection to more than one antenna at a time.

Tag antenna: They operate on the same principle as reader antennas, but face some different practical challenges (Dobkin, 2008). In the case of passive RFID tags, the tag antenna is responsible for receiving the electromagnetic wave from the reader antenna and reflecting the modulated backscatter signal to the reader. For active RFID tags, the antenna is responsible for emitting the internally generated signal. The size and shape of the antenna determines the operating frequency as well as the application and ideal orientation of the tag (Fuschini et al., 2008). Tag antenna must also be small enough to fit the item it is identifying; have omnidirectional and hemispherical coverage; have a polarization that matches with the reader; and be robust and low cost (Keskilammi et al., 2003).

Polarization: Propagating electric fields point in a certain direction in space. Polarization refers to the orientation of the electric field radiated by the antenna. If the

vector rotates with time, then the wave is elliptically polarized. The degree of ellepticity from a circle to a straight line gives circular and linear polarization. For linear polarization (vertical / horizontal), the vector oscillate on one plane as the wave propagates whereas in circular polarization it rotates through 360 degrees per cycle (Figure 2-4).

Gain: The gain, or amplification factor, is the factor by which the input power is amplified. Ideally a reader antenna has a high gain due to the fact that the received power at the tag is directly proportional to the reader antenna gain.

Tags

An RFID tag is a device that can store and transmit data to a reader in a contactless manner using radio waves. Tags have three main components: an integrated circuit (IC or chip), an antenna and a substrate (Meyers et al., 2007). They are available in a wide variety of sizes, shapes and functionality which determines their unit cost (Jedermann et al., 2009). The tag is responsible for storing and sharing user defined information regarding the item to which it is attached. It may be constantly in an active state whereby it may record storage conditions in its immediate environment or it may remain in a dormant state until activated by an interrogating wave from a nearby reader depending on its classification (Nikitin and Rao, 2006). It communicates with the reader by superimposing its stored data (through signal coding and demodulation). Transponders can be classified according to sources of energy:

- Passive tags
- Active tags
- Semi-active tags
- Semi-passive tags

Passive tags: Passive RFID tags have no internal power source (no battery). In inductively coupled systems, when the tags are present in the RF field of an RFID interrogator, the energy induced on the tag circuitry is used for transmitting back the ID of the tag. In UHF systems, electromagnetic backscatter coupling is used at the tag circuitry for changing the impedance of the tag antenna according to its ID. A passive tag is simple in its construction and has no moving parts. As a result, such a tag has a long life and is generally resistant to harsh environmental conditions. Passive tags can be very small and low cost to manufacture. On the other hand, they have limited data capacity and shorter read range. In tag-to-reader communication for this type of tag, a reader always communicates first, followed by the tag. The presence of a reader is mandatory for such a tag to transmit its data (Lahiri, 2006).

Active tags: Active tags are beaconing in a defined period of time by using integrated power supplies (battery for example). It does not need the reader's emitted power for data transmission. The on-board electronics can contain microprocessors, sensors (temperature, humidity, motion, etc.), and input / output ports powered by the on-board power source. Therefore, for example, these components can measure the surrounding temperature and generate the average temperature data (Keskilammi et al., 2003). The components can then use this data to determine other parameters such as the expiry date of the attached item. The tag can then transmit this information to a reader. In tag-to-reader communication for this type of tag, a tag always communicates first, followed by the reader (Lahiri, 2006). Active tags also have longer read ranges than passive tags. They are ideal in environments of high electromagnetic interference because of their ability to broadcast a stronger signal with the aid of their internal power

source (Jeddermann et al., 2009). Some advantages and disadvantages of active tags are:

- Increased functionality (sensor, monitoring, recording)
- Long read ranges
- Large memory capacity
- Physically bulky
- High production costs
- Fragile because of moving parts in the design
- Life span limited to power source

These tags are commonly used in RTLS (Real Time Location Systems) in which the tag continuously reports its ID to the receiver units and location of the tag is usually calculated by using RSS (Received Signal Strength) information and triangulating between different receivers (Altunbas, 2010).

Semi-active tags: The name associated with this type of tag is not yet widely accepted. It is somewhat a type of active tag that enters a sleep or a low-power state in the absence of interrogation by a reader. A reader “wakes up” such a tag from its sleep state by issuing an appropriate command. This state saves the battery power, and therefore, a tag of this type generally has a longer life compared to an active transmitter tag. In addition, because the tag transmits only when interrogated, the amount of induced RF noise in its environment is reduced.

Semi-passive tags: These combine both passive and active type technology. Semi-passive systems have internal batteries but are not beaconing signals in a defined period. In the presence of the RF field of an interrogator, the tag wakes up and starts to backscatter its ID to the interrogator (like a passive tag); but using its integrated battery supply to increase the signal (McCarty, 2009). The trade off for energy efficiency is to

have reduced response time caused by the time slot needed to wake up the transponder.

Tag generation and classification. Tags can be classified according to their power source, as seen earlier, but they may also be grouped according to their functionality (Meyers et al., 2007). This classification is based on EPCglobal standard as shown in Table 2-1. This classification of tag is based on the format, read / write capability and programming capability. The EPC classification consists of Class and Generation. The Class describes a tags basic functionality, for example whether it has memory or an on-board power source, whereas Generation refers to a tag specification's major release or version number (Khan et al., 2009).

Frequencies

Commercial RFID systems designed for different applications can work at different frequencies, such as:

Low frequency (LF): Frequencies between 30kHz and 300kHz are considered low, and RFID systems commonly use the 125kHz to 134kHz frequency range. At LF, the power supply to the transponder is generated by inductive coupling, which means short read ranges between the tags and reader antenna. RFID systems operating at LF generally have low data-transfer rates from the tag to the reader, and are especially good if the operating environment contains metals or liquids (Lahiri, 2006), which is why LF systems are commonly used in animal identification applications.

High frequency (HF): HF ranges from 3MHz to 30MHz, with 13.56MHz being the typical frequency used for HF RFID systems. A typical HF RFID system uses passive tags, has a slow data-transfer rate from the tag to the reader, and offers fair performance in the presence of metals and liquids (Lahiri, 2006). Moreover, HF systems

also work within short read ranges (generally within 1m), it is used in smart cards applications like access control or contactless payments.

Ultra-high frequency (UHF): UHF is the most common passive RFID tags used in supply chain applications worldwide. While the entire UHF spectrum ranges from 300MHz to 1GHz, it operates between 902-928MHz in the Americas; 865-868MHz in Europe, middle east and Russia; and 866-869MHz and 923-925MHz in Asia, Australia and the Pacific. The accepted standard for passive UHF frequency is ISO 18000-6C (UHF Gen2). Active or semi-active RFID systems in UHF frequencies operate at 433MHz. ISO 18000-7 is the accepted standard for parameters of active air interface communications at 433MHz. A UHF system can therefore use both active and passive tags and has a fast data-transfer rate between the tag and the reader, but performs poorly in the presence of metals and liquids (not true, however, in the cases of low UHF frequencies such as 433MHz) (Lahiri, 2006). UHF systems working in the electromagnetic field offer a much longer read range than lower frequencies.

Microwave frequency: Microwave frequencies range upward from 1GHz. A typical microwave operating frequency is either at 2.45GHz or 5.8GHz in the Industrial Scientific and Medical (ISM) band. Microwave systems can be either passive or semi-passive and provide the fastest data communication rates compared to the other frequencies (Lahiri, 2006). Microwave frequency, like UHF, offers long read ranges, especially when working in an active RFID system. Read range performance for passive systems in the presence of water and metallic surfaces is very poor because of the higher signal attenuation at higher frequency (Friis, 1946).

National licensing regulations. In the USA, RFID systems must be licensed in accordance with licensing regulation *FCC Part 15* from the Federal Communications Commission. This regulation covers the frequency range from 9kHz to above 64GHz and deals with the intentional generation of electromagnetic fields by low and minimum power transmitters (intentional radiators) plus the unintentional generation of electromagnetic fields (spurious radiation) by electronic devices such as radio and television receivers or computer systems. The category of low power transmitters covers a wide variety of applications, for example cordless telephones, biometry and telemetry transmitters, on-campus radio stations, toy remote controls and door openers for cars. Inductively coupled or backscatter RFID systems are not explicitly mentioned in the FCC regulation, but they automatically fall under its scope due to their transmission frequencies, which are typically in the ISM bands, and their low transmission power (Finkenzeller, 2003). Table 2-2 lists some of the frequency ranges that are important for RFID systems.

Air Cargo

Aviation History

Times have changed since the Wright Brothers and the first flight of a powered aircraft in 1903 (Taylor 1989; Bilstein 1994; Wegener 1997). They were not only pioneers of flight, they also were the first ones to ship goods by air, when in November 1910, a department store from Ohio made arrangement with them to have a bolt of silk flown up from Dayton to Columbus (Bilstein, 1994). Not long after, in 1911, the first official airmail flight is made in India, where 6,500 letters were carried over about 10 km (Taylor, 1989). It is only after World War I, on May 15, 1918 that airmail service began in the US between New York City, Philadelphia and Washington D.C. with a JN-4, which

was built as an Army training airplane. In 1919, American Railway Express made an unsuccessful attempt to deliver cargo to Chicago (Bilstein, 1994). In the mean time, the Airmail Act (1925) and the Air Commerce Act (1926) were created. Later, in 1927, plans were made for four commercial airlines (National Air Transport, Colonial Air transport, Boeing Air Transport and Western Air Express) to fly express. From hesitant beginnings to slow progress, commercial air cargo made great strides in the post-World War II era. Wartime experience in long-range cargo operations helped, but the postwar availability of dozens of surplus military multiengine transports was more important. Unfortunately, the maintenance cost of those aircraft only allowed a handful of companies to survive. On the other hand, the scheduled passenger lines, sensing lost revenues, began to pay more attention to cargo services in their normal passenger routes and began to operate their own all-cargo services (Bilstein, 1994).

Air Cargo Supply Chain

The air cargo system consists of a large, complex distribution network linking manufacturers and shippers to freight forwarders to airport sorting and cargo handling facilities where shipments are loaded and unloaded from aircraft (Elias, 2007).

The airport forms an essential part of the air cargo supply chain, because it is the physical site at which a modal transfer of transport is made from the air mode to land mode. It is the point of interaction between the airline and the user (Ashford et al., 1983). Airports are divided into landside (parking lot, access roads, etc.) and airside (all areas accessible to aircraft, including runways, taxiways and ramps) areas. In addition to people, airports move cargo around the clock. Cargo airlines often have their own on-site and adjacent infrastructure to transfer parcels between ground and air.

Air cargo warehouse operations

Figure 2-5 presents the layout of an airline's new cargo facility. The cargo terminal is divided into an import area and an export area. The flow of goods through the terminal is either from the airside to the landside (terminating freights or connecting freights requiring the road feed service), from the landside to the airside (originating freights or connecting freights arriving from a road feeder service), or from the airside to the airside via the terminal (connecting freights).

Export area: The export area is dedicated to receiving, processing and preparing outbound freights, which refers to all shipment moving from an outside customer, and going onto a flight. All freight arrives at the cargo facility from the "landside export" area, either as bulk or as shipper loaded unit device. The freight gets weighed and dimensioned by the acceptance agent and stored at the appropriate location depending on its flying time and destination. If items are bulk, they ultimately go to the build-up area to be put in a ULD (Unit Load Device) or are transported in a tub cart directly to the airplane if this airplane is bulk loaded. ULDs are transported onto roller system through the cargo facility and onto trailers to the airside. All export shipments leave the warehouse via the "airside export" doors.

Import area: The import area is dedicated to receiving, processing and releasing inbound freights which refers to all shipments coming from a flight, going to an outside customer. ULDs are transported the same way between the airside and cargo facility (trailers). Bulk is unloaded from the aircraft directly into tub carts. Everything is brought back to the cargo warehouse via the "airside import" area, is broken-down when needed and stored until customer pick-up.

The movement of transiting goods (from one flight to another flight) also goes through the warehouse. It is considered “import” as it enters via the import airside, and becomes “export” as is it processed in the cargo facility and moves to the export side before exiting the warehouse through the “airside export” doors to reach its next flight.

Unit load device (ULD)

Unit Load Devices (ULDs) play a vital part in ensuring that as air-cargo volumes increase; they are moved safely, quickly and cost-effectively (IATA, 2002). ULD is the correct terminology used by the air transport industry for containers and loading units that are used for the carriage of cargo by air. It allows large quantities of cargo to be bundled into large units. Pallets and nettings as well as rigid containers are commonly used for freight transport by air. Each ULD is required to have a marking that identify its type code, maximum gross weight and actual tare weight (IATA, 2002). Currently, technical specifications for unit load devices are set by the International Air Transport Association (IATA).

While the world is talking about climate change, the airline industry is looking at ways to be more fuel efficient to minimize their operational costs as well as their impact on the environment. One way to do so is to reduce weight, minimizing weight without compromising the business volume is feasible by using lighter containers, or ULDs. Composite ULDs can save up to 25% of the tare weight of a traditional aluminum ULD (Nordisk, 2010). Kevlar® ULDs are constantly replacing older aluminum containers and account for approximately 39% of a major airline’s ULD fleet. Aluminum ULDs still add up to 43% of their fleet, whereas Lexan® containers count for the remaining 18%.

Market

During the late 1960s, the total tone kilometerage of freight doubled every four years, an average annual growth rate of 17%. At that time, the aviation world was replete with extremely optimistic forecasts of a burgeoning air cargo market. The prolonged and recurrent economic recessions and the tenfold increase in oil prices of the 1970s militated against sustained growth in North America (Ashford et al., 1983).

Today's trend. World air cargo traffic grew 5.1% in 2007, which followed 3.2% growth in 2006 and 1.7% growth in 2005, making those three years the weakest growth period for the industry since the first Gulf War, 1990-1992. Tepid traffic growth can be largely attributed to high fuel prices, which were increasing from late 2003 through July 2008. In response to the ongoing rise in jet fuel prices, freighter operators have accelerated fleet renewal activities, most notably in the large wide-body sector. Freighters count for about 10% of the total airplane fleet (Boeing, 2008). A wide-body aircraft is a large airliner with two passenger aisles, whereas a narrow-body only has one passenger aisle.

A few decades ago, it was hard to foresee the present degree of traffic volume in aviation. An increase of up to 5.8% per year is estimated for the next two decades which will mean triple the amount of the present cargo traffic volume in the next 20 years (Boeing, 2008). As a result of this increase, the focal point in aviation research has changed: Socio-economic aspects are coming to the fore. The reduction of emissions such as noise and pollutants is becoming more significant. In particular, the reduction of the weight of the structure of future aircraft is a central task that will enable a reduction of fuel consumption and an increase in the payload (Wilmes et al., 2002).

The international competitive situation and the related increase in global competition in the aircraft industry is additionally making it necessary to considerably reduce costs in the development, production, and maintenance of the next generation of aircraft. The development time must be considerably shortened in order to enter aircraft faster into service. In addition to weight and cost, additional challenges in the future will be increased safety requirements for aircraft in the case of accidents, etc. Improvements in these areas are indispensable in order to ensure a high acceptance of this means of transportation in the future (Wilmes et al., 2002).

Materials in Commercial Aircrafts

Commercial aircraft include types designed for scheduled and charter airline flights, carrying both passengers and cargo. The larger passenger-carrying types are often referred to as airliners, the largest of which are wide-body aircraft. Some of the smaller types are also used in general aviation. Aircraft construction materials used to be mostly aluminum alloys, but nowadays more and more composites are utilized in aircrafts design.

Composites

The development of composite materials is considered to be one of the most important advances in aviation design since aluminum was introduced in the 1920s. Development of various composite materials has had a very positive impact on the performance, shape, reliability, weight, cost and composition of modern aircraft. Composites are a combination of two or more significantly different inorganic or organic components. Although the components together form a composite material they each maintain their original form and do not blend together. In a composite material, one component serves as a “matrix”, being the component that holds everything together,

with the other component or components serving as reinforcement. An epoxy resin matrix with glass fiber reinforcing is one of the more commonly known composite materials, but continuing research is resulting in the production of various other composite materials which are proving beneficial in aviation design as well as in other industries (Anonym, 2007). Despite their strength, light weight, long life expectancy, corrosion resistance, and resistance to damage from cyclic loading (fatigue); composites have not been a miracle solution for aircraft structures. Composites are hard to inspect for flaws and can sometimes be brittle. Some of them absorb moisture. Most importantly, they can be expensive, primarily because they are labor intensive and often require complex and expensive fabrication machines. Aluminum, by contrast, is easy to manufacture and repair (Day, 2009).

Modern airliners use significant amounts of composites to achieve lighter weight. About 10% of the structural weight of the Boeing 777, for instance, is composite material (Day, 2009). The new Boeing 787 Dreamliner has made extensive use of composite materials, resulting in a lighter weight airplane which is expected to have a number of benefits including greater fuel efficiency. This twin-engine, wide-body jet airliner is constructed from 50% composite with aluminum, titanium and steel making up 45% and a variety of components making up the balance of 5%. The composite material most used in the Boeing 787 Dreamliner's construction is carbon fiber reinforced plastic (Boeing, 2010a).

Metals

Aluminum still remains a remarkably useful material for aircraft structures and metallurgists have worked hard to develop better aluminum alloys (a mixture of aluminum and other materials). Aluminum is a very tolerant material and can take a

great deal of punishment before it fails. It can be dented or punctured and still hold together (Day, 2009). Aluminum alloys used in the aerospace industry are high strength and able to perform well in harsh and challenging environments. 7075 Aluminum is the alloy of choice when it comes to manufacturing aircraft parts, and 5052 aluminum, which is not quite as strong but has more weldability, is sometimes used. 7075 contains zinc and copper, which is ideal for highly stressed parts and is considered the strongest type of aluminum. It has good high temperature resistance and corrosion resistance, both necessary characteristics in aircraft aluminum. Aircraft metal must be strong yet lightweight at the same time, and aluminum exhibits a good strength-to-weight ratio, making it the first choice in airplane construction. The airframe of a typical commercial transport aircraft is 80% aluminum by weight (The Aluminum Association, 2008).

Electrical Systems in Commercial Aircrafts

Aircraft power can be generated by DC or AC power sources. DC systems usually supply 28 VDC at all times. Most of today's commercial aircrafts use AC power sources, which are three-phase systems where three sine waves are generated 120 degrees out of phase from each other. In this layout the phase voltage of a standard aircraft system is 115 VAC and the standard frequency is 400Hz; which is the same standard for ground power at most airports (Moir and Seabridge, 2001).

Avionics: This is a portmanteau word of "aviation electronics". It comprises electronic systems for use on aircraft, comprising communications, navigation and the display and management of multiple systems. Table 2-3 lists the main systems and their respective working frequencies.

Temperature Profile in Commercial Aircraft

Temperature is well regulated in the cabin of most passenger flights, but it is not necessarily the case inside the cargo hold or of freighter flights. Temperature distribution around cargo depends on many factors, to name a few: weather, duration of flight, type of aircraft (ability to control cargo ambient temperature), altitude, transit time (on tarmac), etc. As shown in Figure 2-6, a study on an international shipment of live mice during summer showed that both heating problems (during airport handling) and cooling problems (during flight) can occur (Syversen et al., 2008).

Aircraft Safety

Every day approximately six million people board airplanes and arrive safely at their destinations. Flying is one of the safest modes of transportation today. The overall safety record of commercial airplanes is excellent and has been steadily improving over time. During the 1950s and 1960s, fatal accidents occurred about once every 200,000 flights. Today, the worldwide safety record is more than ten times better, with fatal accidents occurring less than once every 2 million flights (Boeing, 2010b).

Cargo security and monitoring

The air cargo system is a complex, multi-faceted network that handles a vast amount of freight, packages, and mail carried aboard passenger and all-cargo aircraft. The air cargo system is vulnerable to several security threats including potential plots to place explosives aboard aircraft; illegal shipments of hazardous materials; criminal activities such as smuggling and theft; and potential hijackings and sabotage by persons with access to aircraft. Several procedural and technology initiatives to enhance air cargo security and deter terrorist and criminal threats have been put in place or are under consideration. Procedural initiatives include industry-wide

consolidation of the “known shipper” program; increased cargo inspections; increased physical security of air cargo facilities; increased oversight of air cargo operations; security training for cargo workers; and stricter controls over access to cargo aircraft and air cargo operations areas. Technology being considered to improve air cargo security includes tamper-resistant and tamper-evident packaging and containers; explosive detection systems (EDS) and other cargo screening technologies; blast-resistant cargo containers and aircraft hardening; and biometric systems for worker identification and access control (Elias, 2007). While the primary policy focus of legislation has been on cargo carried aboard passenger aircraft, air cargo security also presents a challenge for all-cargo operators (FAA, 2006).

History shows that very few accidents were caused by hazardous cargo content. According to the National Transportation Safety Board’s aviation accident database (NTSB, 2010), in the last 15 years, less than 20 accidents occurred from that cause, which corresponds to less than 0.1% of all accidents and incidents within that period of time. Moreover, only one major (fatal) accident was caused by fire in a cargo hold. Fortunately, the low numbers of accidents do not slow down the aviation authorities in encouraging the design of safer aircrafts.

Fire detection

For some aircraft compartments a fire / smoke detection system is required by the regulations JAR (Joint Aviation Requirements) and/or FAA. In addition, aircraft manufacturers install supplementary fire / smoke detection systems to increase the level of safety. These systems must comply e.g. with the regulations (Schmoetzer, 2001). The urgency of the corrective action subsequent to a fire / smoke warning depends directly on the risk and is reflected in the procedures to be applied by cockpit or cabin

crew. For example, a cargo compartment smoke warning is indicated to the flight deck crew as a red warning, this means the crew has to perform the action immediately. As long as the crew is unable to differentiate between a true and a false warning, it has to follow the certified procedure. The impact of a false fire / smoke warning in non accessible compartments is extensive and might include: flight diversion, declaration of emergency situation, eventually passenger evacuation, compartment inspection, fire extinguisher replacement, passenger disappointment, loss of confidence in the warning system, etc (Schmoetzer, 2001).

Technologies

Because the capability of available technology is seen as a significant constraining factor on the ability to screen, inspect, and track cargo, initiatives to improve cargo screening technology have been a focus of recent legislation to enhance air cargo security. Various technologies are under consideration for enhancing the security of air cargo operations, such as:

- Tamper-evident and tamper resistant packaging and container seals
- Cargo screening technology using x-rays, chemical trace detection systems, or possibly neutron beams
- Canine teams
- Hardened cargo container technology
- Biometric technologies

In addition, technologies to better track cargo shipments are being considered to maintain better control and tracking of cargo shipments along the supply chain. Both global positioning system (GPS) and radio-frequency identification (RFID) technologies are seen as emerging technologies for improving the tracking of air cargo in the supply chain (Elias, 2007). And within that supply chain, there is a definite weak point during air transit. Therefore, there is a growing interest to know which cargo is on board, where is

it in the cargo hold and what is its temperature, humidity, acceleration, etc (Schmoetzer, 2005).

RFID in Aviation

Cerino and Walsh (2000) stated that RFID technologies and systems with potential application to the worldwide aviation industry will most likely operate in the international Industrial, Scientific and Medical (ISM) frequency spectrum. Operation in an ISM band has the distinct advantage of not requiring the user to obtain specific licenses on a site-by-site basis. In fact, only an “honor system” compliance with the defined ISM regulations on a band-by-band and geographical region-by geographical region is required to allow completely unrestricted site operation anywhere within that ISM region.

In addition, for the most part, the application of RFID for aviation has focused on the “electronic baggage tag” as a replacement for a barcode baggage tag. However, the FAA and others have also addressed issues such as RFID for use with baggage containers, passenger and cargo tracking and as such have considered other additional frequencies; one such is the 915MHz ISM band (Cerino and Walsh, 2000). The International Air Transport Association (IATA) member airlines unanimously approved the IATA Recommended Practice (RP) 1740C document, which endorses the use of ultra-high frequency tags and readers compliant with the EPCglobal Gen2 protocol as a global air interface standard for RFID baggage tags (O’Connor, 2005).

ISM Frequency and Aviation RFID Considerations

The US Federal Aviation Administration (FAA) to a large extent, and other aviation industry vendors and / or air carriers to a lesser extent, has completed testing of various technologies to ascertain their potential performance for aviation operational utility. Each system (being comprised of reader and tag) was not tested side-by-side, nor

under identical simulated or operational conditions, yet a rather extensive matrix of frequency (ISM frequencies of 125kHz / 132kHz, 13.56MHz and 2.45GHz) versus operational performance was obtained as result of the totality of FAA trials. In total, seven test phases – geared at addressing the full range of aviation functional requirements – along with other additional site-specific operational RFID usage evaluations contributed to the following results.

Cerino and Walsh (2000) analyzed the results of three years of testing and research to develop an effective RFID system for the airline/airport environment. It was found that the 2.45GHz system has better performance, is more flexible in design, can be assembled off-the-shelf, and the system and tags (about 1/3 the cost of 13.56MHz disposable tags) are least expensive. The 13.56MHz system requires a mostly customized design, is less mature than the 2.45GHz technology, and interference concerns at 13.56MHz add significant complexity and cost to the system. The system at 125kHz / 132kHz presents significant tag cost disadvantages, which are not likely to be overcome for aviation use.

It is important to recognize that for each ISM band there exists specific transmitter power, signal modulation, duty cycle and other technical parameters that effectively comprise the band's operating regulation. These regulations are not consistent from band-to-band and (coupled with the natural differences in propagation characteristics for each band) result in significant differences as they relate to efficient aviation industry use.

2.45GHz: At this frequency the communication is entirely propagation coupling. Propagation in this band is via directional antennas, and hence reader energy can be

directed to the area of greatest tag likelihood. The 2.45GHz band essentially evolved with the understanding that ISM interference exists at every band, and hence offers several advanced communications protocols which counter the potential interference effects.

Aviation Applications

Although the FAA's interest in RFID stemmed from mandates associated with the Vice President's Commission on Anti-Terrorism, in particular its application to RF baggage tags and positive passenger bag matching, the use of RFID for commercial aviation extend beyond one security application. The fact is, there are many business and security reasons for applying RFID to the airport environment. Communications and RFID technology programs represent the key to integrating all the components of airport security, including perimeter intrusion detection, personnel screening, checkpoint screening, vehicle and cargo screening, digital video surveillance and recording, and RFID baggage and vehicle tracking (Hallowell and Jankowski, 2005).

Passenger baggage sortation

In aviation industry, major airports have been looking for opportunities to use RFID technologies in baggage handling areas since 1999. Many pilot tests have been done at numerous airports including Gimpo (Korea), Las Vegas, Jacksonville, Seattle, Los Angeles, San Francisco, Boston, New York, Heathrow and Rome (Chang et al, 2006). Ouyang et al. (2008) presented an intelligent RFID reader and its application in the airport baggage handling system. Jacinto et al. (2009) presented an RFID equipment tuning and configuration methodology developed in a project to support baggage tracking and feed dashboards with real time status of Service Level Agreements between the airport, the airliner and the ground operators.

A survey of the aviation industry would quickly identify that most air carriers utilize optical barcode “baggage tags” to identify the travel itinerary for each individual baggage item. The aviation industry is working towards standardization of an RF baggage tag, in hopes of eliminating current barcode read-rate limitations. These limitations become particularly evident with transfer baggage where the use of automated sortation systems is essential to keep connection times to a minimum. The FAA has, with the cooperation of many vendors, airlines and airports, clearly demonstrated the ability to utilize RF baggage tags to enhance baggage sortation (Cerino and Walsh, 2000; Chang et al., 2006).

Passenger / baggage matching. This process necessitates insuring that only boarded passenger’s baggage is loaded onto the aircraft. This process today can be accomplished either totally manually or semi-automatic (using handheld barcode). Either way, a significant amount of baggage handling is required and as such there exists a dependence on human accuracy and barcode quality. The later becomes particularly suspect with transfer baggage where the tags are no longer in the “pristine” condition as when originally issued. In addition, certain low-cost, high-performance RFID tags afford the opportunity to “add to the tag” more than just the IATA license plate data. Information such as: the results of security screening; passenger biometrics; baggage images; and, flow timing through the baggage handling process all provide for significant core business and security benefits (Cerino and Walsh, 2000).

Verification / authentication

From a security standpoint, few processes are considered complete without featuring a verification / authentication element. For example, if a certain passenger-checked bag is screened and considered to be cleared, this “cleared status” may be

used as basis for loading on to an aircraft. Consequently, it is imperative that the overall process be able to accurately verify that the bag in question definitely is the bag that has been deemed to be cleared for loading – versus any other bag in the system. A robust RFID system implementation could easily track that bag based on its physical characteristics (with the support of other sensors); unique data (securely) added to the tag and/or overall RFID carrier IT system; and, know path / timing for the bag through the baggage handling process (Cerino and Walsh, 2000). McCoy et al. (2005) investigated an automatic tacking system to improve airport security and efficiency by means of a cellular network of passive RFID receivers, combined with far-field active RFID tags which may be issued within boarding cards or as security badges.

Tracking and locating

The tracking and rapid locating of baggage, cargo and containers (and the associated integrity assurance of those items) is essential to the overall security of a commercial flight. This tracking / locating of “transport items” is accomplished today, for the most part, only by a very labor-intensive manual process. The application of RFID not only would be more time and labor efficient, but also more accurate. Sensors and electronic systems do not fall asleep, forget their assignments, become distracted, or otherwise perform in an unpredictable manner. The introduction of RFID to provide this asset tracking and locating offers the opportunity for: centralized monitoring; continuous surveying; automatic event logging; and, of course, more rapid finding of items when retrieval is mandatory (Cerino and Walsh, 2000).

Boeing and Airbus are also promoting the adoption of industry solutions for RFID on commercial aircraft parts. They believe that RFID could provide major benefits for the entire industry. They will get more accurate information about their demand for parts

and will be able to reduce their parts inventory and cut the time it takes to repair planes. Part suppliers will also be able to reduce inventory, improve the efficiency of their manufacturing operations and reducing the amount of unapproved parts that enter the supply chain (Chang et al., 2006).

Cargo

A natural evolution, beyond the sortation of passenger baggage, is the use of RF tags to handle sortation of cargo. For this application, the process is quite similar to passenger baggage sortation, with exception that cargo parcels often can have a rather large form factor. As such, only an RFID system with enough flexibility and performance features to allow achievement of cargo and passenger baggage sortation requirements would be a realistic option for most of the aviation community. Naturally, for carriers such as FedEx and UPS this restriction do not directly apply, however, even in those examples, there is benefit in commonality with passenger air carrier systems. With cargo, however, the concept of “tagging” entire palletized shipments becomes a consideration. This could demand fixed station RFID readers requiring an even greater read volume or, more practically, implementation of an area read capability (such as the entire cargo hanger or even the entire tarmac area) to cover widely dispersed assets. This concept of broad coverage area for very large parcels also relates to passenger baggage, as in containerized luggage for stowage on wide-body aircraft. And, as it relates to efforts accomplished and planned by the FAA, the application of RFID to ensure the integrity (from a security standpoint) of ULDs from the time they are filled until the time they are loaded onto the aircraft (Cerino and Walsh, 2000).

Containers. According to Cerino and Walsh (2000), passenger baggage containers (ULDs), are an important aspect of commercial aviation. For wide-body

aircraft, they are used to store up to 70 individual pieces of luggage (depending, of course, on the size of the individual pieces) and are loaded as a single unit. Whenever possible, baggage handlers segment passenger baggage by destination, in an effort to reduce the amount of handling time for luggage. This process of sorting luggage by destination and container positioning, besides supporting minimized ground turn-around time, is important to support the security process of passenger bag matching. Accordingly, the use of RFID to: manifest exactly which baggage is in which container; support the matching of the baggage to passenger “aboard aircraft” status; and exactly locate the container which holds the passenger baggage, in valuable from both security and operational efficiency standpoints.

Monitoring. With air freight increasing rapidly; just in time delivery being a real challenge; ULDs being packed by third parties; inspection time being very limited and transportation security being linked to volume, monitoring of goods within containers may contribute to security. Moreover, customers and insurance providers want to know what happens to their shipment (liability issue) and forwarders need to increase the monitoring of goods. Improvements may be feasible for temperature sensitive goods, hazardous materials and high value cargo, and such monitoring require communication between the container and the aircraft (Schmoetzer, 2005). If readers are installed in the aircraft, they can be used to interrogate the cargo, acquire data from dedicated goods, enhance the monitoring, set off warnings, etc (Figure 2-7). Therefore, automated onboard identification of cargo can contribute to enhance of security (Schmoetzer, 2005). Benefits of RFID assisted air freight handling include:

- Automated tracing of goods
- Automated verification of aircraft load instruction

- Reduction of false loading
- Reduction of ground time
- Paperless data transfer
- Electronic Bill of Loading
- Wireless interface can be used to enable more services than simply RF-Identification e.g.:
    - Change / update information on relevant item
    - Self control / monitoring means
    - Memorize what is of interest
    - Data exchange (e.g. actual temperature, history, etc.)

Cold chain

Products, such as food, pharmaceuticals and flowers, are at high risk of perishing from various adversities along the cold chain. The parties involved should control when possible, and at the very least monitor the conditions of the goods in order to ensure their quality and to comply with all legal requirements. Among environmental parameters during transport, temperature is the most important in maintaining the shelf life of the products (Nunes et al., 2006; Zweig, 2006; Jedermann et al., 2009).

With today's globalization, there is a growing need for fresh products to be delivered year round all over the world, thus, temperature sensitive items are likely to be shipped by air because of their relatively short shelf life. Unfortunately, a faster transit time does not always imply controlled temperature throughout transportation. In contrast, during airport operations, loading, unloading, air transportation or warehouse storage, perishable goods often suffer from temperature abuse either due to difficulties in controlling the temperature, absence of refrigerated facilities, or lack of information about produce characteristics and needs (Nunes et al., 2003). Of approximately 2.6 million tons of perishables air freighted in 2008, nearly 30% is estimated to be lost due to handling and temperature abuse (Catto-Smith, 2006). In a previous study, Émond et al. (1999) showed that the environmental conditions during airport operations could, in

fact, be very far from the optimum for fruits and vegetables. Moreover, in a strawberry quality study, Nunes et al. (2003) showed that greater losses in quality occurred during simulation of the airport handling operations, in-flight, and retail display than during warehouse storage at the grower, truck transportation to or from the airport, or during backroom storage at the supermarket. The relative success of growing exotic perishables in countries such as Colombia, Ecuador, and Peru in South America, and its successful distribution and commercialization in distant markets such as the US and the EU, have been made possible due to advances in transportation and refrigeration technologies. Yet the transportation systems of exotic perishables are far from perfect. Transportation and logistics costs can be high both monetarily and in terms of loss of quality during handling (Vega, 2008).

While passenger business is generally bidirectional, cargo is not. Consequently, freighter routes are often imbalanced. This implies that when transporting goods from point A to point B, the freight rate charged must also cover the return trip from B to A (Vega, 2008).

Temperature monitoring. Currently, most digital temperature loggers have to be connected to a host device to download data, and as a result, have limited real-time data interactivity, which results in after-the-fact analysis for claims, loss in quality and related issues. Radio frequency identification (RFID) temperature loggers function wirelessly which allows for real-time information transfer. Active or semi-passive RFID tags can support one or many sensors as well as the unique ID that RFID technology provides by design. The RFID tag, with associated hardware and software adds the benefit of having the item scanned on receipt, so that if an alert (alert triggers are

programmable prior to shipping) is active, the receiver knows immediately (not after-the-fact) that there is a potential problem with the shipment and can spend the time required on specific shipments rather than going through random inspections (Jedermann et al., 2007). Many studies have already shown the effectiveness of RFID in monitoring product temperature during transit (Émond, 2007; Jedermann and Lang, 2007; Jedermann et al., 2007; Ketzenberg and Bloemhof-Ruwaard, 2009).

Wireless Interference

Portable electronic devices' (PEDs) interference risk to aircraft radio systems is a concern during flights. For various reasons, many devices such as laptop computers are allowed during flights, while intentional transmitters such as wireless devices and phones are prohibited. There have been many past studies addressing the three elements. Examples include emissions measurements from wireless devices in aircraft radio bands (Nguyen et al., 2004, 2005). Aircraft radio receiver interference thresholds data may be found in "Environmental Conditions and Test Procedures for Airborne Equipment" (DO-160F) published by the Radio Technical Commission for Aeronautics (RTCA).

Devereux et al. (1997b) reported research and experimental results of commercial aircraft avionics and control systems exposed to conducted and radiated electromagnetic interference. This experiment, conducted inside a CV-580 aircraft, determined how susceptible installed avionics are to different low power RF sources located in passenger cabin and baggage compartments, and avionics and cargo bay areas. This study showed that avionics certified to the special 100V/m high intensity radiated field requirements are still highly vulnerable to low to moderate levels of onboard RF energy when installed in the aircraft system. Various sources of

electromagnetic interference can be easily transmitted at these frequencies. Also, many of the avionics bays and cable routes onboard today's modern aircraft are unshielded and easily accessible. Many of the aircraft cargo bays are located adjacent to the avionics bays with only fiberglass walls and access doors separating the two (Cerino et al., 1997). A cargo hold could easily contain a RF transmitter system which emits enough RF energy to seriously interfere with and upset today's avionics systems. Further analysis of the CV-580 aircraft was made by Devereux et al. (1997a) which emphasizes the aircraft receiver in-band frequency susceptibility, primarily the microwave frequency bands used for aircraft Global Positioning Satellites (GPS) and Satellite Communication (SATCOM) navigation. This report also includes VOR, VHF, UHF and DME navigation and communication frequency bands (refer to Table 2-3). The evaluation is focused on coupling behavior from inside the aircraft cavity, coupling through the windows, to the aircraft receive antennas. It was found that path loss coming from the cargo bay is likely to travel up through the mostly non metallic ceiling of the cargo bay into the passenger cabin and out the passenger windows or through the non metallic avionics bay doors located in the cargo bay through to the cockpit window and to the receiver antennas. Moreover, the path losses from a transmitting antenna at a central position inside the fuselage were greater than that from any window and about 10 to 20 dB greater than from the optimum window.

Furthermore, in a study by Nguyen et al. (2007) interference coupling factor (or interference path loss) data were measured for multiple radio systems on ten small aircraft. The data show significant data variations between different aircraft models. The

data also show stronger interference coupling than for previously measured larger aircraft, and potentially result in higher interference risks.

Electronic devices

Unlike aircraft installed equipment, passenger carry-on devices such as wireless phones are not required to pass the rigorous aircraft radiated field emission limits. Previous studies were made to measure the emissions from wireless phones in aviation bands and to assess interference risks to aircraft systems (Ely et al., 2003; Nguyen et al., 2004). Results from a recent study showed that the spurious emissions from 33 phones tested were below the aircraft installed equipment limits (RTCA/DO-160 cat. M), even with the consideration of the 5-8dB uncertainty associated with the phones expected directivity (Nguyen et al., 2005).

RFID interference

Passive tags are considered less of an interference concern for aircraft since they do not transmit without an interrogator, whose electromagnetic fields power the tags. Active tags, on the other hand, are powered with internal batteries. Active tags can be of higher interference risks since many can transmit on their own without an interrogator. The actual interference risks depend on several factors, including the tags' intentional and unintentional emission levels, the propagation path loss factor, and the victim system's susceptibility threshold to the emissions type. Nguyen et al. (2008) studied the emission measurements of active tags and their interference potential on aircraft sensitive radio receivers. Specifically, this study measured the unintentional emissions from several popular RFID tags used for cargo tracking. Results showed that many tags' peak total radiated power exceeded RTCA/DO-160E category L and M EIRP emission limits, one of which surpassed the limit by as much as 35 dB in the GS band

(328.60 – 335.40MHz). Another study made with two active tags at 433MHz showed that emissions from both tags were higher than the limit of DO-160E at the operation frequency and the harmonics. It was also found that the emission level depends greatly on the location and material on which a tag is placed (Yonemoto et al., 2007).

For a complete interference assessment, other factors such interference path loss and receiver interference thresholds should also be considered. These factors were addressed previously, for example, Nguyen et al. (2006) documented the measurement of interference path loss for cargo bays on a Boeing 747 and an Airbus A320 aircraft. Nguyen et al. (2004) provided a summary of passenger cabin path loss data for many commercial transport aircraft. Nguyen et al. (2007) reported the path loss measurements for general aviation aircraft. These path loss data represent the propagation loss between the tag locations and the victim receiver's antenna port. Aircraft radio receiver interference thresholds for continuous interference signal transmission were addressed in RTCA/DO-294B (Guidance on allowing transmitting portable electronic devices (T-PEDs) on aircraft). LaBerge (2007) analytically determined thresholds for intermittent interference signals similar to RFID emissions. Moreover, the work in Nguyen and Mielnik (2008) reports the laboratory effort to determine the GS system interference threshold to an RFID interference signal.

RFID airworthiness policy

The current Federal Aviation Administration (FAA) RFID policy document is AC20-162 "Airworthiness approval and operational allowance of RFID systems" (FAA, 2008). It incorporates and supersedes jointly-issued AIR-100, AFS-200 and AFS-300 RFID policy. This advisory circular offers guidance on installing and using RFID systems on aviation products and equipment. Specifically, it provides an acceptable way to use

RFID readers or interrogators installed on aircraft, and advice on allowing use of RFID devices on baggage, mail containers, cargo devices and galley / service carts. It also covers using portable RFID readers or interrogators carried onboard aircraft. This advisory circular is not mandatory and does not constitute a regulation. It describes an acceptable means, though it is not the only means, to show compliance with applicable installation and operational requirements. Through this AC, the FAA does not prohibit any use of RFID devices, it provides specific requirements that the equipment must meet to be safe and airworthy.

Concluding Remarks

This review showed that RFID has long been thought to have the potential to help the air cargo industry by increasing its safety, operation efficiency, monitoring capability, customer satisfaction, etc. Before implementation can take place, some questions have to be answered and more research has to be done. This is why this study will cover the following subjects: interference and frequency assessment in air cargo warehouses; RF propagation study inside the cargo hold; RF propagation through ULD materials; and temperature distribution in the cargo hold during transit.

Table 2-1. EPCglobal tag class structure

EPC Class	Functionality	Type
Class 0 – Gen 1	Read only	Passive
Class 1 – Gen 1	Write once, read many	Passive
Class 1 – Gen 2	Write many, read many	Passive
Class 2	Write once, read many	Passive
Class 3	Read and write	Semi-passive
Class 4	Read and write	Active
Class 5	Reader tags	Active

Table 2-2. Permissible field strengths for RFID systems in accordance with FCC Part 15 (FCC, 2008).

Frequency range (MHz)	Max. E field (mV/m)	Measuring distance (m)
13.553–13.567	10	30
433.5-434.5	11	3
902.0–928.0	50	3
2435–2465	50	3
5785–5815	50	3

Table 2-3. Aircraft radio systems

Aircraft Band	Description	Receive Spectrum (MHz)
LOC	Localizer	108.10 – 111.95
VOR	Very high frequency omnidirectional range	108.00 – 117.95
VHF-Com	Very high frequency voice communication	118.00 – 138.00
GS	Glideslope	328.60 – 335.40
DME	Distance measuring equipment	962.00 – 1213.00
ATC	Air Traffic control radar beacon system	1030.00
TCAS/TCAD	Traffic collision avoidance system / Traffic collision alert device	1090.00
GPS (L5)	Global positioning system	1176.45
GPS (L2)	Global positioning system	1227.60
GPS (L1)	Global positioning system	1575.00 ± 2
MLS	Microwave landing system	5031.00 – 5090.70

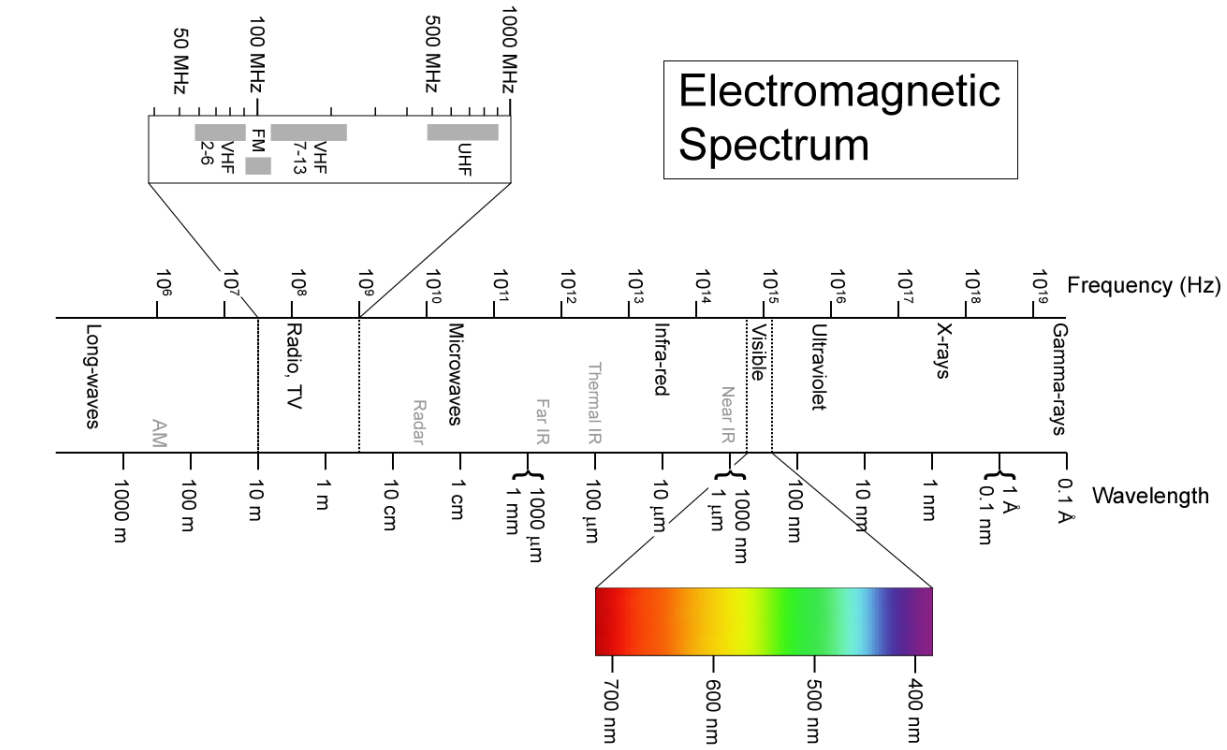

Figure 2-1. Electromagnetic spectrum

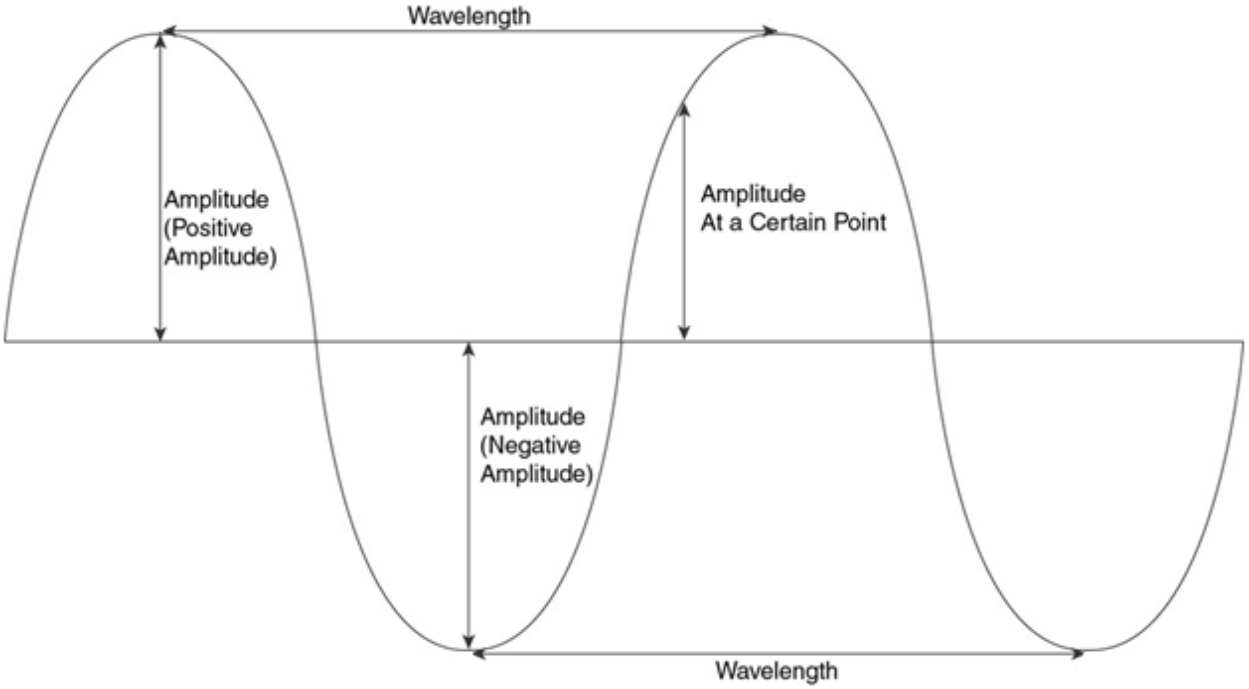

Figure 2-2. Different parts of a wave (Lahiri, 2006)

Figure 2-3. Example of an RFID system on conveyor belt.

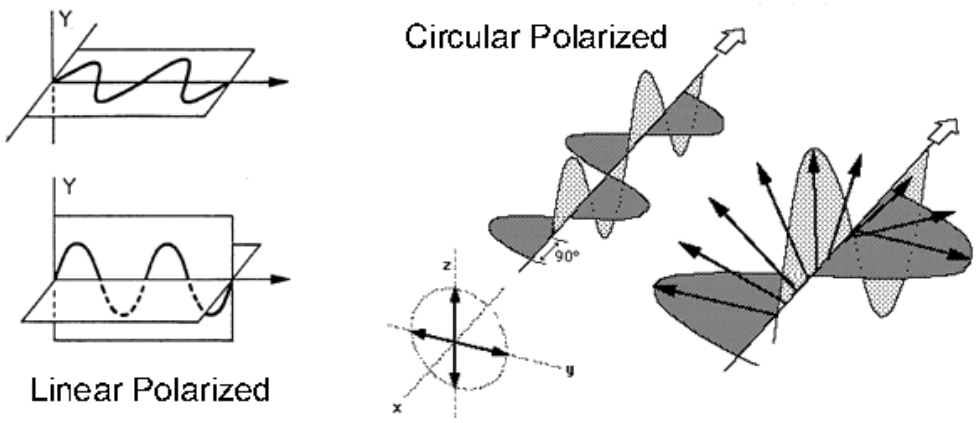

Figure 2-4. Wave propagation for linear and circular polarization

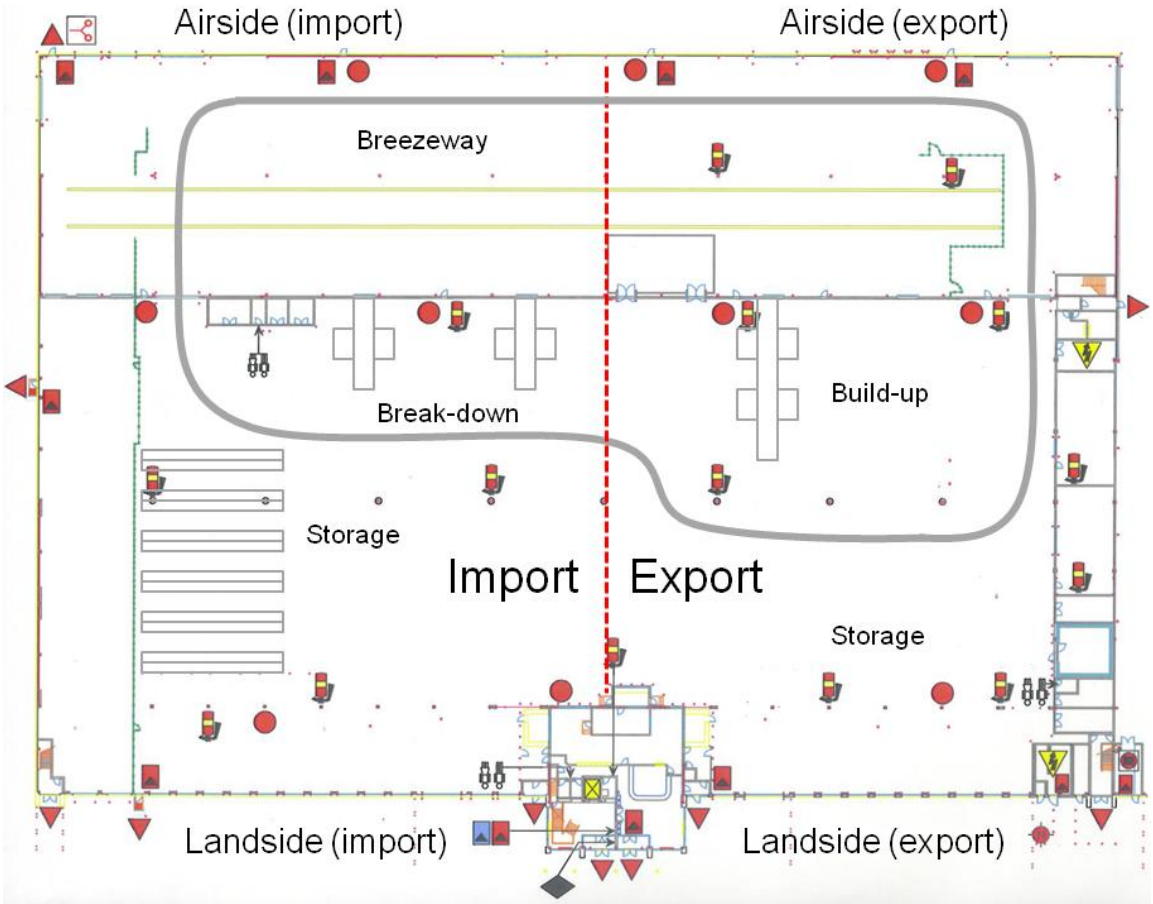

Figure 2-5. Cargo warehouse floor plan and activity areas.

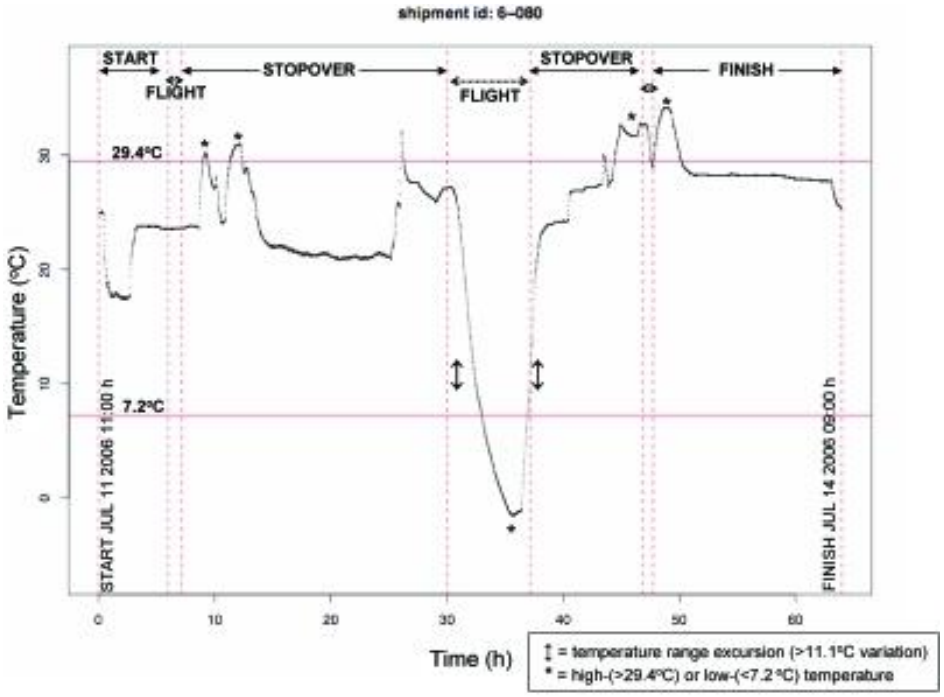

Figure 2-6. International flight temperature profile with both high-temperature excursions (during stopovers) and low-temperature excursions (in flight) (Syversen et al., 2008).

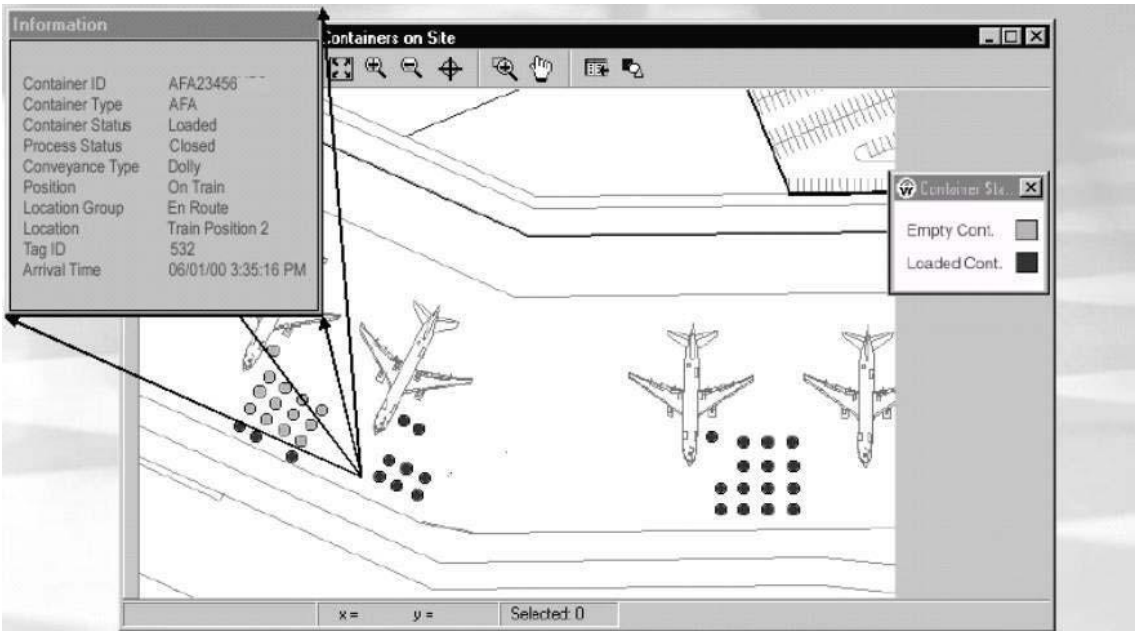

Figure 2-7. Example of a GSM/GPS capable RFID system for real time data acquisition (Schmoetzer, 2005).

CHAPTER 3
AIR CARGO WAREHOUSE ENVIRONMENT AND RF INTERFERENCE

Introduction

The air cargo system is a complex network that handles a vast amount of freight, packages, and mail carried aboard passenger and all-cargo aircraft. With air freight increasing rapidly; just in time delivery being a real challenge; unit load devices (ULDs) being packed by third parties; inspection time being very limited and transportation security being linked to volume, monitoring of goods within containers may contribute to enhanced security (Schmoetzer, 2005). Moreover, monitoring the movement of goods within the air cargo warehouse can enhance operation efficiency and provide valuable real-time information.

Cargo warehouse. A typical cargo terminal is divided into an import area and an export area. The import area is dedicated to receiving, processing and releasing inbound freights. The export area is dedicated to receiving, processing and preparing outbound freights. The flow of goods through the terminal is either from the airside to the landside (terminating freights or connecting freights requiring the road feed service), from the landside to the airside (originating freights or connecting freights arriving from a road feeder service), or from the airside to the airside via the terminal (connecting freights). These movements of goods in many directions can easily lead to item misplacement, and therefore it can be time consuming for the air cargo agents to locate the pieces when they are needed for build-up. Item level radio frequency identification (RFID) tagging, as well as ULD tagging, can address this issue by allowing real-time access to location of all shipments present in the warehouse. Moreover, RFID could permit automated and efficient ULD / item association during container build-up. This

technology could also give time stamp data on the movement of ULDs in and out of the building. There are many applications for which RFID could be helpful in an air cargo warehouse, but for a reliable system to be working properly, interference assessment needs to be done.

RF interference. Interference is typically interpreted as other sources of radio frequency (RF) energy that compete with an existing implementation. Any devices operating at the same frequency have the potential to interfere with each other. There exist many short range consumer devices operating at UHF frequencies. For example, devices like automotive remotes, alarm systems, home automation and wireless temperature sensors, can operate at 433MHz. At 915MHz, GSM 900 is a potential threat, as well as cordless phones, stereo, older wireless local area network (WLAN), amateur radio, etc. At 2.45GHz, interference is possible from devices such as newer WLANs, cordless phones, microwave ovens, fluorescent lighting and Bluetooth technology to name a few. There are ways to work around this issue by setting up these systems so that they do not use the same RF channels at the same time, but their consideration as potential interference threat to any UHF RFID system is of prime importance.

Frequency allocation. RFID is a radio technology and as such requires the use of radio spectrum to operate. Generally, when discussing spectrum issues, focus tends to be on tags that make use of the ultra high frequency (UHF) range. UHF (together with VHF) is the most common frequency band for television. In addition, it is used for mobile telephony, two-way radio communication and increasingly for digital services. Since RFID shares the UHF range with other applications, only a limited bandwidth within

UHF is available for short range devices and RFID, which is 902-928 MHz in North America. Although there are RFID tags and applications that make use of other frequency bands (for example 433MHz and 2.45GHz), most spectrum issues seem to concentrate around the UHF range and many sectors and applications (e.g. in retail and supply chains) use UHF tags (van de Voort and Ligtvoet, 2006).

ISM band. The Industrial, Scientific and Medical (ISM) bands are defined by the International Telecommunication Union Recommendation (ITU-R) in 5.138, 5.150, and 5.280 of the Radio Regulations. Individual countries' use of the bands designated in these sections may differ due to variations in national radio regulations. Because communication devices using the ISM bands must tolerate any interference from ISM equipment, these bands are typically given over to uses intended for unlicensed operation, since unlicensed operation typically needs to be tolerant of interference from other devices anyway. In the US, the use of ISM bands is governed by Part 18 of the FCC rules, while Part 15 Subpart B contains the rules for unlicensed communication devices, even those that use the ISM frequencies. All frequencies considered in this study are part of the following ISM bands: 433.05–434.79MHz, 902-928MHz (North America only) and 2400-2500MHz.

Spectrum analyzer. The sensitivity (or threshold) of a spectrum analyzer is defined as its ability to detect signals of low amplitude. The maximum sensitivity of the spectrum analyzer is limited by the noise generated internally (Anritsu, 2008). Noise level is directly proportional to the resolution bandwidth (RBW) of the system. Therefore, by decreasing the bandwidth by an order of 10dBm on the logarithmic scale (from 100KHz to 10KHz, for instance), the system noise floor is also decreased by 10dBm. As

an additional example, when the RBW is increased from 100Hz to 10kHz, the noise floor moves up 20dBm (Figure 3-3). When comparing spectrum analyzer specifications it is important that sensitivity is compared for equal bandwidths since noise varies with bandwidth. For this test, all data were taken at 10kHz RBW, which was the maximum sensitivity achievable with this specific spectrum analyzer. In other words, the real noise floor could have been lower than what was recorded.

Reader sensitivity. RFID communication goes two ways, first the reader-tag link, then the tag-reader link. The reader sends an RF signal with initial output power, which attenuates while traveling in the medium between the reader and the tag. If the tag received enough signal to respond, it sends its info back to the reader, which is also attenuated on the way back. When the reader receives this much attenuated signal, if it is above reader sensitivity levels, the communication is complete. The reader sensitivity defines the minimum signal level needed to be able to communicate with the transmitter. For passive RFID, it is usually the reader-tag link that is the limiting one, whereas for a semi-passive tag, the reader-tag link requirement is much more lenient since the received power must only be decoded not exploited (Dobkin, 2008). Reader sensitivity is dependent on several design choices, particularly, antenna configuration, and will become more important as tag IC power is scaled to lower values. Moreover, when interference is present, it is the tag-reader link or reader sensitivity that limits the system the most. The sensitivity of the receiver is limited by the noise that enters it and the largest source of noise for an RFID receiver is usually the leakage from its own transmitted signal (Dobkin, 2008). Nevertheless, any other sources of interference, within the specific UHF band used, can affect the performance of an RFID system when

its noise level is above the reader sensitivity limit. For example, a few years ago the typical passive RFID reader had a sensitivity of -65dBm, whereas in 2007 the most sensitive reader had a sensitivity of -77dBm (Impinj, 2007), but today Intelleflex's new XC3 reader has a receive sensitivity of -120dBm (Intelleflex, 2010). This does not mean that any noise above -120dBm would completely disable the communication link between a tag and reader. Interference can only be expected in the case where the noise level would be well above the tag-reader link; and that is not taking into account the fact that most RFID readers have their own interference filtering system. In other words, each RFID reader will tolerate up to a certain level of signal-to-noise-ratio (SNR in dB) which indicates how much higher the signal level is compared to the noise level. For instance, if a reader with sensitivity Y dB requires an SNR of X dB for a successful read, this means that in order to use the reader at its maximum capacity, the noise level present in the environment has to be less than (Y – X) dB. If this is not the case, than the effective distance between the tags and the readers need to be adjusted accordingly to compensate for the environmental noise.

For RFID technology to be implemented into an air cargo warehouse, many RF assessments need to be done. In particular, interference levels might dictate which frequency is most suitable for a specific RFID application. Therefore, the objective of this study was to identify the multiple RF interferences encountered inside air cargo warehouses.

Materials and Methods

RF interference readings were taken at different locations throughout two air cargo warehouses. One warehouse was located near the Pierre-Elliott Trudeau airport (YUL) in Montreal, Canada, whereas the other one was near Pearson airport (YYZ) in Toronto,

Canada. All interference readings were taken with a handheld spectrum analyzer (HSA 9101, Willtek, Parsippany, NJ) at three different UHF frequencies: 433MHz, 915MHz and 2.45GHz. Each frequency was measured using a specific receiving antenna, as detailed in Table 3-1. Signal data were adjusted to account for receiving antenna gain. In other words, readings at 915MHz were lowered by 2.5dBm and readings at 2.45GHz were lowered by 8dBm.

All interference data are in dBm and the range considered for each frequency is in accordance with the Federal Communication Commission part 15 regulations (FCC, 2008). For 433MHz, the range of device operation is between 433.5 and 434.5MHz; for 915MHz, the range is between 902 and 928MHz; and for 2.45GHz, the range is from 2.435 to 2.465GHz.

Export: All freight arrives at the cargo facility either as bulk or as shipper loaded unit devices (SLUD), which can be air containers or pallets, pre-loaded by the customer. The freight gets weighed and dimensioned by the acceptance agent and stored at the appropriate location depending on its flying time and destination. If items are bulk, they ultimately go to the build-up area to be put in a ULD (pallet or container) or are transported in a tub cart directly to the airplane if this airplane is bulk loaded. ULDs are transported onto roller systems or forklifts through the cargo facility, after which they are carried out to the ramp onto trailers.

Import: ULDs are transported between the aircraft and cargo facility on special trailers pulled in a train by small tractor vehicles. Bulk items are unloaded from the aircraft directly into tub carts. Everything is brought back to the cargo warehouse and is broken-down when needed and stored until customer pick-up.

Montreal Warehouse

This location is in a very new building (constructed in 2008) and covers an area of 16,300m^2. Figure 3-1 presents the layout of the warehouse, including most activity areas (export, import, storage, build-up, break down, airside and landside). Interference reading points are circled on the layout and correspond to the following areas:

- Office area
- Export landside, near unloading dock doors
- Breezeway, export airside, near doors
- Breezeway, import airside, near doors
- Center of warehouse, between import and export; pallet break-down and build-up area; and storage
- Import landside, near loading dock doors

Toronto Warehouse

This location is slightly older building, built in 2002, and covers an area of 26,700m^2, which is more than 60% bigger than the Montreal warehouse. Figure 3-2 presents the layout of the warehouse, including most activity areas (export, import, storage, build-up, break down, airside and landside). Interference reading points are circled on the layout and correspond to the following areas:

- Import landside, near loading dock doors
- Office area
- Export landside, near unloading dock doors
- Build-up area
- Center of warehouse, between import and export
- Break-down of imported ULDs
- Breezeway, import airside
- Middle of breezeway
- Breezeway, export airside

Results and Discussion

As stated earlier, frequency ranges are as follows: 433.5 to 434.5MHz; 902 to 928MHz; and 2.435 to 2.465GHz. Table 3-2 and 3-3 show minimum and maximum

electromagnetic signal levels recorded inside these ranges for Montreal and Toronto respectively. The “maximum” data point is the worst interference level recorded in the area (Table 3-2 and 3-3). The “minimum” data is only present to show a comparison base for peak signal identification. It represents the sensitivity of the spectrum analyzer. When minimum and maximum data points are similar for a single location, it can be concluded that no “peak” is present and therefore no specific interference was observed above noise floor.

433MHz

Around 433MHz, the study did not show any important signal peaks that could interfere with an RFID system operating in this range. The average minimum background noise is -107.3dBm and the maximum signal level recorded is -103.7dBm in Montreal for position 1 and 3 (Table 3-2); and -89.8dBm in Toronto, position 4 (Table 3-3). Figure 3-4 shows the spectrum analyzer graphs for 433MHz in Toronto, position 4. Only one graph per frequency has been chosen as illustration, which represents the worst case scenario recorded within all locations and positions at that frequency. According to the National Telecommunications & Information Administration (NTIA, 2003, 2010) the small signal peaks visible around 433MHz (Figure 3-4) corresponds to “RADIOLOCATION and Amateur” (Capital letters are primary activity and lower cases are secondary) in the range of 420-450MHz.

The ISM range 433.05–434.79MHz can be heavily occupied by a wide range of ISM applications. In addition to backscatter (RFID) systems, baby intercoms, telemetry transmitters (including those for domestic applications, e.g. wireless external thermometers), cordless headphones, unregistered LPD walkie-talkies for short range radio, keyless entry systems (handheld transmitters for vehicle central locking) and

many other applications are crammed into this frequency range. Unfortunately, mutual interference between the wide range of ISM applications is not uncommon at this frequency (Finkenzeller, 2003). However, as far as the results found in this experiment are concerned, the very minimal peak recorded as the worst case scenario does not cover the entire band and is not present at a high power level. It is in fact lower than reader sensitivity of RFID readers designed three years ago. Therefore, it would be safe to say that the level of interference recorded would not significantly affect the performance of an RFID system.

915MHz

As shown in Figure 3-5, there is very low activity within the 902-928MHz range in the Toronto warehouse, which represents again the worst case scenario recorded. The maximum signal level recorded was -99.8dBm for Montreal and -92.2dBm for Toronto, whereas the average minimum is -109.5dBm (Table 3-2 and 3-3). As explained earlier, this level of noise could possibly only interfere with state of the art readers that have sensitivities below -90dBm and are being used at their maximum capacity (maximum range which allows for successful communication). In the event that this level of noise would not be blocked or filtered by the reader, it would still only interfere with tags that are further away from the reader, and require this much sensitivity to communicate. Typically, when the interference level is close to the reader sensitivity, it can only affect the tags that have communication links “power levels” between the interference noise and the receiver sensitivity. Moreover, systems working in that frequency range in North America use frequency hopping techniques; which means that the reader utilizes a slim portion of the band for a maximum of 0.4 seconds at a time. In other words, if the

interfering signal is only present on a small portion of the band, the likelihood of interference becomes lesser.

As seen in Figure 3-6, activity surrounding this band corresponds to (NTIA, 2003, 2010), where capital letters are primary activity:

- 851-894: FIXED + LAND MOBILE (GSM 850)
- 929-932: FIXED + LAND MOBILE
- 932-935: FIXED
- 935-940: FIXED + LAND MOBILE

Wireless applications that operate license-free in the 900 MHz ISM band include supervisory control and data acquisition, industrial automation, building automation and control, wireless sensor networks, and consumer devices such as cordless telephones, wireless speakers and baby monitors. In the U.S., most such systems utilize frequency hopping spread spectrum over 902-928MHz.

2.45GHz

Around 2.45GHz, the study shows much more activity that could interfere with an RFID system operating in this range (Figure 3-6). The maximum signal level recorded is -74.6dBm in Montreal for position 4; and -66.5dBm in Toronto for position 9, whereas the average minimum is -112.6dBm (Table 3-2 and 3-3). RFID readers working at this frequency have similar sensitivities as readers for 915MHz and frequency hop within the specified range. As mentioned earlier, frequency hopping only allows a small portion of the band to be used at a time; therefore if the interfering signal is only present on a portion of the band, the likelihood of interference becomes smaller. Signal level of around -66dBm is well above most reader sensitivity, which could cause unwanted interference in the event that those readers are not capable of filtering the interfering signal.

The signal peaks visible around 2.45GHz for Montreal (Figure 3-6) corresponds to (NTIA, 2003, 2010), where capital letters are primary activity and lower cases are secondary:

- 2417-2446: Amateur + radiolocation
- 2454-2472: FIXED + MOBILE + radiolocation

In the 2.4GHz ISM band there are several sources of interfering signals, including but not limited to: microwave ovens, baby monitors, wireless phones, wireless camera, Bluetooth enabled devices, WLANs, WIFI, and 2 way radios.

Conclusion

This study showed interference levels at three UHF frequencies recorded in two air cargo warehouses. The interference levels from highest to lowest were at 2.45GHz, 433MHz, and 915MHz respectively. Even in the case where interference is above a typical reader sensitivity, it is hard to say that these signals will or will not interfere with and RFID system since every system is designed differently. When the interference is on the edge of the spectrum, it is possible to reduce the used RF band in order to avoid such noise. When the interference is more towards the middle or across the entire band, RFID system design must take this into consideration to filter the noise out. RFID systems working at 915MHz and 2.45GHz use frequency hopping, therefore, when noise is only present on a certain part of the band, interference is also only encountered when the frequency is “hopping” on that part of the band, which should only create interference for a short period of time (depending on the percentage of the band covered by the interfering signal). This test was performed inside two warehouses, which may or may not give a realistic average representation of any air cargo warehouse in North America. But as far as these locations are concerned, it would be

safe to say that implementation of RFID systems at 915MHz or 433MHz would bring the best results, interference-wise.

Table 3-1. Receiving antenna specifications

Frequency	Polarization	Gain	Model & Manufacturer
433MHz	Linear (omni)	0dBi	B-368-1, How Tsen Intl. Electronics Metal Co.,Ltd. Shin Wu Hsiang, Tao Yuan Hsien, Taiwan
915MHz	Linear (omni)	2.5dBi	EXR902TN, Laird Technologies, Schaumburg, IL
2.45GHz	Linear (omni)	8dBi	MRN-24008SM3, AntennaWorld, Miami, FL

Table 3-2. Minimum and maximum interference readings (in dBm) for six positions and three frequencies at the Montreal warehouse.

Frequency (MHz)	Position in the warehouse											
	1		2		3		4		5		6	
	min	max	min	max	min	max	min	max	min	max	min	max
433	-107.3	-103.7	-107.8	-103.8	-106.6	-103.7	-106.7	-104.4	-108	-104.5	-108.1	-105
915	-109.8	-103.8	-109.8	-100.0	-109.0	-101.9	-109.0	-99.8	-108.6	-100.4	-108.6	-105.9
2450	-113.7	-82.9	-113.9	-79.3	-113.1	-76.1	-112.6	-74.6	-112.4	-82.0	-113.7	-88.7

Table 3-3. Minimum and maximum interference readings (in dBm) for nine positions and three frequencies at the Toronto warehouse.

Frequency (MHz)	Position in the warehouse									
	1		2		3		4		5	
	min	max	min	max	min	max	min	max	min	max
433	-106.6	-103.9	-106.4	-104.2	-107.1	-103.8	-107.4	-89.8	-106.7	-104.5
915	-110.5	-99.9	-110.1	-103.7	-108.9	-95.9	-110.1	-98.1	-110.5	-94.4
2450	-112.0	-90.0	-111.8	-91.3	-112.1	-86.5	-112.4	-76.1	-112.0	-80.5

Table 3-3. Continued.

Frequency (MHz)	Position in the warehouse							
	6		7		8		9	
	min	max	min	max	min	max	min	max
433	-107.8	-104.2	-107.2	-105.3	-107.3	-101.8	-108.2	-103.9
915	-109	-98.4	-110.1	-102.2	-110.1	-92.2	-108.9	-93.4
2450	-112.1	-90.1	-112.4	-69.4	-112.5	-71.6	-112.5	-66.5

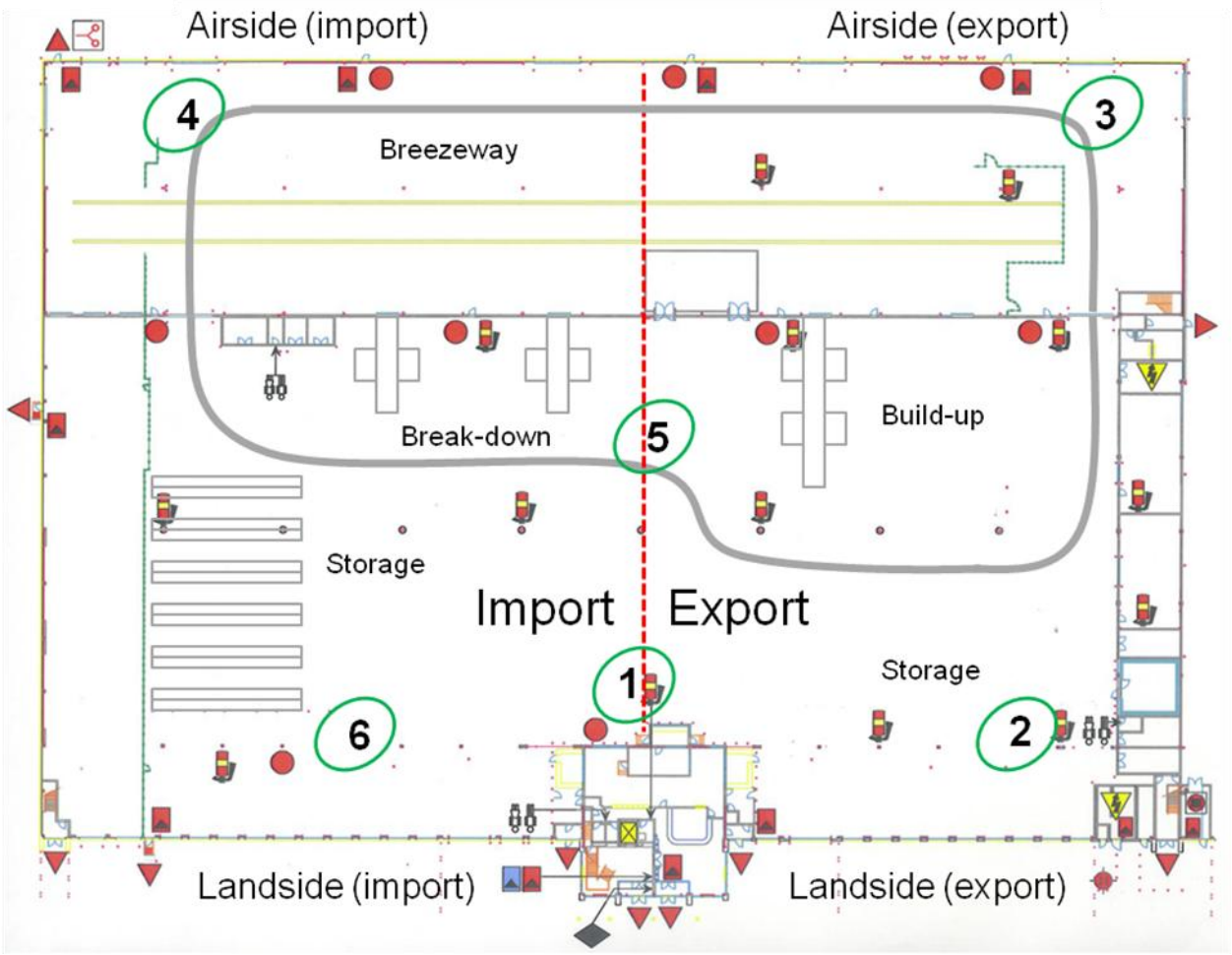

Figure 3-1. Montreal cargo warehouse facility floor plan and interference reading points (numbered 1 to 6).

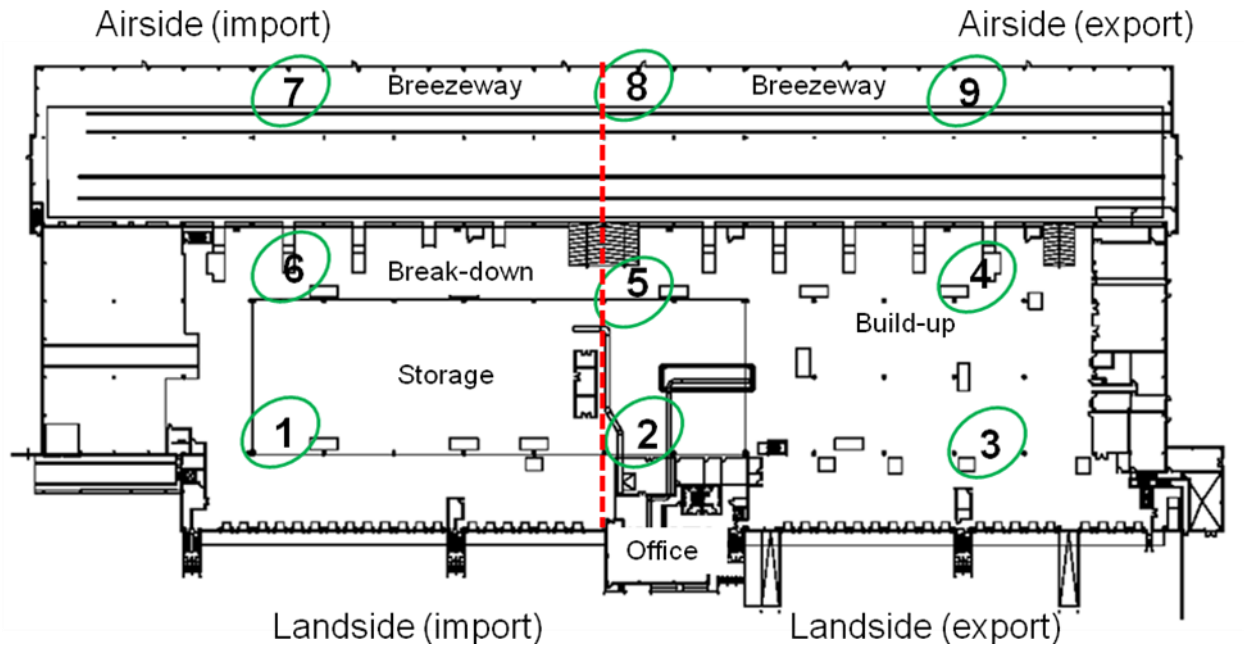

Figure 3-2. Toronto cargo warehouse facility floor plan and interference reading points (numbered 1 to 9).

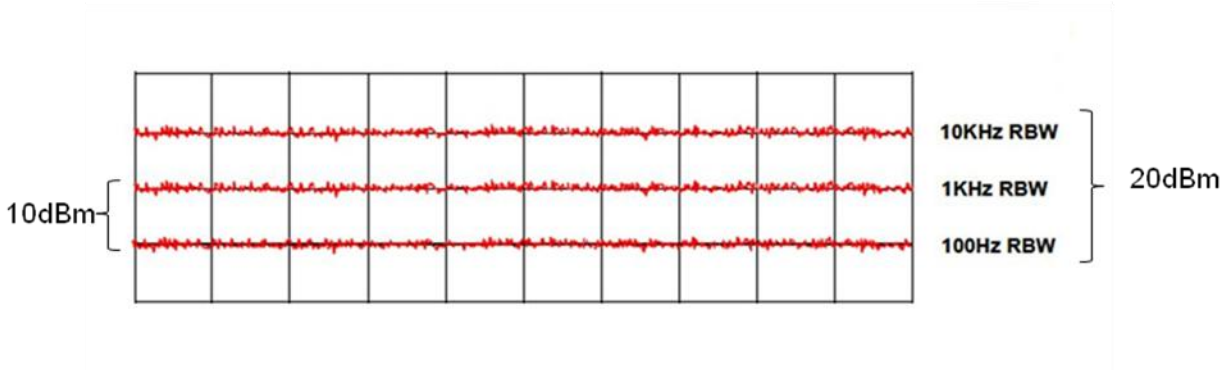

Figure 3-3. Noise floor of spectrum analyzer at three different resolution bandwidths.

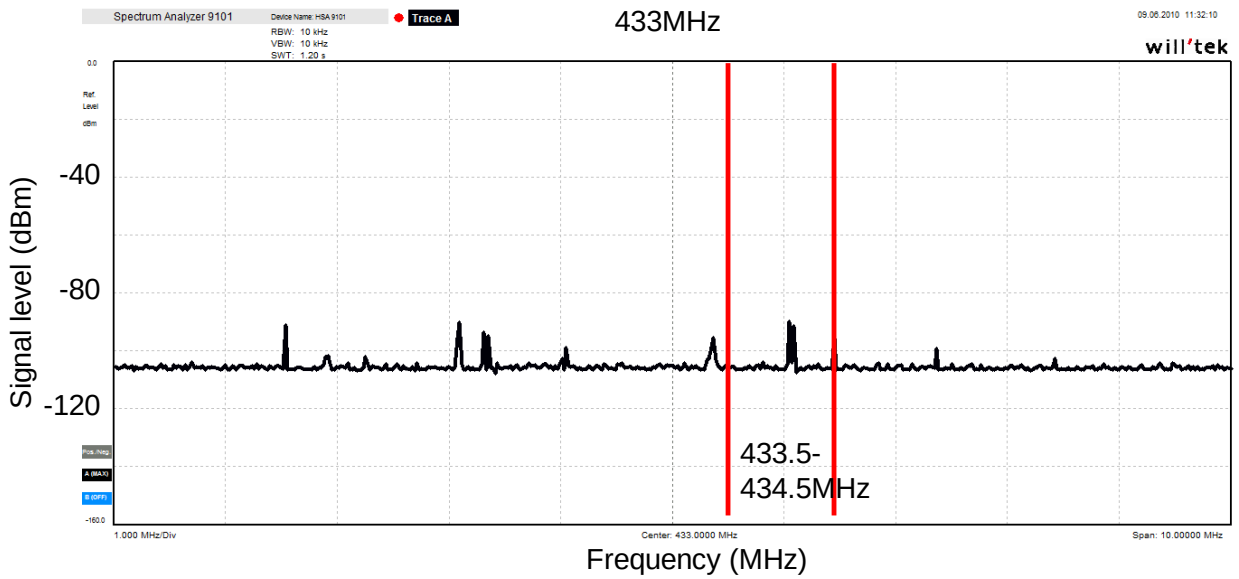

Figure 3-4. Worst case scenario for signal interference readings around 433MHz (Toronto, position 4). Span: 10MHz, RBW: 10kHz, attenuation: 0dB, gain: 0dBi.

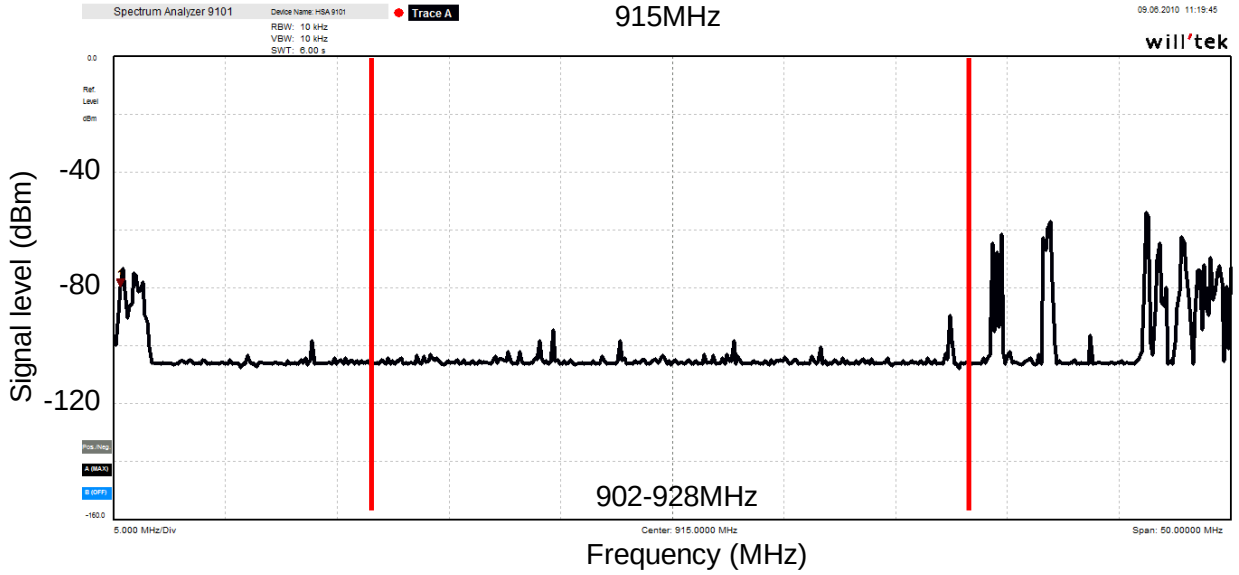

Figure 3-5. Worst case scenario for signal interference readings around 915MHz (Toronto, position 8). Span: 50MHz, RBW: 10kHz, attenuation: 0dB, gain: 2.5dBi.

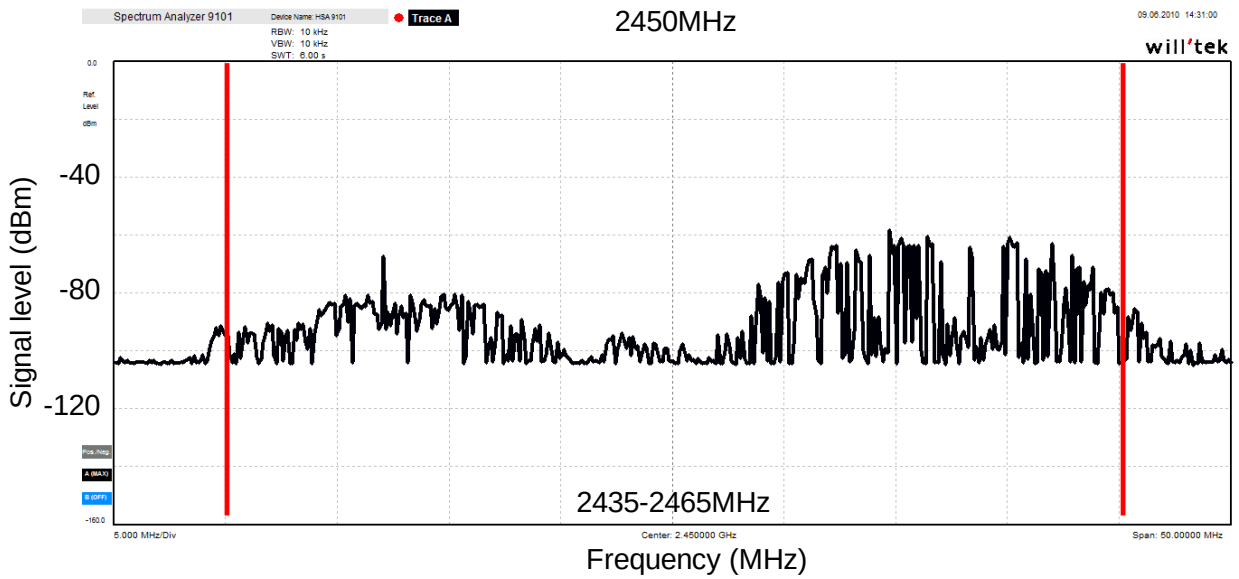

Figure 3-6. Worst case scenario for signal interference readings around 2450MHz (Toronto, position 9). Span: 50MHz, RBW: 10kHz, attenuation: 0dB, gain: 8dBi.

CHAPTER 4
RADIO FREQUENCY PROPAGATION INSIDE THE CARGO HOLD OF A DC-10 AIRCRAFT

Introduction

New technologies to better track cargo shipments are responsible for maintaining improved control and tracking along the supply chain. Both global positioning system (GPS) and radio frequency identification (RFID) technologies are emerging technologies for improving the tracking of air cargo in the supply chain (Elias, 2007). Within that supply chain, there is a definite weak point during air transit. Therefore, there is a growing interest to know which cargo is on board, where it is in the cargo hold and what some variables such as its temperature, humidity, acceleration, etc, are. (Schmoetzer, 2005). With air freight increasing rapidly; just-in-time delivery being a real challenge; customers and insurance providers want to know what happens to their shipment (liability issue) and forwarders need to increase the monitoring of goods. Improvements may be feasible for temperature sensitive goods, hazardous materials and high value cargo, and such monitoring requires communication between the container and the aircraft (Schmoetzer, 2005). If RFID readers are installed in the aircraft, they can interrogate the cargo, acquire data from dedicated goods, enhance the monitoring, set off warnings, etc. Therefore, automated onboard identification of cargo can contribute to enhanced security (Schmoetzer, 2005).

RFID airworthiness policy. The current Federal Aviation Administration (FAA) RFID policy document is AC20-162 “Airworthiness approval and operational allowance of RFID systems” (FAA, 2008). It incorporates and supersedes jointly-issued AIR-100, AFS-200 and AFS-300 RFID policy. This advisory circular offers guidance on installing and using RFID systems on aviation products and equipment. Specifically, it provides

an acceptable way to use RFID readers or interrogators installed on aircraft, and advice on allowing use of RFID devices on baggage, mail containers, cargo devices and galley or service carts. It also covers using portable RFID readers or interrogators carried onboard aircraft. The FAA airworthiness concerns about RFID systems installed on aircraft include:

- Integrity, accuracy, and authenticity of both safety-related and identification data from RFID devices
- Fire and electrical safety, crashworthiness, and environmental effects
- RFID device-generated RF intended transmissions or spurious emissions, both of which can interfere with aircraft electrical and electronic systems and components
- Maintenance required for RFID devices and readers

Therefore, some of the current requirements that passive and/or active RFID must meet are:

- Safety assessment
- Major alterations (if it might appreciably affect the aircraft's weight, balance, structural strength, performance, flight characteristics, or other qualities affecting airworthiness)
- Electromagnetic compatibility (EMC) demonstration (for active RFID and readers)
- Battery safety (for active RFID)
- Flammability and fire safety
- Mounting and attachment integrity
- Instructions for continued airworthiness (documentation)

This advisory circular is not mandatory and does not constitute a regulation. It describes an acceptable (though not the only) means, to show compliance with installation and operational requirements. Through this document, the FAA does not prohibit any use of RFID devices, instead it provides specific requirements that the equipment must meet to be safe and airworthy.

RF Propagation. While previous research (Rappaport and McGillem, 1989; Valenzuela et al., 1997; Mayer et al., 2006) documents indoor propagation of radio waves, very little work (Laniel et al., 2009) specializes on RF behavior inside a metal

environment. In contrast, the behavior of radio frequency around metal has been studied extensively (Dobkin and Weigand, 2005; Griffin et al., 2006; Prothro et al., 2006; Sydanheimo et al., 2006). Because aluminum is a very good conductor, incident electromagnetic wave totally reflects from the metallic surface with a phase reversal (Cheng, 1993; Reitz et al., 1993). Such materials are generally referred to as being “RF-opaque”. Moreover, metallic surface of the object in the vicinity of an antenna changes its radiation pattern, input impedance, radiation efficiency and resonant frequency. These changes depend on the size and shape of the metallic object and also on the distance of the antenna from the object (Raumonen, 2003; Mo and Zhang, 2007). Mo and Zhang (2007) also demonstrated that RFID tags placed 1/4 wavelength away from the metallic surface enhances the readability of the tags. On the other hand, little or no reflection occurs when electromagnetic waves penetrate directly through objects such as paper, non conductive plastics or textiles (Penttilä et al., 2006). These materials, including most composites, are non-absorbing and possess low refractive indexes. Such materials are generally referred to as being “RF-lucent”.

Aircraft. Whether it is inside the cargo hold or the cabin, RFID installed inside an aircraft would encounter a lot of metal in its environment. The entire fuselage of most aircrafts is made of aluminum alloy. Even if the use of composite materials is continuously growing and that big steps forward have been reached on the newest aircrafts, the material distribution on an aircraft structure predominantly remains aluminum based alloys. For example, only a mere three to four percent of the original Airbus A300 was made of composites, but they now account for 25% of the A380 structural weight and will account for more than 50% on the future A350 (Airbus, 2009).

The shape of the metal enclosure is not only cylindrical, but also has many cross beams as shown in Figure 4-1 which creates a very uneven reflective surface. This metal environment leads to highly unpredictable RF propagation behavior.

DC-10-30F. According to Boeing (2010c), the multi-range DC-10 was designed and built in Long Beach, California, by Douglas Aircraft Company, now the Long Beach Division of Boeing Commercial Airplanes. Production was started in January 1968 and extended to 1989, where 386 commercial DC-10s were delivered. The DC-10 Series 30F, an all-freighter model, was ordered by Federal Express in May 1984. This pure freighter version carries palletized payloads of up to 79,380kg on more than 6,115km. This is the model used for study in this chapter (Figure 4-2).

RFID is becoming more and more accepted for air cargo applications. Moreover, RF propagation inside aircrafts is not well documented. As a result, the objective of this study is to evaluate the RF propagation behavior inside the cargo hold of a wide body aircraft (DC-10-30F) at different frequencies.

Materials and Methods

Three radio frequencies (433MHz, 915MHz and 2.45GHz) were tested inside the forward lower cargo hold of a DC-10-30 freighter aircraft (Figure 4-3). The aircraft cargo door was kept open during the entire testing period, which simulates loading or unloading environment. Each frequency was generated by either an RFID reader or an RF transmitter (Table 4-1). Each RF system was connected to its respective set of antennas as described in Table 4-1. The RF systems were installed inside the cargo hold and the corresponding emitting antenna, connected via cable, was positioned either at the front of the cargo hold (top end), or in the center of the ceiling (Figure 4-4). Only one frequency and one antenna position was tested at a time. The only thing

present inside the cargo hold during testing was the RF testing equipment and one person, who was standing on the step just outside the cargo door while operating the spectrum analyzer. Details of the cargo hold and cargo door dimensions can be seen in appendix A.

Test 1: Propagation Study

Signal strength data was measured in dBm (power level in decibels relative to 1 mW) via a spectrum analyzer (RSA3303B, Tektronix, Beaverton, OR) connected to the appropriate RF receiving antenna (Table 4-1) and a 50m long LMR-400 low-loss cable. The receiver antenna was mounted on a plastic tripod, which was moved every meter along the length of the cargo hold at three different height and three different width positions. This created a 3x3x12 signal strength data grid for each frequency, antenna position and antenna type tested (Figure 4-5). The definition of a data point in this experiment is a 200 sample “max hold” of the peak signal power observed at each tested frequency.

Data analysis

All raw data was acquired via the spectrum analyzer in terms of signal strength measured in dBm. Radio frequencies being tested were chosen from commercially available products which have to obey RF spectrum regulations. In the United States, Federal Communications Commission (FCC) regulates operating frequencies and their respective maximum allowed output power (MAOP). Since all three systems do not use the same output powers, antennas, connectors and cables, a calculation had to be done to allow comparison of the systems. Link budget analysis (Shahidi, 1995; Clampitt, 2006) takes into consideration transmitter output power (P_t), measured signal strength

(P_r), transmitter antenna gain (G_t), receiver antenna gain (G_r), and various system losses such as connectors, adapters and cables (L_{sys}).

RF propagation and link budget analysis

Radio signal propagation can be analyzed with various models, one of the fundamental RF propagation equations is known as Friis transmission equation (Friss, 1946), which models line of sight propagation in free space as follow:

$$\frac{P_r}{P_t} = G_t G_r \left(\frac{\lambda}{4\pi R}\right)^2 \quad (4\text{-}1)$$

P_r: Measured signal strength
P_t: Transmitter output power
G_t: Transmitter antenna gain
G_r: Receiver antenna gain
R: Distance of the receiver antenna to the transmitter
λ: Wavelength

Wavelength is equal to the speed of light ($3x10^8$m/s) over the frequency (in Hz).

Therefore, λ_0 (433MHz) = 0.692m; λ_0 (915MHz) = 0.327m; λ_0 (2.45GHz) = 0.125m.

According to Friss propagation model (Eq. 4-1), Free Space Path Loss can be calculated as (in dB, using Log base 10);

$$PL_{Free\ Space} = 20Log\frac{4\pi R}{\lambda} \quad (4\text{-}2)$$

Equation 4-2 shows that received power is equal to the power flow through the effective area of the receiving antenna which is also related to the wavelength and the distance (Friis, 1946). This model (Eq. 4-2) does not account for reflections that are caused by the high metallic environment inside the cargo hold. A better path loss (PL) model (Nikitin and Rao, 2006) would be;

$$PL = \left(\frac{\lambda}{4\pi d}\right)^2 \left|1 + \sum_{n=1}^{N} \Gamma_n \frac{d}{d_n} e^{-jk(d_n - d)}\right|^2 \quad (4\text{-}3)$$

d: length of the direct ray path
Γ_n: reflection coefficient of the n[th] reflecting object
d_n: length of the n[th] reflected ray path
N: total number of reflections

It can be seen from equation 4-3 that reflections have an important impact on path loss calculations. The effects of reflection inside a metal environment was not added to the link budget calculation but was instead being considered as attenuation. So far the propagation model can be improved as follows:

$$P_r = P_t + G_t + G_r - PL - L_{sys} \ (dB) \quad (4\text{-}4)$$

Where L_{sys} are the system losses due to connectors, adapters and cables. Those losses were measured in the lab using an RF signal generator and spectrum analyzer. In this research attenuation is more specifically defined as path loss and other losses that are not taken into consideration such as; loss due to pointing error, atmospheric loss, polarization loss and path loss.

$$Attenuation = P_t - P_r + G_t + G_r - L_{sys} = P_{sys} - P_r \quad (4\text{-}5)$$

P_{sys} is the system's total output power. Signal strength data was put in equation 4-5 to calculate the attenuation. Values of each parameter and calculated attenuation (Eq. 4-5) are shown in Table 4-2. These new attenuation equations were then used to compare results between each test. Data obtained generated a 3-D map of signal attenuation. Full observation of the data can be seen in 12 vertical slices, as shown in the result section in Figures 4-7 to 4-14 or in more details in Appendix B.

Link budget analysis also allows comparing data in terms of signal strength. This is useful to evaluate the relationship between signal strength and tag reads. To be able to compare each system to one another, it is optimal to offset the data to simulate the maximum allowed output power (MAOP). In the case of 915MHz and 2.45GHz, the systems used were commercially available readers that should follow FCC regulations, but lab testing still showed deviations. On the other hand, for 433MHz, the RF transmitter used did not have the capability to be set to the MAOP. FCC regulations are written for measured power at a specific range. Regulation for operation in the band 433.5-434.5 MHz states (FCC, 2008):

> "The field strength of any emissions radiated within the specified frequency band shall not exceed 11,000 microvolts per meter measured at a distance of 3 meters."

Regulation for operation in the bands 902-928 MHz and 2400-2483.5 MHz states:

> "For frequency hopping systems operating in the 2400-2483.5 MHz band employing at least 75 non-overlapping hopping channels: 1 watt. For frequency hopping systems operating in the 902-928 MHz band: 1 watt (for systems employing at least 50 hopping channels). The conducted output power limit specified in this section is based on the use of antennas with directional gains that do not exceed 6 dBi."

The following calculation provides the MAOP for each frequency based on the above FCC regulations.

$$PD = \frac{PtGt}{4\pi r^2} = \frac{E^2}{\mu o} \tag{4-6}$$

In equation (4-6), *PD* is the power density, *E* is the electric field strength and μ_o (impedance of free space) $= 377\Omega$. The equation can be re-written as:

$$Pt\ Gt = \frac{E^2 r^2}{30} = 0.3\ E^2 \text{ (at r = 3m)} \tag{4-7}$$

The attenuation loss (*Al*) comes from $\log_{10}$ the received power (*Pr*) equation:

$$Pr = Pt\ Gt\ Gr\ Al \quad \text{where} \quad Al = \frac{\lambda^2}{(4\pi r)^2} \tag{4-8}$$

Therefore for 433MHz, since the maximum allowed output power measured at 3m is 11mV/m (using log base 10),

$$Pt\ Gt\ (at\ 3m) = 0.3\ (0.011)^2 = 36.3 * 10^{-6}\ W = 0.0363\ mW$$

$$10\log(0.0363) = -14.4\ dBm$$

$$Al = \frac{\lambda^2}{(4\pi r)^2} = 3.35 * 10^{-4}\ W = 0.000335\ mW$$

$$10\log(0.000335) = -34.8\ dBm$$

$$MAOP\ (at\ reader) = -14.4 - (-34.8) = 20.4\ dBm$$

For 915MHz and 2.45GHz, the limit for 1W at the reader corresponds to 30dBm, plus 6dBi antenna gain, therefore MAOP (at reader) is 36dBm. Each system's MAOP is shown in Table 4-2. The adjustment is the difference between the MAOP and each system's measured output power (P_{sys}). The adjustment was added or subtracted from the data set to mimic an optimal system and permit data comparison.

Statistical analysis

A mixed linear model was used to test the effect of frequency on attenuation. The main effect of location of the antenna (two antenna positions) was tested on attenuation levels for each frequency and antenna polarization; as well as the effect of antenna polarization (circular vs. linear) for each frequency and antenna location with a mixed analysis of variance (ANOVA) model (Littell and Milliken, 2006). The effects of width (three vertical slices), height (three horizontal slices), and depth (12 widthwise slices) of the receiving antenna was also tested on the attenuation level. A residual analysis was performed to check normality and homogeneity of variance (Ott and Longnecker, 2004).

All statistical analyses were computed using SAS 9.1 (SAS Institute Inc., Cary NC) and significance was accepted at level $\alpha = 0.01$. A more conservative level of acceptance was chosen due to the very large dataset (108 data points per test).

Test 2: Validation of Relation between Signal Strength and Tag Reads

In an ideal scenario, the measured power levels inside the cargo hold would directly indicate the probability of having successful tag-reader communication at a specific point. However, the cargo hold is far from being an ideal space in terms of wave propagation due to the fact that there is interference from metals inside the cargo hold as well as outside sources. Hence, another test was conducted as a proof-of-concept to show that the measured power levels correspond adequately with a real RFID system performance in terms of tag read rates.

Signal strength data acquired in Test 1 were used to compare tag readability at 915MHz using the “top end” position for circularly and linearly polarized antennas. Tag readability was tested using 29 AD-210 Gen 1 Class 1 tags (Avery Dennison, Flowery Branch, GA) and the ALR-9780 Gen1 915MHz reader (Alien Technology, Morgan Hill, CA). All tags were attached on a sheet of Tyvek® material which covered half of the cargo hold cross section as shown in Figure 4-6. The top of the sheet was taped to a cardboard tube which was held by a plastic tripod. The tripod’s front leg was set longer to allow the sheet to stand as vertical as possible. This set-up was moved every meter along the length of the cargo hold on one side (starboard or port), then it was pivoted (along the central axis of the aircraft) to the other side to gather the other half of the readability data. Data were acquired with the Alien software developer’s kit (Alien Technology, Morgan Hill, CA) installed on a laptop computer. Read rates obtained correspond to the number of reads per 30 seconds.

Data point comparison

Since the signal strength readings only provide 9 data points per cross section and the readability test uses 58 tags, the data obtained is averaged for each of the 12 slices. Figure 4-6 shows the location of the 29 tags on the Tyvek® sheet, which covers half of the cargo hold cross section. To obtain data on the other half of the cargo hold, the sheet pivots along the edge that is in the center of the compartment (Figure 4-6).

Results and Discussion

Test 1: Propagation Study

All raw data obtained inside the cargo hold (signal level in dBm) were offset by the amount calculated with the link budget as shown in Table 4-2 to permit comparison in terms of attenuation or signal strength. Comparison of raw measured signal was not appropriate since initial output power was different from one system to the other.

Attenuation

Attenuation levels for each frequency show how the RF signal fades or attenuates with distance. The attenuation levels observed from this experiment are shown in Figures 4-7 to 4-14. These graphs are color coded following the visible color spectrum, where red represents high attenuation (70dBm) and purple stands for low attenuation (30dBm). Detailed illustration of each slice is shown in Appendix B.

Comparison of all graphs makes it apparent that 433MHz suffers less attenuation than 915MHz, which also suffers less attenuation than 2.45MHz. As shown earlier in this chapter, lower frequencies have longer wavelengths, which tend to travel longer distances easier or suffer less path loss. From the graphs it can also be observed that signal variation is more present at lower frequencies than at higher ones. Standard

deviations for each test are shown in Table 4-3. Despite the higher attenuation, a more uniform dataset is observed at higher frequencies.

Effect of frequency on attenuation

Figure 4-15 shows a simple graph of the distribution of attenuation levels between frequencies for circular antenna tests only (and two antenna locations). Linear antenna testing were omitted from the comparison since, because of time constraint, there was no such test done at 433MHz. Figure 4-15 shows a proportional relationship between frequency and attenuation. In other words, lower frequencies lead to lower attenuation levels inside the cargo hold. Significant difference between frequencies was statistically tested with a mixed linear ANOVA model ($p < 0.0001$) (Appendix C, Table C-1).

Effect of antenna location and polarization on attenuation

The effect of antenna location as well as polarization on attenuation levels for all frequencies mixed up was tested. The results lead to highly significant differences with p-values <0.0001 (Appendix C, Table C-1). However, what is mostly important in reality is the significance of this effect for each frequency and location or polarization. This is explained in the following paragraphs.

Location. The main effect of location of the antenna (top end vs. ceiling) was tested on attenuation levels for each frequency and antenna polarization with a mixed linear model (Littell and Milliken, 2006). Table 4-4 shows statistical results for each test. None of which is significantly different at $\alpha = 0.01$ level.

Polarization. The effect of antenna polarization (circular vs. linear) on attenuation for each frequency and antenna location was tested with a mixed linear model (Littell and Milliken, 2006). Again, comparison of antenna polarization was not possible at

433MHz due to the lack of time to perform linear antenna testing on site. Statistical analysis, as shown in Table 4-5, demonstrates a significant difference between circular and linear polarization at 2.45GHz only. Although statistically different, the mean value of each test differs by 2.59dBm, which may or may not have a significant effect on an RFID system. This only depends on how close the signal level is to the sensitivity threshold of the tags.

Effect of width, height and depth on attenuation

The effect of width, height and depth on attenuation for each frequency, antenna location and antenna polarization was tested with a mixed linear model (Littell and Milliken, 2006).

Width. The effect of width was only significant at 2.45GHz for the top end antenna position and linear polarization (Appendix C, Table C-2). Statistical means were as follows: 62.60dBm (port), 58.39dBm (center) and 61.75dBm (starboard); with p-value <0.0001. Difference was significant between center and port as well as center and starboard. Port and starboard were statistically similar.

Height. The effect of height was only significant at 915MHz for the top end antenna position and linear polarization (Appendix C, Table C-3). Statistical means were as follows: 52.66dBm (high), 46.37dBm (middle) and 45.03dBm (low); with p-value <0.0001. Difference was significant between high and middle as well as high and low. Middle and low were statistically similar.

Depth. The effect of depth was significant in all cases except at 2.45GHz for the top end antenna position and linear polarization (Appendix C, Table C-4). It is interesting to see how antenna polarization affects wave propagation. Just like it is the

case for free space propagation, linear antennas have a longer, but narrower footprint (Dobkin, 2008). This can be observed here by the significant effect of width and height, combined with a non significant effect of depth for linear antenna tests only. In other words, RF signal from a linear antenna attenuates much faster as the receiver moves sideways from the antenna, than it does as the receiver moves away in front of the antenna. Although the width and height results were not significant for all linear antenna tests, p-values for linear polarization was lower than for circular polarization in all cases (Appendix C, Tables C-2 and C-3).

Signal strength

Signal strength comparison allows studying how an actual RFID system would behave if it was installed inside the cargo hold, which will be explained in better detail in test 2 later in this chapter. For this part of the test, the goal is to compare pure signal propagation for each test performed (three frequencies, two antenna positions and one or two antenna polarizations). As mentioned previously, the signal propagation data were offset by the amount calculated in the last column of Table 4-2 (adjustment), which brings the dataset to the maximum allowed output power as per FCC regulations. It is important to repeat that regulations for 433MHz are much more strict that those for 915MHz and 2.45GHz. Signal propagation for each test follows the same distribution as for attenuation since both datasets come from the same original data. However, results show a significantly higher signal level at 915MHz compared to the two other frequencies, with averages between -10dBm and -12dBm for 915MHz, compared to between -21dBm and -25dBm for the other two (Table 4-6). This is due to the fact that 915MHz and 2.45GHz start with higher power levels than 433MHz; however, as observed earlier, 915MHz has much lower attenuation levels than 2.45GHz. Therefore,

when following FCC regulations, more energy is available in the cargo hold at 915MHz. Graphical results of each slice can be seen in Appendix D.

Test 2: Validation of Relation between Signal Strength and Tag Reads

As previously mentioned, the purpose of this test is to show that there exists a relationship between the measured power levels by the spectrum analyzer and the tag read rate by a commercial reader. In an ideal scenario, the power levels would be directly proportional to read rates except irregularities such as saturation at very high power levels. However, the substantial existence of metals inside the cargo hold will result in antenna detuning, negatively affecting the read rates. In order to smooth out such effect, both the read rates and the power levels across the 58 tag reads and 9 signal data points are averaged for each of the 12 cross sectional planes along the cargo hold. This will help understand the relationship between the signal strength and read rates while approximating the proportionality between the two quantities.

Two different antennas; circular and linear, were used for the experiment with the same reader. The read rates and measured power levels across the 9 data points were averaged for each of the 12 cross sectional planes. In addition, for better comparison between the power levels and the read rates, each cross sectional power level and read rate average are normalized by the corresponding global averages. For instance, the global average for power levels in this study including both circular and linear antennas is -13.5dB whereas the global average for read rates across all dimensions and antenna types is 10.9. Hence, as Table 4-7 indicates, all the recorded values will be adjusted by the aforementioned averages for improved statistical representation. The first column in table 4-7 is explained as follows:

Pc: Average power levels for each cross sectional plane for the circular antenna in dB

Pc-adj.: Adjusted average power levels for each cross sectional plane for the circular antenna in dB (by -13.5dB)

Rc: Average read rates for each cross sectional plane for the circular antenna

Rc-adj.: Adjusted average read rates for each cross sectional plane for the circular antenna (by 10.9)

Pl: Average power levels for each cross sectional plane for the linear antenna in dB

Pl-adj.: Adjusted average power levels for each cross sectional plane for the linear antenna in dB (by -13.5dB)

Rl: Average read rates for each cross sectional plane for the linear antenna

Rl-adj.: Adjusted average read rates for each cross sectional plane for the linear antenna (by 10.9)

Table 4-7 shows that for the cross sections further from the emitting antenna, both the power level and the read rate averages decrease in general confirming the initial assumption that the two values are directly proportional to some extent. Furthermore, figure 4-16 shows the adjusted average power levels and read rates for both circular and linear antennas. In this figure, blue diamonds and red squares show the average power levels and read rates for circular and linear antennas respectively across 12 cross sectional planes. Solid lines show the best fitted curves via linear regression with the corresponding R-squared values. One can observe from this figure that there are points in the system where higher average power levels do not necessarily correspond to higher average read rates. Heavy concentration of metals around these points and the detuning properties of the metal could have caused such discrepancies as well as the relatively high number of tags being interrogated by the reader resulting in trafficking problems. Nonetheless, the general trends for either antenna as well as the R-squared values clearly show the direct proportionality between the two quantities.

Another useful observation is to look at the correlation coefficient between the adjusted power level and read rate curves for both circular and linear antennas. In the case of the circular antenna, $\rho_{circular} = 0.91$, whereas for the linear antenna $\rho_{linear} = 0.96$. Although both figures show a strong relationship between average power levels and read rates for either antenna, the relationship is stronger for the linear case. This is expected and can be explained by the fact that all the tags were carefully placed on the Tyvek® sheet in the best possible orientation with respect to the linear emitting antenna, which confirms the fact that linear antennas perform better in use case scenarios where tag orientation is known or controllable.

The results for both tests show that, even though there are many factors to be considered when estimating a commercial RFID reader performance in a given environment, measuring the signal strength at key locations in the application space would indicate the weak and strong points in the system. It is well-known that each system built by different manufacturers will have technical differences in terms of sensitivity, coding technology, etc. However, this experiment indicates that the power measurements explained in this chapter which include the three frequencies of 433MHz, 915MHz and 2.4GHz can all serve as a guideline when determining which system would perform better in terms of RFID tag read rates under the same circumstances and technical specifications.

Conclusion

This test demonstrated that frequencies have a major influence on signal propagation, especially inside a metal environment. Lower frequencies suffer less attenuation over distance, but have higher variation within the cargo hold. It was also shown that antenna location did not deliver significantly different results. However,

antenna polarization can have a significant effect on signal propagation in some cases, and therefore should not be omitted when designing an RFID system for air cargo transportation. Moreover, FCC regulations restrict output powers at 433MHz more than at 915MHz and 2.45GHz, which leads to the conclusion that more RF signal is available in the cargo hold at 915MHz. It was also demonstrated that the relationship between signal strength and tag reads is an important factor to take into account when considering the installation of an RFID system inside an application space with nonzero interference.

Table 4-1. Specifications of the three RF systems used.

Frequency	RF system	Antenna			
		Type	Polarization	Gain	Model & Manufacturer
433MHz	Chipcon CC1100 RF transmitter (Texas Instruments Inc., Dallas, TX)	Emitter	Circular	9dBi	SPA 430, Huber + Suhner AG, Essex, VT
		Receiver	Linear (omni)	0dBi	B-368-1, How Tsen Intl. Electronics Metal Co.,Ltd. Shin Wu Hsiang, Tao Yuan Hsien, Taiwan
915MHz	915 MHz Alien RFID reader ALR-9780 (Alien Technology, Morgan Hill, CA);	Emitter	Circular	6dBi	ALR-9610-BC, Alien Technology, Morgan Hill, CA
		Emitter	Linear	5.9dBi	ARL-9610-AL, Alien Technology, Morgan Hill, CA
		Receiver	Linear (omni)	2.5dBi	EXR902TN, Laird Technologies, Schaumburg, IL
2.45GHz	2.45 GHz Alien RFID reader ALB-2484 (Alien Technology, Morgan Hill, CA)	Emitter	Circular	6dBi	2AC-001, Alien Technology, Morgan Hill, CA
		Emitter	Linear	15dBi	Com-24015p, Antenna World, Miami, FL
		Receiver	Linear (omni)	8dBi	MRN-24008SM3, Antenna World, Miami, FL

Table 4-2. Calculated parameters for the attenuation equation (Eq. 4-5) and maximum allowed output power adjustment.

Systems	P_t (dBm)	G_t (dBi)	G_r (dBi)	L_{sys} (dBm)	Attenuation P_{sys} - P_r (dBm)	MAOP (dBm)	Adjustement for MAOP (dBm)
433MHz circular	10.34	9.0	0.0	2.50	16.85 – P_r	20.4	+3.55
915MHz circular	34.97	6.0	2.5	3.95	39.52 – P_r	36	- 3.52
915MHz linear	34.97	5.9	2.5	3.95	39.42 – P_r	36	-3.42
2.45GHz circular	32.24	6.0	8.0	7.26	38.99 – P_r	36	-2.99
2.45GHz linear	32.24	15.0	8.0	6.71	48.54 – P_r	36	-12.54

Table 4-3. Averages and standard deviations of attenuation levels for each test.

	433MHz		915MHz			2.45GHz		
	circular		circular		linear	circular		linear
	top end	ceiling	top end	ceiling	top end	top end	ceiling	top end
Average	44.20	44.17	48.00	46.91	48.02	58.32	58.79	60.91
Std dev.	4.75	4.72	3.53	3.39	5.72	3.19	3.06	4.16

Table 4-4. Statistical analysis results for the effect of antenna location.

Frequency	Polarization	Location	Mean	F value	p value
433MHz	Circular	Top End	41.70	0.00	0.9615
		Ceiling	41.67		
915MHz	Circular	Top End	48.00	5.27	0.0227
		Ceiling	46.91		
2.45GHz	Circular	Top End	58.32	1.20	0.2744
		Ceiling	58.79		

Table 4-5. Statistical analysis results for the effect of antenna polarization.

Frequency	Location	Polarization	Mean	F value	p value
433MHz	Top End	Circular	N/A	N/A	N/A
		Linear	N/A		
915MHz	Top End	Circular	48.00	0.00	0.9683
		Linear	48.02		
2.45GHz	Top End	Circular	58.32	26.34	< 0.0001
		Linear	60.91		

Table 4-6. Signal strength data for each test, averaged per vertical slice, and total cargo hold (Avg).

		433MHz		915MHz			2.45GHz		
Slices		circular		circular		linear	circular		linear
(m)		top end	ceiling	top end	ceiling	top end	top end	ceiling	top end
1	average per slice (dBm)	-16.2	-26.6	-7.6	-14.8	-6.2	-18.6	-24.0	-24.0
2		-18.6	-23.7	-9.5	-13.5	-8.5	-19.4	-23.6	-24.7
3		-17.3	-20.1	-10.0	-10.8	-8.9	-20.8	-22.6	-24.8
4		-19.3	-19.6	-10.5	-11.3	-9.0	-22.4	-21.6	-23.8
5		-18.8	-20.4	-11.2	-8.7	-9.4	-21.6	-20.3	-24.7
6		-21.9	-16.5	-11.7	-7.3	-11.3	-21.8	-18.8	-25.1
7		-23.1	-18.6	-11.9	-6.4	-13.1	-22.3	-19.9	-23.1
8		-22.9	-19.7	-12.7	-9.2	-13.6	-23.4	-22.4	-25.4
9		-24.0	-22.6	-12.3	-10.9	-16.0	-23.1	-23.2	-24.6
10		-23.1	-22.9	-15.0	-11.4	-15.6	-24.0	-25.2	-25.6
11		-23.8	-22.2	-16.7	-12.6	-16.5	-24.7	-25.8	-26.9
12		-26.7	-22.5	-14.9	-14.3	-15.9	-25.9	-26.1	-26.2
	avg	-21.3	-21.3	-12.0	-10.9	-12.0	-22.3	-22.8	-24.9

Table 4-7. Table summarizing the recorded and adjusted power levels (P) and read rates (R) for circular and linear antennas across the 12 cross sectional planes.

	Sectional planes											
	1	2	3	4	5	6	7	8	9	10	11	12
Pc	-10.6	-12.5	-13.0	-13.5	-14.2	-14.7	-14.9	-15.7	-15.3	-18.0	-19.7	-17.9
Pc-adj.	2.9	1.0	0.5	0.0	-0.7	-1.2	-1.4	-2.2	-1.8	-4.5	-6.2	-4.4
Rc	18.6	14.7	16.2	14.3	13.2	9.6	4.6	5.1	1.3	0.7	0.4	0.0
Rc-adj.	7.7	3.8	5.3	3.4	2.3	-1.3	-6.3	-5.8	-9.6	-10.2	-10.5	-10.9
Pl	-6.2	-8.5	-8.9	-9.0	-9.4	-11.3	-13.1	-13.6	-16.0	-15.6	-16.5	-15.9
Pl-adj.	7.3	5.0	4.6	4.5	4.1	2.2	0.4	-0.1	-2.5	-2.1	-3.0	-2.4
Rl	20.1	19.8	20.9	16.0	18.4	13.8	11.7	11.0	8.4	7.0	6.1	10.0
Rl-adj	9.2	8.9	10.0	5.1	7.5	2.9	0.8	0.1	-2.5	-3.9	-4.8	-0.9

Figure 4-1. Section of an aircraft fuselage (Airbus A380)

Figure 4-2. DC-10-30F from Arrow Cargo.

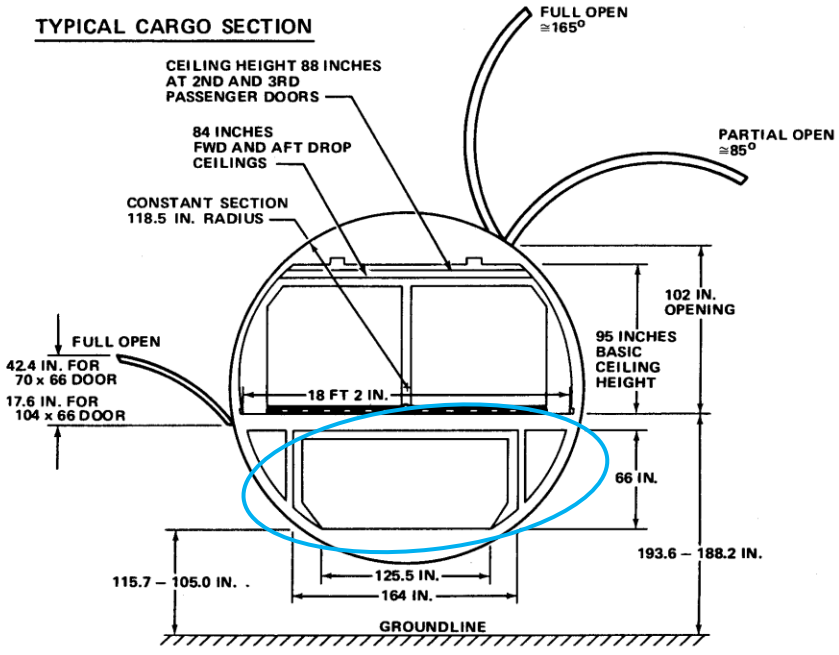

Figure 4-3. Typical fuselage section of a DC-10-30F, lower cargo hold circled in blue (Boeing, 2010c)

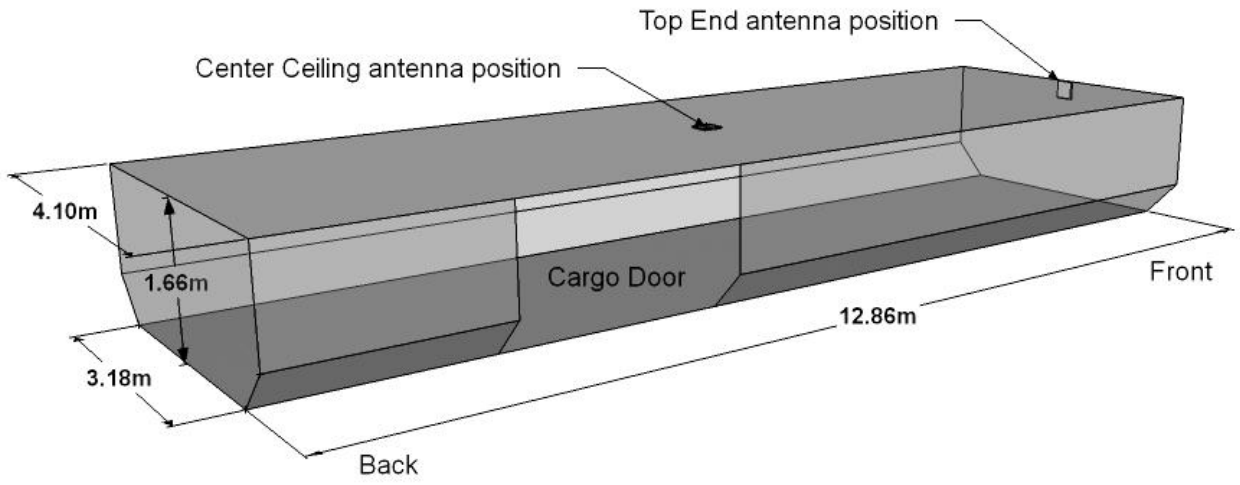

Figure 4-4. Cargo hold dimensions and RF emitting antenna positions.

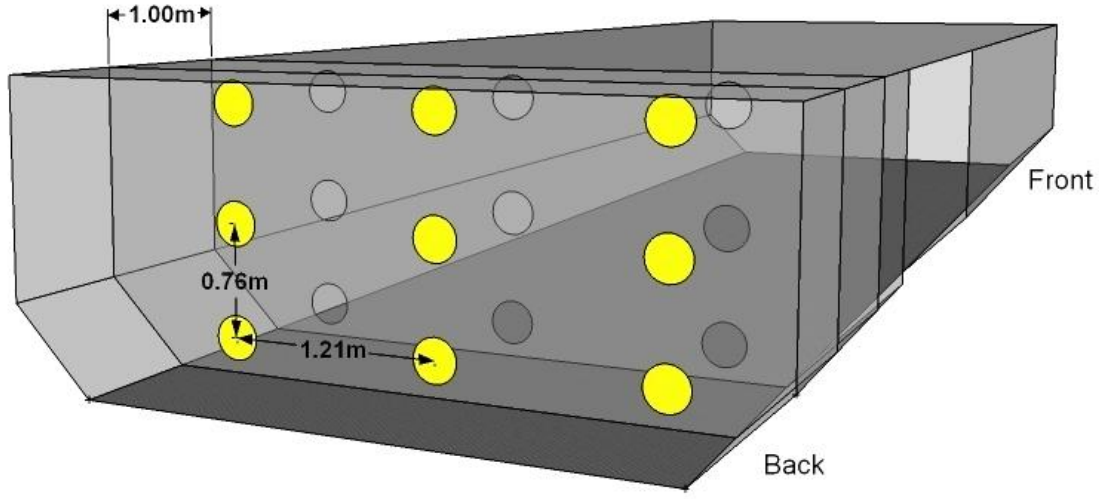

Figure 4-5. Data point positions in the 3x3 grid. Twelve 3x3 grids are measured long the length of the cargo hold, every meter.

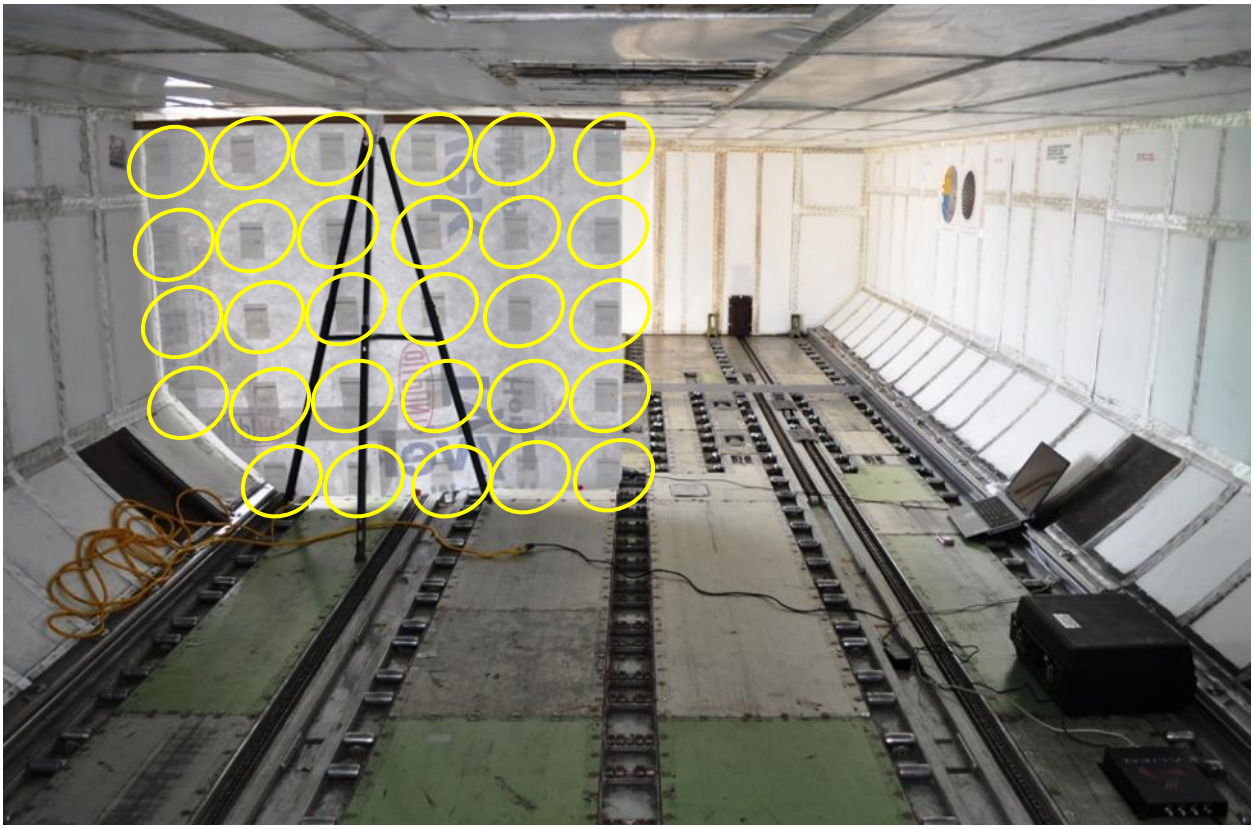

Figure 4-6. Tag readability test configuration. Tyvek® sheet with 29 RFID tags (circled) covering half of the cargo hold cross section.

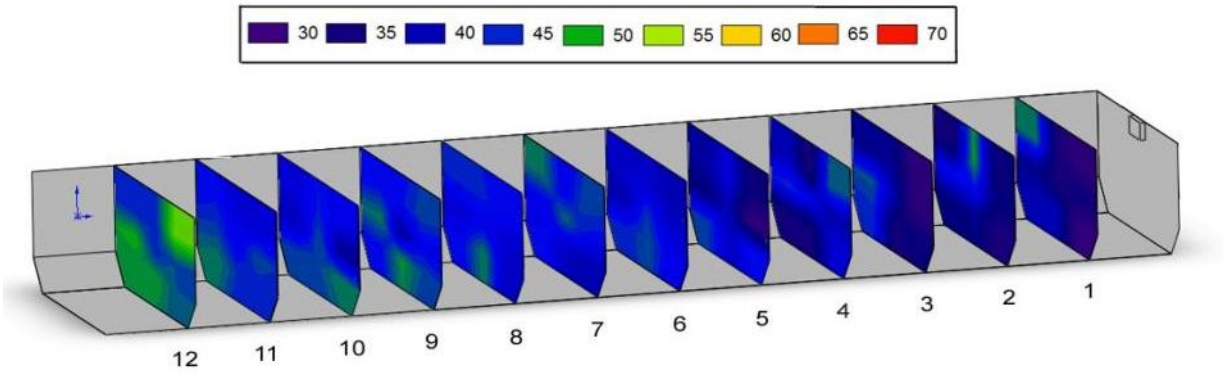

Figure 4-7. Attenuation surface plots for each vertical slice of 3x3 data point at 433MHz, circular antenna and top end antenna position.

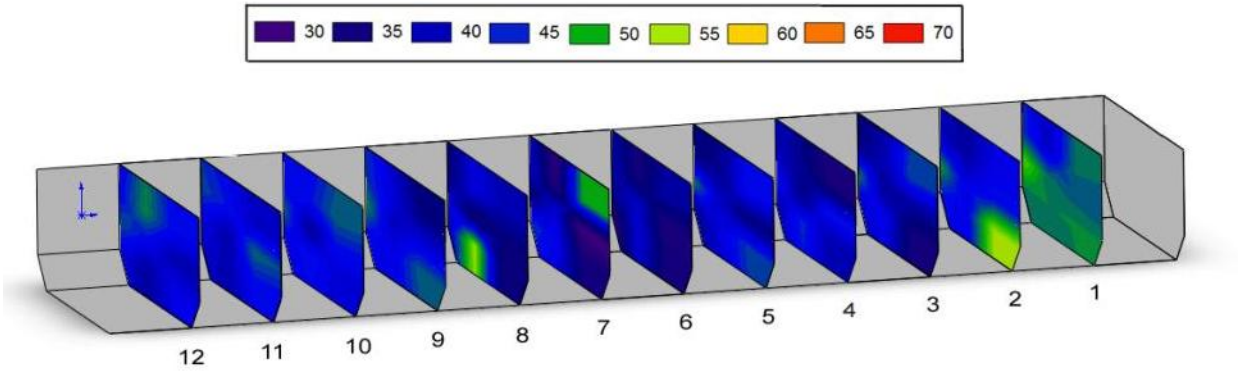

Figure 4-8. Attenuation surface plots for each vertical slice of 3x3 data point at 433MHz, circular antenna and center ceiling antenna position.

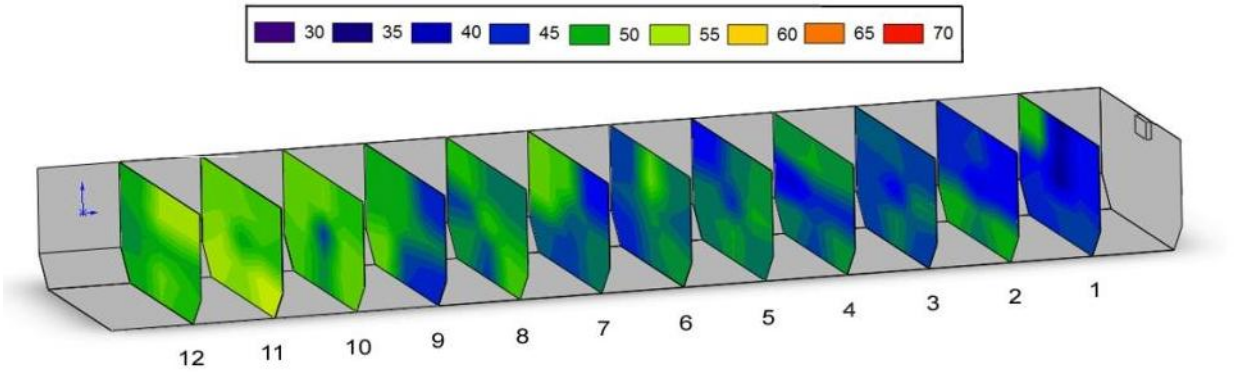

Figure 4-9. Attenuation surface plots for each vertical slice of 3x3 data point at 915MHz, circular antenna and top end antenna position.

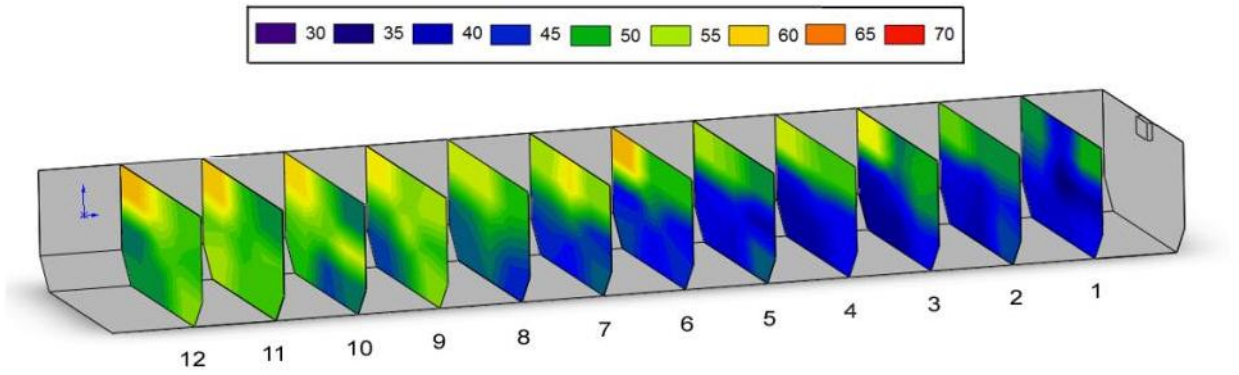

Figure 4-10. Attenuation surface plots for each vertical slice of 3x3 data point at 915MHz, linear antenna and top end antenna position.

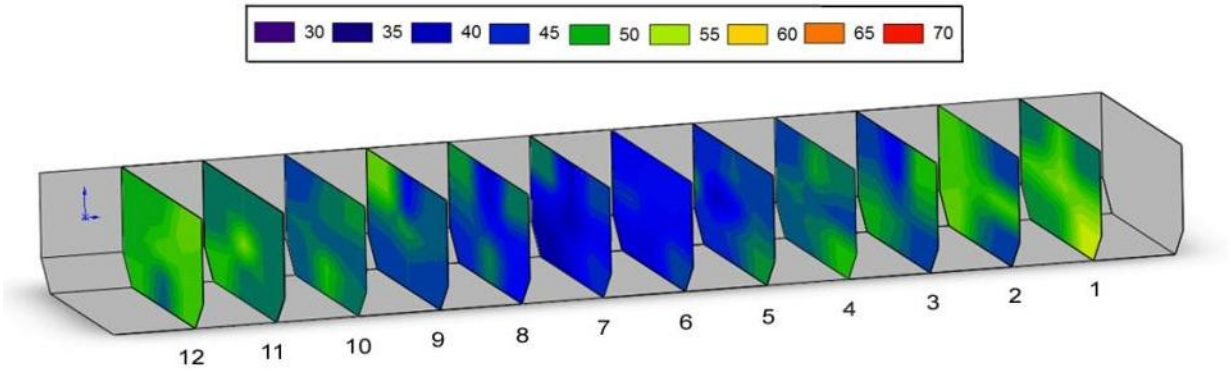

Figure 4-11. Attenuation surface plots for each vertical slice of 3x3 data point at 915MHz, circular antenna and center ceiling antenna position.

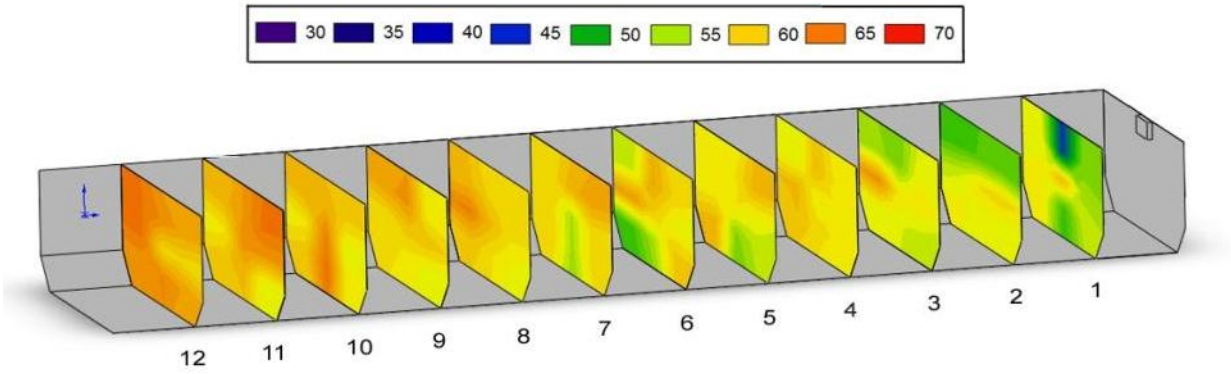

Figure 4-12. Attenuation surface plots for each vertical slice of 3x3 data point at 2.45GHz, circular antenna and top end antenna position.

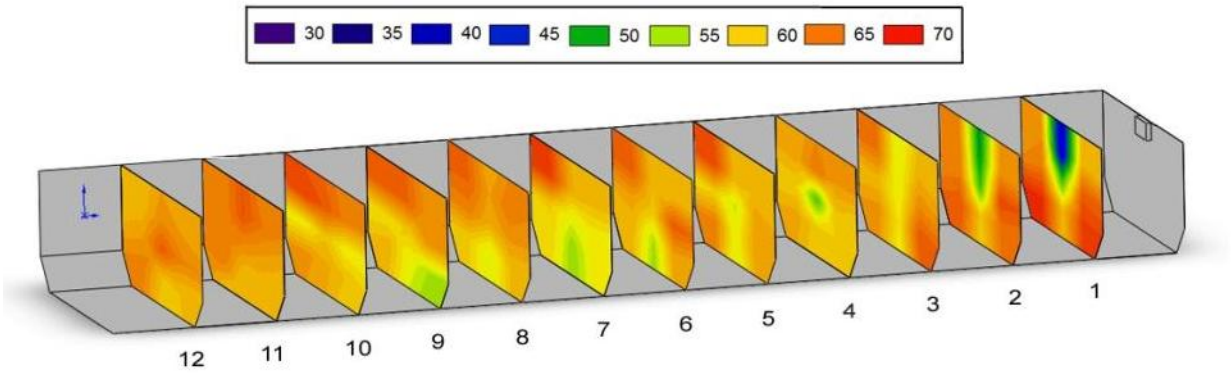

Figure 4-13. Attenuation surface plots for each vertical slice of 3x3 data point at 2.45GHz, linear antenna and top end antenna position.

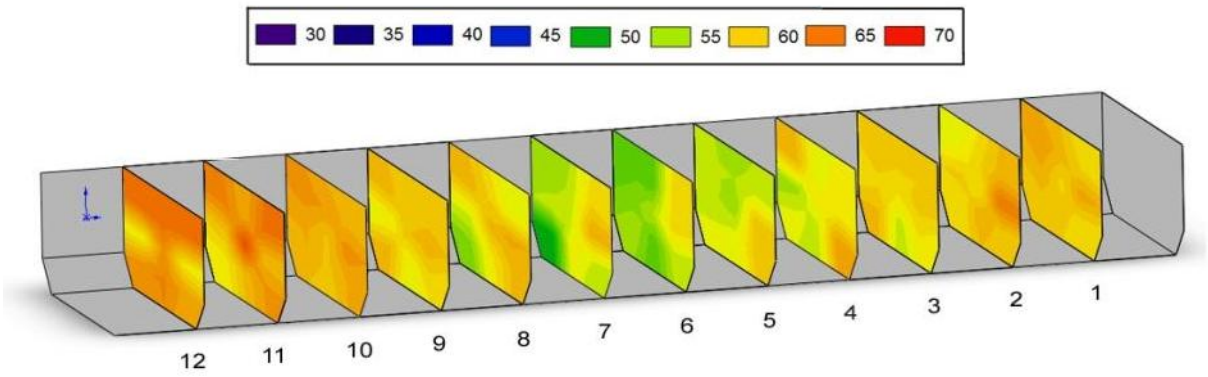

Figure 4-14. Attenuation surface plots for each vertical slice of 3x3 data point at 2.45GHz, circular antenna and center ceiling antenna position.

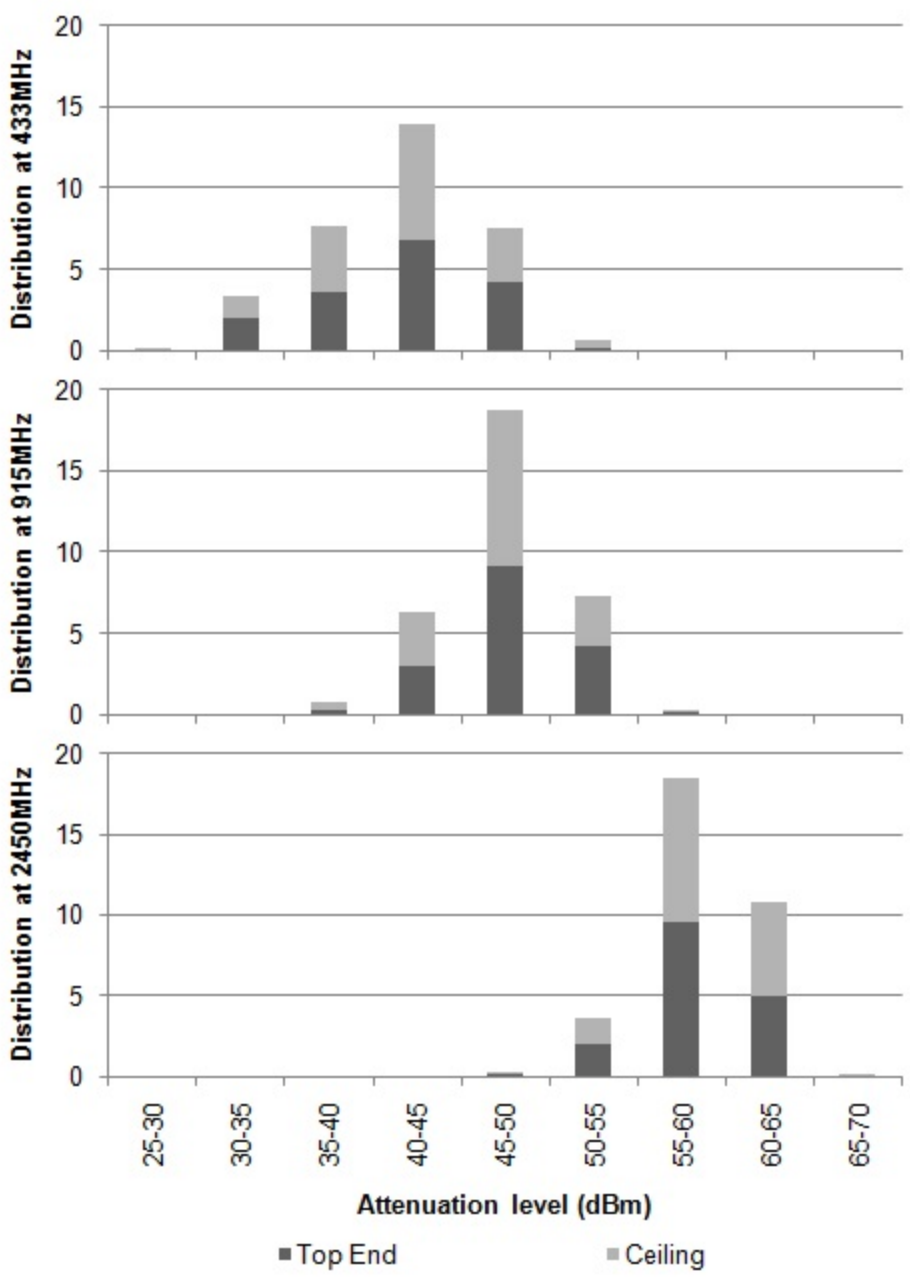

Figure 4-15. Distribution (in percentage) of each frequency tested, for circular antenna only and two antenna locations.

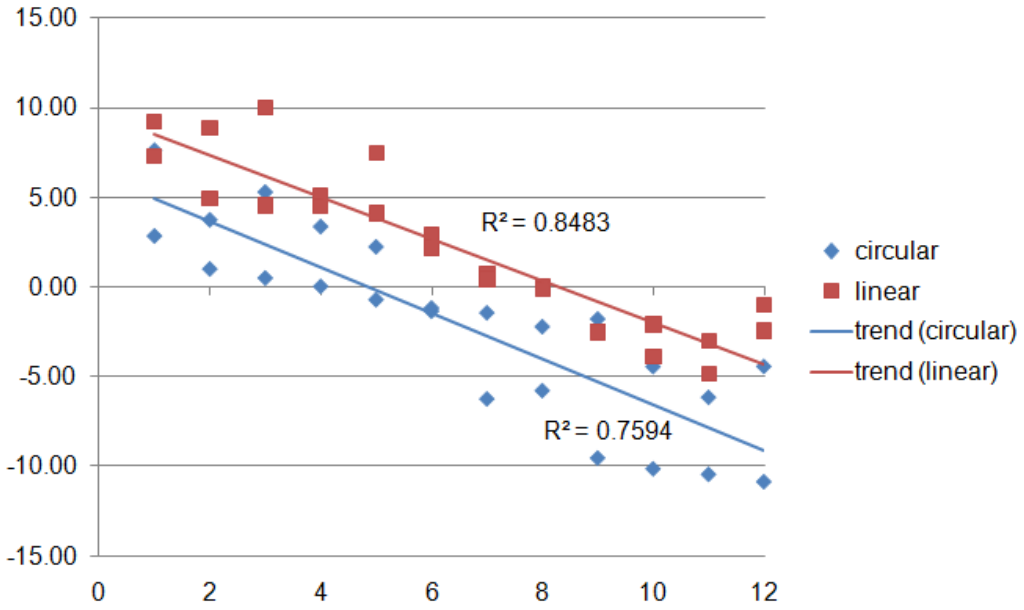

Figure 4-16. Comparison of the change in average power levels and tag read rates for both antennas through linear regression.

CHAPTER 5
RADIO FREQUENCY INTERACTIONS WITH AIR CARGO CONTAINER MATERIALS FOR REAL-TIME MONITORING

Introduction

Products, such as food, pharmaceuticals and flowers, are at high risk of perishing from various adversities along the cold chain. The parties involved should control when possible, and at the very least monitor the conditions of the goods in order to ensure their quality and to comply with all legal requirements. Among environmental parameters during transport, temperature is the most important in maintaining the shelf life of the products (Nunes et al., 2006; Zweig, 2006; Jedermann et al., 2009).

Cold chain. With today's globalization, there is a growing need for fresh products to be delivered year round all over the world, thus, temperature sensitive items are likely to be shipped by air because of their relatively short shelf life. Unfortunately, a faster transit time does not always imply controlled temperature throughout transportation. In contrast, during airport operations, loading, unloading, air transportation or warehouse storage, perishable goods often suffer from temperature abuse either due to difficulties in controlling the temperature, absence of refrigerated facilities, or lack of information about produce characteristics and needs (Nunes et al., 2003). Of approximately 2.6 million tons of perishables air freighted in 2008, nearly 30% is estimated to be lost due to handling and temperature abuse (Catto-Smith, 2006). In a previous study, Émond et al. (1999) showed that the environmental conditions during airport operations could, in fact, be very far from the optimum for fruits and vegetables. Moreover, in a strawberry quality study, Nunes et al. (2003) showed that greater losses in quality occurred during simulation of the airport handling operations, in-flight, and retail display than during

warehouse storage at the grower, truck transportation to or from the airport, or during backroom storage at the supermarket.

Temperature monitoring. Currently, most digital temperature loggers have to be connected to a host device to download data, and as a result, have limited real-time data interactivity, which results in after-the-fact analysis for claims, loss in quality and related issues. Radio frequency identification (RFID) temperature loggers function wirelessly which allows for real-time information transfer. Active or semi-passive RFID tags can support one or many sensors as well as the unique ID that RFID technology provides by design. The RFID tag, with associated hardware and software gives the added benefit of having the item scanned on receipt, so that if an alert (alert triggers are programmable prior to shipping) is active, the receiver knows immediately (not after-the-fact) that there is a potential problem with the shipment and can spend the time required on specific shipments rather than going through random inspections (Jedermann et al., 2007). Many studies have shown the effectiveness of RFID in monitoring product temperature during transit (Émond, 2007; Jedermann and Lang, 2007; Jedermann et al., 2007; Ketzenberg and Bloemhof-Ruwaard, 2009).

RFID technology. Although RFID's effectiveness has been proven for many cases, the technology is not flawless. Certain materials, like metals and water-based liquids, are challenging for RFID systems (Foster and Burberry, 1999; Émond, 2008) and are generally referred to as being RF-Opaque. The behaviour of radio frequency around metal has been studied extensively (Dobkin and Weigand, 2005; Griffin et al., 2006; Prothro et al., 2006; Sydanheimo et al., 2006). Because aluminum is a very good conductor (conductivity 38 MS/m), an incident electromagnetic wave totally reflects from

the metallic surface with a phase reversal (Cheng, 1993; Reitz et al., 1993). Moreover, metallic surface of the object in the vicinity of an antenna changes its radiation pattern, input impedance, radiation efficiency and resonant frequency. These changes depend on the size and shape of the metallic object and also on the distance of the antenna from the object (Raumonen, 2003; Mo and Zhang, 2007). Mo and Zhang (2007) also demonstrated that RFID tags placed 1/4 wavelength away from the metallic surface enhances the readability of the tags.

Not only metallic materials, but also dielectrics (or electrical insulators) cause reflections. Other materials affect part of the incident energy and transmit the rest. The exact amount of transmission and reflection is also dependant on the angle of incidence, material thickness, and dielectric properties (Blaunstein and Christodoulou, 2007). On the other hand, little or no reflection occurs when electromagnetic waves penetrate directly through objects such as paper, non conductive plastics or textiles (Penttilä et al., 2006). These materials, including most composites, are non-absorbing and possess low refractive indexes. Such materials are generally referred to as being RF-lucent.

Air Cargo. While the world is talking about climate change, the airline industry is looking at ways to be more fuel efficient to minimize their operational costs as well as their impact on the environment. One way to do so is to reduce the weight, and minimizing weight without compromising the business volume is feasible by using lighter containers, or Unit Load Devices (ULDs). Composite ULDs can save up to 25% of the tare weight of a traditional aluminum ULD (Nordisk, 2010). For illustration: A Boeing 747-400 aircraft, equipped with 16 standard aluminum ULDs normally has a total of

1216kg empty container weight. Alternatively, by using ultra light composite ULDs, the combined empty container weight total would be approximately 880kg. Furthermore, composites containers are easier to repair and require fewer visits to a repair station than aluminum units (Saunders, 2003). Kevlar® ULDs are constantly replacing older aluminum containers and account for approximately 39% of a major airline's ULD fleet. Aluminum ULDs still add up to 43% of their fleet, whereas Lexan® containers count for the remaining 18%. Considering that ULDs have an approximate usable life of 10 years, Aluminum ULDs will most likely be outnumbered by composite containers relatively quickly.

This study focuses on the air transportation part of the cold chain. RFID is not yet a widespread technology in the transportation industry, but its potential value makes it worth the investigation effort. The objective of this study is to explore the possibility of real time temperature monitoring during air cargo operations by researching the effect of container wall materials on RF propagation. Five different ULD materials were chosen for this study: Aluminum, Duralite, Herculite, Kevlar® and Lexan®. Due to the fact that the RF behavior of materials depends on size, shape and thickness, all samples used for this study were collected from an airline container maintenance facility and therefore represent the true properties for each material. Initial hypotheses are that only Aluminum samples will not allow RF transmission, whereas all other materials will transmit radio waves with negligible interference.

Materials and Methods

Three radio frequencies (433MHz, 915MHz and 2.45GHz) were tested against five different air cargo materials as described in the introduction: Aluminum, Duralite, Herculite, Kevlar® and Lexan®. Duralite is a thick fibreglass woven composite. Herculite

(or Twintex® P PP) is a thermoplastic glass reinforcement panel made of commingled E-Glass and thermoplastic filaments. Kevlar® is made with high strength para-aramid fiber and Lexan® is a translucent polycarbonate. For the first two tests, each sample was a square sheet of 0.305m long sides and thicknesses of 1.00, 1.80, 1.00, 0.50 and 1.80mm respectively. For the third test both samples were squares of sides 1.22m long.

This series of tests was performed inside an anechoic chamber of dimensions 2.05m high, 1.90m wide and 2.70m deep. The wall materials were Eccosorb VHP-12-NRL and Eccosorb FS-100-NRL (Emerson & Cuming Microwave Products N.V., Westerlo, Belgium), a solid, pyramidal shaped, carbon loaded urethane foam absorber. Each frequency was generated by an RF signal generator (Agilent N9310A, Agilent Technologies, Santa Clara, CA); power supply (XTR 33-25, Xantrex technology, Burnaby, BC, Canada); and power amplifiers (5803039A and 5303081, Ophir RF, Los Angeles, CA). This equipment was located outside of the anechoic chamber during testing. The RF output of this system was conveyed to the anechoic chamber via a 50m long LMR-400 low-loss cable. Each frequency was tested with a particular set of emitter and receiver antennas (Table 5-1) and only one frequency was tested at a time.

Three tests were administered to determine the effects of the materials on RF propagation. For all tests, the received signal was measured with a spectrum analyzer (RSA3303B, Tektronix, Beaverton, OR), also kept outside the door of the anechoic chamber during testing. The definition of a data point in this experiment is a 200 sample average of the peak signal power observed at each tested frequency. One frequency was tested at a time and all data were analyzed with reference to the control data point (no material sample present).

Test 1

The goal of this test was to quantify the reflection and absorption characteristics of each material. Inside the chamber, the emitting antenna, receiver antenna and material samples were arranged in a row on a Plexiglas table with a Styrofoam plate to help hold everything in place (Figure 5-1). The table was centered in the room 0.38m above the floor, just over the anechoic chamber surface material responsible from absorbing outside RF radiation. The emitting antenna was positioned vertically, beaming towards the back of the room. The receiving antenna was also positioned vertically with specific intervals based on the radiation wavelength (at $\lambda/2$, $3\lambda/4$, $\lambda+\lambda/4$ or $\lambda+\lambda/2$), and the material sample was positioned at λ in front of the emitting antenna.

Wavelength in meters is calculated as; $$\lambda = \frac{c}{f} \quad (5\text{-}1)$$

Where c is the speed of light in m/s and f is the frequency in Hz. In other words, the sample was 0.692m from the 433MHz antenna; 0.328m away from the 915MHz antenna; or 0.125m away from the 2.45GHz antenna. The respective receiver antennas were consecutively placed ¼ and ½ wavelengths away from the sample, on both sides (Figure 5-1). Ideally, test 1 should have been accomplished with infinite planes of each sample. Reality is different, and material availability was limiting. This design is interesting in the way that it procures information on more aspects of radio frequency behavior, such as wave scattering and diffraction around sharp obstacles. In reality, those effects exist and are inevitable components in RFID applications.

Test 2

In order to achieve a more uniform dataset, the goal of this test was to isolate the receiver antenna from the knife-edge diffraction effect. The sample was framed with a

solid, pyramidal shaped carbon loaded urethane foam absorber (anechoic chamber wall material). The foam pyramids were glued onto a 0.05m thick Styrofoam sheet and were positioned to leave the center part of the 0.305m by 0.305m square empty to place the samples as shown in Figure 5-2A. The samples were again positioned one wavelength away from the emitting antennas, and the receiver antenna was taped behind the sample (Figure 5-2B). Three repetitions of each data point were performed for statistical analysis. Statistical analysis consisted of one-way ANOVA to show significant differences between the materials for each frequency. Multiple comparisons of means were performed with Bonferroni adjustments. All statistical analyses were computed using SAS 9.1 (SAS Institute Inc., 2003).

Test 3

Following the thought process from test 1 to test 2, it was determined that an additional test was needed to clarify the effect of using a smaller sample and therefore show more realistic properties of RF-lucent and RF-opaque materials. Since larger samples were not available in all materials, Aluminum and Kevlar ® were chosen and samples of 1.22m x 1.22m were tested (which is 16 times larger than the previous sample size). Those two materials were chosen because of availability, but also because of their wide use in the air cargo container fleet. Aluminum and Kevlar ® containers cover together over 80% of today's container fleet at a major airline. Moreover, those two materials can represent typical RF-lucent and RF-opaque materials encountered in the air cargo industry.

The same set-up as test 1 was used, which means that the emitting antenna was positioned vertically, beaming towards the back of the room. The receiving antenna was also positioned vertically with specific intervals based on the radiation wavelength (at

λ/2, 3λ/4, λ+λ/4 or λ+λ/2); and the material sample was positioned at λ in front of the emitting antenna. Except this time because of sample size, the antennas and samples were hung from the ceiling of the chamber with strings, instead of being held in place on the table. Three repetitions of each data point were performed for statistical analysis

Results and Discussion

Test 1

The results showed a very strong effect for Aluminum on RF transmission, and minimal interaction for all other sample materials. All comparisons were made between the control and each sample. Table 5-2 shows values obtained for the control measurements (no material present), whereas Table 5-3 illustrates the signal deviations from the control (control subtracted from each signal strength measurement). Receiver antenna positions are measured from the emitting antenna and sample materials are positioned at λ.

433MHz

Results show weaker signal levels in front of the Aluminum sample at λ/2 (-1.52dBm) and higher signal strength at 3λ/4 (+2.39dBm) (Table 2-3). This confirms the observation made by Mo and Zhang (2007), which is when an electromagnetic wave hits a metallic surface, it reflects with a 180° phase reversal. This causes signal cancellation at λ/2 and signal amplification at λ/4 from the metallic surface. In our case, λ/4 from the Aluminum sample is 3λ/4 distance from the emitting antenna. All other samples show no considerable loss or gain from reflections when the receiver antenna was positioned in front of the samples (within ±0.09dBm from control). As far as signal transmission through the samples, it is understandable that only the Aluminum sample

offers considerable signal blocking, with signal loss of -5.45dBm at λ+λ/4 and -2.70dBm at λ+λ/2. All other materials were within ±0.50dBm from the control.

915MHz

In this part of the experiment, signal strength in front of the Aluminum sample was increased in both λ/2 and 3λ/4 cases, although the increase was greater at 3λ/4 (+7.11 vs. +3.98). This could be caused by signal scattering since the plate size (0.305m) was slightly smaller but very close to the wavelength at 915MHz (0.325m). Since for the case of 915MHz the wavelength and the dimensions of the material (obstacle) were of similar sizes, the set-up was in the resonance range (Finkenzeller, 2003). Therefore, the behavior of RF radiation may not follow traditional rules such as the one stated by Mo and Zhang due to the unpredictable nature of edge diffractions (Longhurst, 1967) as well as resonance. Signal was also slightly reflected from of other materials, Lexan® being the second most reflecting with +1.18dBm gain. In the case of signal transmission, similar results were observed as with 433MHz, except the signal loss is greater, with -19.70 and -11.74 at λ+λ/4 and λ+λ/2 respectively. All other materials were within ±0.17dBm of the control.

2.45GHz

Results for this part of the experiment follow Mo and Zhang's theory of wave reflection with a loss of -6.86dBm and a gain of +2.81dBm at λ/2 and 3λ/4 respectively. All other materials were within ±0.58dBm of the control. Moreover, the signal loss behind the samples was obvious with -37.99dBm at λ+λ/4 and -34.37dBm at λ+λ/2, all other materials being within ±0.55dBm of the control.

Looking at signal transmission behind the Aluminum sample, it was noticeable that the signal loss increases with the frequency. This was caused by the ratio of the wavelengths and the materials sample size. At 433MHz, the wavelength was more than two times longer than the sample size (0.692m and 0.305m respectively); at 915MHz, both dimensions were similar (λ = 0.325m); and at 2.45GHz, the wavelength was about half of the sample size (λ = 0.125m). When a radio wave impinges an obstacle larger than its wavelength, reflection occurs. However, when a wave hits an obstacle smaller than its wavelength, scattering occurs and wave patterns are redirected with random phase and amplitude (Blaunstein and Christodoulou, 2007).

It is also noticeable that there was minor signal amplification behind the non metallic samples at 433MHz and 915MHz. This can be explained by the fact that the sample size was smaller than the wavelengths, which allows waves to travel around the materials' edges. This effect is known as the knife-edge diffraction and explains the redirection of electromagnetic waves when they hit a solid obstacle such as the edge of the material sample in this experiment (Kumar et al., 2007). Knife-edge diffraction is described by Huygens-Fresnel principle which states that such an obstruction (the edge of the material in this case) will act as a secondary source of RF radiation (Longhurst, 1967). Depending on the wavelength of the electromagnetic signal, the effects of this secondary source could be observed at different points in the measurement field, in this case, amplification behind the non-metallic samples, however, the discussion of this phenomenon in greater detail is beyond the scope of this text.

Test 2

When six treatments (material samples) were compared, all results are reported as significant when $P < 0.05$ and the Aluminum sample was the only one significantly different from the others for all three frequencies. Due to the nature of the second experiment it would be expected to obtain higher attenuation at lower frequencies because shorter wavelengths travel more easily inside the open frame within the foam absorber material. However, one should note that this observation is affected by two important parameters: the electromagnetic properties of the container samples as well as the absorption profile of the urethane foam absorber, which is proportional to the frequency (Eccosorb, 2008). For instance, for free air (control) the signal strength at 433MHz is 3.83dBm whereas the signal strength at 915MHz is 9.53dBm. This clearly shows the attenuation from the wavelength dimension at lower frequency as expected. However, at 2.45GHz, the signal power was attenuated to 6.96dBm, which is explained by the fact that the foam absorber material has higher absorption coefficients at higher frequencies.

Test 3

Table 5-5 shows values obtained for the control measurements (no material present), whereas Table 5-6 illustrates the signal deviations from the control (control subtracted from each signal strength measurement). All comparisons were made between the control measurement and each sample. The results showed a very strong effect for Aluminum on RF transmission, and minimal interaction for Kevlar ®, as expected from the previous tests. This test, however, showed a much more important attenuation level behind the Aluminum sample when comparing to the results obtained in test 1 (same test set-up, different sample sizes) for frequencies 433MHz and

915MHz. As stated previously, 433MHz corresponds to a wavelength of 0.692m, whereas 915MHz corresponds to 0.328m and 2.45GHz to 0.125m. As opposed to the earlier tests, the dimensions for the samples in test 3 were 1.22m x 1.22m, which are larger than all three wavelengths in this case.

Similar to the previous tests, the attenuation levels measured behind the Aluminum sample were still proportional to the frequency tested. Attenuation at 433MHz is lower than attenuation at 915MHz and 2.45GHz, but the divergence was not as strong as in test 1 which can be explained by the use of a larger sample between the emitting and receiving antennas. The general trend shows that an infinite aluminum plane would probably lead to similar results in terms of total attenuation for all frequencies. As far as reflection, a similar pattern was observed where the RF waves that reflects from the aluminum surface increase the signal level in front of the sample in all cases. This confirms again what Mo and Zhang (2007) had previously observed, which is when the electromagnetic wave reflects off a metallic surface, it causes signal cancellation at $\lambda/2$ and signal amplification at $\lambda/4$ from the metallic surface.

As previously stated, the goal of this test was to show that a larger-than-wavelength sample size would affect the signal level measurements behind the samples by eliminating secondary effects such as edge reflection discussed in the previous sections and uniformize the results. The values presented in tables 5-5 and 5-6 show that this goal was accomplished by measuring higher power levels in front of the sample material for Aluminum and behind the sample material for Kevlar.

Conclusion

This test demonstrated the effects of five commonly used air cargo container wall materials on RF propagation at three different frequencies. The reflection and absorption characteristics of each material were quantified. Three different tests were utilized to analyze the characteristics of RF propagation in greater detail for each material and the results from all experiments showed a very strong effect of Aluminum on RF transmission and minimal interaction for all other sample materials as expected. These findings suggest that the use of non-metallic containers for air transportation of perishable products should make real time temperature monitoring possible by allowing RF waves to transmit through the wall surface effortlessly. This goes well with the current trend that encourages the use of Kevlar® containers over aluminum ones because of their much lighter tare weight.

Table 5-1. Specifications of the six antennas used.

Frequency	Antenna	Polarization	Gain	Model & Manufacturer
433MHz	Emitter	Circular	9 dBi	SPA 430, Huber + Suhner AG, Essex, VT
	Receiver	Linear (omni)	0 dBi	B-368-1, How Tsen Intl. Electronics Metal Co.,Ltd. Shin Wu Hsiang, Tao Yuan Hsien, Taiwan
915MHz	Emitter	Circular	8 dBi	SPA 915, Huber + Suhner AG, Essex, VT
	Receiver	Linear (omni)	2.5 dBi	EXR902TN, Laird Technologies, Schaumburg, IL
2.45GHz	Emitter	Circular	6 dBi	2AC-001, Alien Technology, Morgan Hill, CA
	Receiver	Linear (omni)	8 dBi	MRN-24008SM3, AntennaWorld, Miami, FL

Table 5-2. Signal strength measurements (dBm) for control (no sample), test 1. Receiver antenna positions are measured from the emitting antenna.

Frequencies	Receiver antenna positions			
	λ/2	3λ/4	λ+λ/4	λ+λ/2
433MHz	11.07	9.25	8.65	1.80
915MHz	13.90	11.03	7.97	6.15
2.45GHz	8.94	7.85	6.64	6.12

Table 5-3. Signal strength deviation (dBm) from control (no sample) for test 1. Receiver antenna positions are measured from the emitting antenna and sample materials are positioned at λ.

Frequencies	Materials	Receiver antenna positions			
		λ/2	3λ/4	λ+λ/4	λ+λ/2
433MHz	Aluminum	-1.52	2.39	-5.45	-2.70
	Duralite	0.02	0.09	0.02	0.18
	Herculite	-0.03	0.02	0.15	0.50
	Kevlar®	-0.02	0.02	0.09	0.40
	Lexan®	0.01	-0.02	0.08	0.14
915MHz	Aluminum	3.98	7.11	-19.70	-11.74
	Duralite	1.09	0.40	0.17	0.12
	Herculite	0.84	0.30	0.08	0.03
	Kevlar®	0.96	0.32	0.09	0.00
	Lexan®	1.18	0.16	0.17	0.10
2.45GHz	Aluminum	-6.86	2.81	-37.99	-34.37
	Duralite	0.22	0.38	-0.32	-0.10
	Herculite	-0.17	0.54	-0.51	-0.50
	Kevlar®	-0.15	0.30	-0.55	-0.16
	Lexan®	-0.07	0.58	-0.29	-0.23

Table 5-4. Signal strength measurements (mean±SD) (dBm) for control, plus signal strength deviation between material samples and control at three frequencies for test 2 (n=3).

Materials	Frequencies		
	433MHz	915MHz	2.45GHz
Control	3.83±0.05	9.53±0.05	6.96±0.01
Aluminum	-15.16±0.06	-20.49±0.18	-35.47±0.23
Duralite	-0.05±0.03	-0.21±0.01	-0.19±0.03
Herculite	-0.04±0.03	-0.29±0.02	-0.33±0.01
Kevlar®	-0.01±0.01	-0.35±0.01	-0.37±0.01
Lexan®	-0.06±0.04	-0.53±0.65	0.07±0.03

Table 5-5. Signal strength measurements (dBm) for control (no sample), test 3. Receiver antenna positions are measured from the emitting antenna.

Frequencies	Receiver antenna positions			
	λ/2	3λ/4	λ+λ/4	λ+λ/2
433MHz	10.60	8.50	4.53	1.97
915MHz	14.93	11.72	7.76	6.41
2.45GHz	11.04	8.97	5.47	4.79

Table 5-6. Signal strength deviation (dBm) from control (no sample) for test 3. Receiver antenna positions are measured from the emitting antenna and sample materials are positioned at λ.

Frequencies	Materials	Receiver antenna positions			
		λ/2	3λ/4	λ+λ/4	λ+λ/2
433MHz	Aluminum	0.36	3.18	-20.01	-15.33
	Kevlar®	0.74	0.30	-1.48	1.27
915MHz	Aluminum	2.17	6.20	-26.84	-24.53
	Kevlar®	0.19	-0.42	-0.13	0.11
2.45GHz	Aluminum	0.84	3.20	-38.12	-37.48
	Kevlar®	0.23	0.40	0.00	0.56

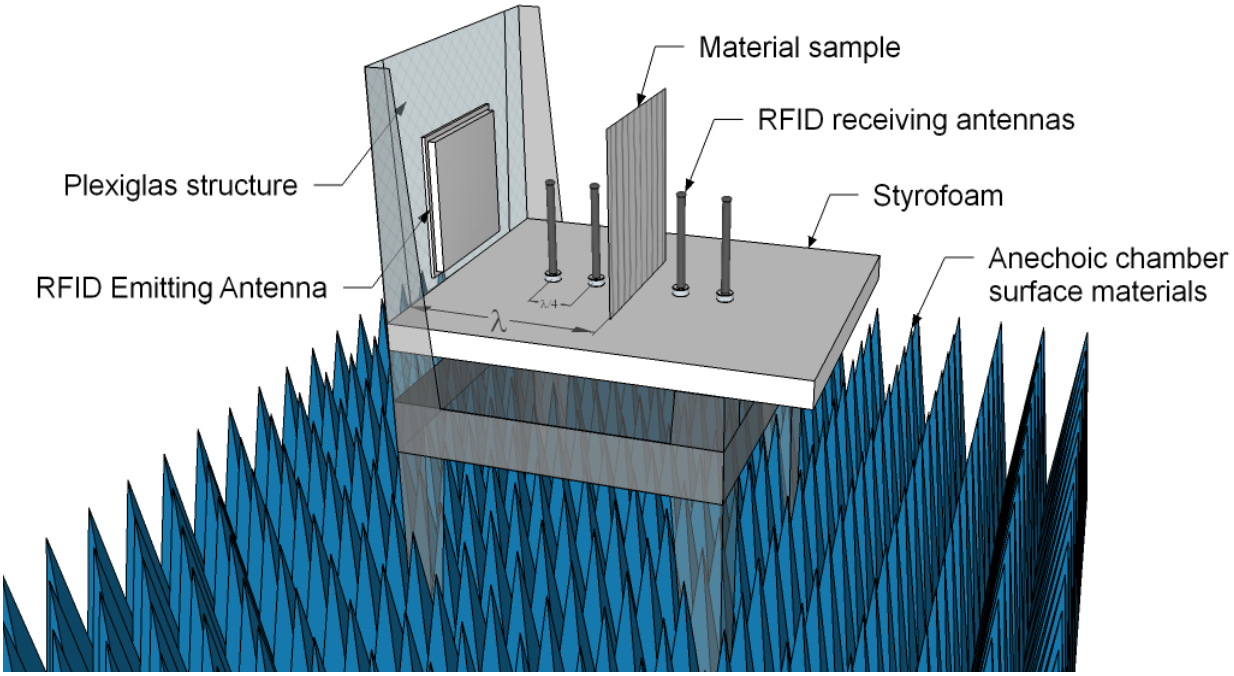

Figure 5-1. Diagram of the anechoic chamber setup for test 1. Note that four receiver antennas are shown for illustrative purposes as only one receiver antenna is used at a time for each test.

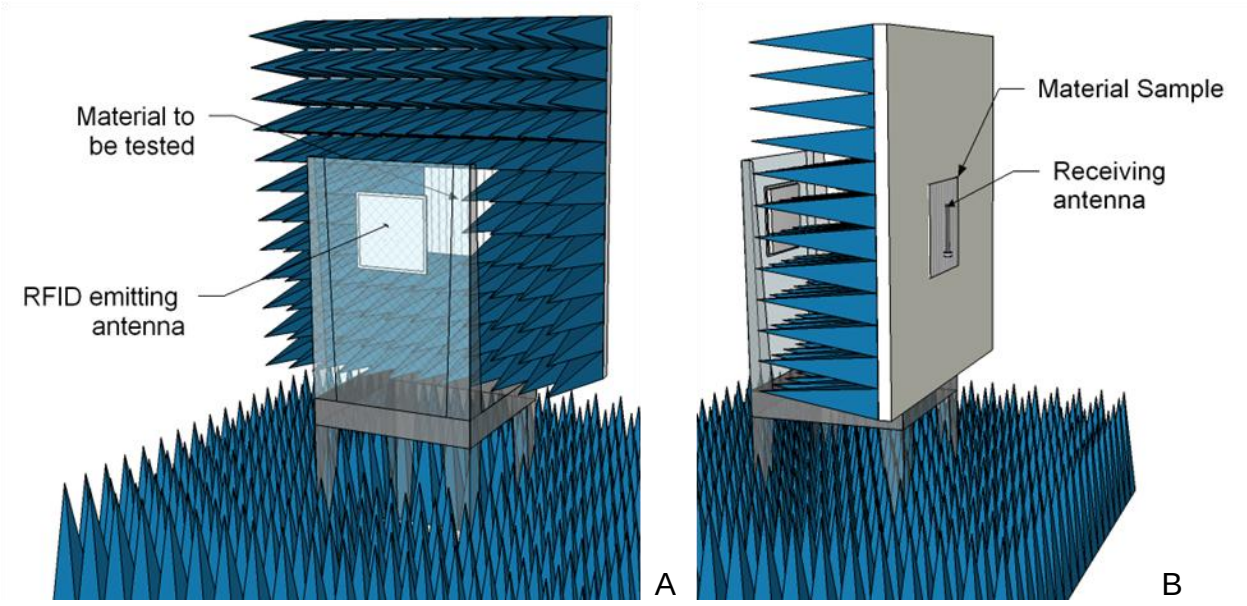

Figure 5-2. Anechoic chamber set-up for test 2. A) The sample material is surrounded by pyramidal shaped, carbon loaded urethane foam absorber and is placed one wavelength from the emitting antenna. B) The receiver antenna is taped behind the material sample.

CHAPTER 6
TEMPERATURE MAPPING INSIDE AIR CARGO CONTAINERS DURING AIRSIDE OPERATIONS

Introduction

Temperature is well regulated in the cabin of most passenger flights, but it is not necessarily the case inside the cargo hold or in freighter flights. Temperature distribution and variability in cargo holds depends on many factors such as weather (air temperature, wind speed, sun radiation), duration of flight, type of aircraft (ability to control cargo ambient temperature), altitude, and transit time on the tarmac.

Aircraft. Temperature control inside the cargo hold can be regulated at different levels. On one end, the only heat available in the cargo hold of some aircraft comes from leaks in the cabin floor; some other airplanes have ventilation systems that can re-circulate the cabin air into the cargo hold; and the more sophisticated ones have their own heating systems designed to keep the cargo from freezing (Air Canada, 2007). Typically, larger and newer aircrafts have more options. When aircrafts are categorized by size, two major categories emerge, which are narrow-body and wide-body aircrafts. Narrow-body aircrafts have one aisle and two rows of seats in the cabin, whereas wide-body aircrafts have two aisles and three rows of seats in the cabin floor. As a consequence, the wide-body aircraft has a larger cargo compartment and can also be used on longer routes. Studies on temperature profiles inside cargo holds state many different temperature ranges. Syversen et al. (2008) found that 49.5% of shipments were exposed to high temperatures (greater than 29.4 °C), 14.6% to low temperatures (less than 7.2 °C), and 61% to temperature variations of 11 °C or more. It was also shown that temperature depends on ULD position inside the cargo hold as well as which cargo hold is used (Émond et al., 1999).

Air cargo operations. All cargo being planned on a flight is built-up onto unit load devices (ULDs) or in tub carts (for bulk) a specific time prior to flight departure. This specific time depends on the airport, destination (domestic vs. international), size of freight, and type of product (priority vs. general freight) (T. Howard, 2010, personal communication). The freight usually leaves the warehouse (on the airside) for a maximum of 2h before flight time, but typically spends between 45 and 90 minutes on the tarmac before being loaded onto the aircraft (T. Howard, 2010, personal communication). In practice, if something happens to delay the loading activity of the plane, the freight can be left on the tarmac for extended periods of time, regardless of weather conditions (Villeneuve, 2006). Many factors can influence ULD's temperature fluctuations while waiting on the tarmac, for example, sun radiation, air temperature, ULD wall material properties, wind speed and direction, etc (Villeneuve et al., 2001).

Perishables. Products, such as food, pharmaceuticals or flowers, are at high risk of perishing from various adversities along the cold chain. Among environmental parameters during transport, temperature is the most important in maintaining the shelf life of the products (Nunes et al., 2006; Villeneuve, 2006; Zweig, 2006; Jedermann et al., 2009). With today's globalization, there is a growing need for fresh products to be delivered year round all over the world, Temperature sensitive items are likely to be shipped by air because of their relatively short shelf life. Unfortunately, a faster transit time does not always imply controlled temperature throughout transportation. In contrast, during airport operations, loading, unloading, air transportation or warehouse storage, perishable goods often suffer from temperature abuse either due to difficulties in controlling the temperature, absence of refrigerated facilities, or lack of information

about produce characteristics and needs (Nunes et al., 2003). On approximately 2.6 million metric tons of perishables air freighted in 2008, nearly 30% is estimated to be lost due to handling and temperature abuse (Catto-Smith, 2006). In a previous study, Émond et al. (1999) showed that the environmental conditions during airport operations could, in fact, be very far from the optimum for fruits and vegetables. Moreover, in a strawberry quality study, Nunes et al. (2003) showed that greater losses in quality occurred during simulation of the airport handling operations, in-flight, and retail display than during warehouse storage at the grower, truck transportation to or from the airport, or during backroom storage at the supermarket. Many more studies showed that important temperature fluctuations can occur during airport ground operations (Bollen et al., 1998; Villeneuve et al., 2000; Villeneuve et al., 2001). Moreover, because perishables are mostly season dependant, transportation companies do not offer special treatments like they would if they were available year round (Villeneuve, 2006).

Temperature monitoring. Currently, most digital temperature loggers have to be connected to a host device to download data, and as a result, have limited real-time data interactivity, which result in after-the-fact analysis for claims, loss in quality and related issues. Radio frequency identification (RFID) temperature loggers function wirelessly which allows for real-time information transfer (Rao, 1999, Lahiri, 2006). Active or semi-passive RFID tags can support one or many sensors as well as the unique ID that RFID technology provides by design. The RFID tag, with associated hardware and software will add the benefit of having the item scanned on receipt, so that if an alert (alert triggers are programmable prior to shipping) is active, the receiver knows immediately (not after-the-fact) that there is a potential problem with the

shipment and can spend the time required on specific shipments rather than going through random inspections (Jedermann et al., 2007). Many studies have already shown the effectiveness of RFID in monitoring product temperature during transit (Émond, 2007; Jedermann and Lang, 2007; Jedermann et al., 2007; Ketzenberg and Bloemhof-Ruwaard, 2009).

Since temperature control inside cargo holds is a weak link in the air cargo cold chain, the objective of this study is to evaluate the temperature distribution inside the ULDs during airside operations. Comparison will be made between long and short flights, as well as between wide- and narrow-body aircrafts. Hypotheses are that temperature will drop lower at the bottom part of containers as well as during longer flights in general.

Materials and Methods

In June 2010, 12 ULDs were shipped on 10 different one-way flights (Table 6-1). The number of ULDs monitored per aircraft was limited by the amount of cargo available to travel on that route that specific day. All flights were managed by Air Canada and originated from Toronto, Canada (YYZ). Three ULDs traveled to Montreal, Canada (YUL); one ULD flew to Vancouver, Canada (YVR); four ULDs flew to London, UK (LHR); and four ULDs were shipped to Frankfurt, Germany (FRA). All these ULDs were reloaded at destination to be shipped back on a returning flight. All containers shipped on Canadian routes were shipped back to Toronto, however, ULDs shipped to Europe either returned to Montreal, Toronto or Vancouver. All flight times varied between 1h and 9.7h (Table 6-1).

ULD capacity. As stated in Table 6-1, domestic flights were made onboard Airbus 320 or 321 narrow-body aircrafts, which hold LD3-45 ULDs (or called by their prefix

AKH). These ULDs take the entire width of the cargo hold. The A320 can hold three in the forward compartment and four in the aft compartment. Being slightly longer, the A321 can hold five ULDs in the front as well as four in the aft cargo hold. On the other hand, international flights were made on wide-body aircrafts which carry LD3 ULDs (prefix AKE). Those ULDs occupy half of the cargo hold width and are loaded side by side. The A330 can hold 18 in the front and 15 in the aft compartment, whereas the Boeing 777 can carry up to 24 in the front and 20 in the aft compartment. Five tags were placed in each AKH and eight tags were installed in each AKE container according to the scheme shown in Figure 6-1.

Temperature control. According to Air Canada Load Control Engineering publications, there is no ventilation and no heating in any of the cargo holds of the A320 and A321 aircrafts except for cargo door leakage when there is a pressure differential between the fuselage interior and exterior. The Airbus specification for the A321 aircraft guarantees a minimum temperature of 2^{o}C in flight (Air Canada, 2005a, b). In the A330, the forward cargo hold is equipped with a temperature controlled heating and cooling system that is ventilated at all times. Under normal conditions, the mean in-flight temperature will be between 5^{o}C and 25^{o}C. The aft cargo compartment is neither provided with ventilation nor heating system (Air Canada, 2006). In the B777, all cargo holds are heated. The forward hold is equipped with an air conditioning system designed to maintain a constant target temperature and provide ventilation both on the ground or during flight. A temperature selector in the cockpit provides a selectable temperature control ranging from 4^{o}C to 27^{o}C. The aft hold is equipped with a basic heating system providing compartment temperature control to two set points

corresponding to settings of LOW (4ºC to 10ºC) and HIGH (18ºC to 24ºC) (Air Canada, 2007).

Temperature sensors. The temperature sensors used for monitoring were TurboTag® (Sealed Air Corporation, Elmwood Park, NJ), which are high frequency (13.56MHz) RFID tags with temperature logging capacity of 702 time-temperature data points. Tag accuracy is ±0.5°C throughout normal operating range (-25°C to +35°C) at 95% confidence interval. They were programmed to read every five minutes, which allowed close to 2.5 days of monitoring time. All tags were started the morning before the first flights and stopped automatically when all 702 points were recorded. Data was downloaded at the end of the experiment.

It is important to note that all “during flight” data shows temperature recorded between the time the aircraft left the origin gate, and the time it sets the brakes at the destination gate, thus including taxi, takeoff and landing. Moreover, “airside operations” refers to everything between the time the cargo leaves the warehouse to go on the tarmac, until it comes back to another warehouse for customer pick-up.

Results and Discussion

During Flight

On a general basis, sensors recorded much lower temperatures in the bottom of ULDs than in the upper part during flight (Figure 6-2). This observation supports one of the initial hypotheses. Moreover, this fact can be explained by a combination of factors such as the distance from the aircraft skin, the heat coming from the passenger cabin and natural convection.

The narrow-body aircrafts used in this study were the Airbus 320 and 321 and are considered as short to medium range aircrafts. As explained earlier, these aircrafts do

not have any means for heating their cargo holds, and consequently temperature distribution depends entirely on outside/surrounding conditions. For narrow-body aircrafts, this study shows that the duration of the flight significantly affects temperature drop (Figure 6-2). Flights under 2h (Toronto-Montreal) stayed above 15°C all around (Figure 6-3), whereas flights to and from Vancouver (4-6h) dropped to 3°C at the bottom of the ULDs (Figure 6-4). Mostly, it is the temperature on the floor of the cargo hold that cools the most, but the overall temperature also drops. Cold or warm temperature does not necessarily mean good or bad. Temperature sensitive goods do not always require refrigeration. Tropical fruits, for example, should never be exposed to close to freezing temperatures, and berries, on the other hand, should be kept as close to 1°C as possible.

For wide-body aircrafts (A330 and B777), temperature shows a decreasing trend while in the air (Figure 6-5 and 6-6). When averaging all curves on Figure 6-5, the general slope becomes negative after only 1h. As a result, flight time is inversely proportional to overall temperature in the cargo compartments, at least for flights over 7h. Nonetheless, the temperature drop during flight was steeper for the narrow-body (Figure 6-4) for the same length of time when comparing with the first 5h of wide-body aircrafts' flights (Figure 6-5, 6-6). This could be due to the temperature control ability of wide-body aircrafts. However, the only ULD carried in the narrow-body A321 (Figure 6-4) was placed at the same position on both flights (Figure E-2), therefore results could change with data from other locations inside the aircraft.

For shipments in the A330, some ULDs were carried aboard the forward or aft compartment, which means that some loads were "heated and ventilated" while some

were not. Averaging all tag temperatures carried in the forward (heated) compartment during flight compared to those transported in the aft (unheated) cargo hold (Table 6-2) leads to the conclusion that there is no significant difference in temperature profiles. This conclusion might be biased by the fact that all ULDs transported in the heated compartment were positioned at the very front of the aircraft, right next to the cargo door. Moreover, if there was no requirement for heating the cargo hold during those specific flights, the system would have been set to default, which is ventilation “on” but no heat. Those two factors could have strongly contributed to this almost homogeneous result, which is counterintuitive.

Before and After Flight

ULDs are brought to the gate up to 2h before each flight, and can typically spend the same amount of time waiting on the tarmac after being unloaded from the aircraft (an ideal, no delay situation) (T. Howard, 2010, personal communication). But as the present study showed, even a short period of time waiting on the tarmac can lead to very high temperatures on top of the UDLs (in summer season). Maximum recorded temperatures at the top of the ULD peaked at 45^{o}C in less than 20 minutes from arrival at the gate (see 7h-mark in Figure 6-7). The goods pulp temperature certainly do not warm up as fast, but sensitive shipments placed near the top of the containers could easily suffer from a major break in the cold chain. On the other hand, goods loaded in the bottom part of the container would take much longer to experience the temperature raise. Other examples can be found in appendix E where each ULD’s temperature profile (2h before first flight until 2h after second flight) is plotted separately. Each graph also shows the container positions inside the aircrafts. Throughout the year, the effect of

ground weather on ULD temperature should see much more variation than during the in-flight transportation since air temperatures at high altitudes do not vary as much.

Conclusion

Cold chain is always hard to keep intact when goods transfer from one hand to another, especially when the transportation methods do not offer refrigeration during transit. This temperature distribution study showed that a major temperature gradient can be found within the same ULD during tarmac operations as well as during flight, especially when the flight time exceeds 4h. Moreover, temperature seems to drop faster inside the cargo holds of narrow-body aircrafts, but further similar studies are required to verify that statement. Since this study was performed in the summer, it would be both interesting and informative to measure temperature distribution and variability for similar tests performed during the winter. Furthermore, one could investigate transportation with longer flights (>10h) to measure temperature variability and distribution and to see if temperature in the bottom of the ULDs would reach critical freezing temperatures.

Table 6-1. Routes, aircraft and ULD specs from Toronto (YYZ).

Destination 1	Destination 2	ULDs		Aircrafts	Flight time
		qty	type	to/from	to / from (h)
YUL	YYZ	3	AKH	Airbus 320	1.1/ 1.4
YVR	YYZ	1	AKH	Airbus 321	5.4 / 4.3
LHR	YUL	2	AKE	Airbus 330	7.2 / 7.5
LHR	YYZ	1	AKE	Airbus 330	7.2 / 8.0
LHR	YVR	1	AKE	A330/B777	7.2 / 9.7
FRA	YUL	4	AKE	Boeing 777	7.5 / 7.5

Table 6-2. Temperature comparison between heated and unheated cargo holds inside an Airbus 330.

Heated compartment				Unheated compartment			
Flight	AKE #	Temperature means (°C)		Flight	AKE #	Temperature means (°C)	
		Top tags	bottom tags			Top tags	bottom tags
YYZ - LHR	03782	19.20	12.71	YYZ - LHR	04090	17.60	13.97
YYZ - LHR	04969	21.26	15.58	LHR - YYZ	04090	20.20	14.71
LHR - YUL	04969	20.78	13.18	YYZ - LHR	05335	17.54	14.01
				LHR - YUL	05335	22.02	16.79
Total averages		20.41	13.82	Total averages		19.34	14.87
		17.12				17.11	

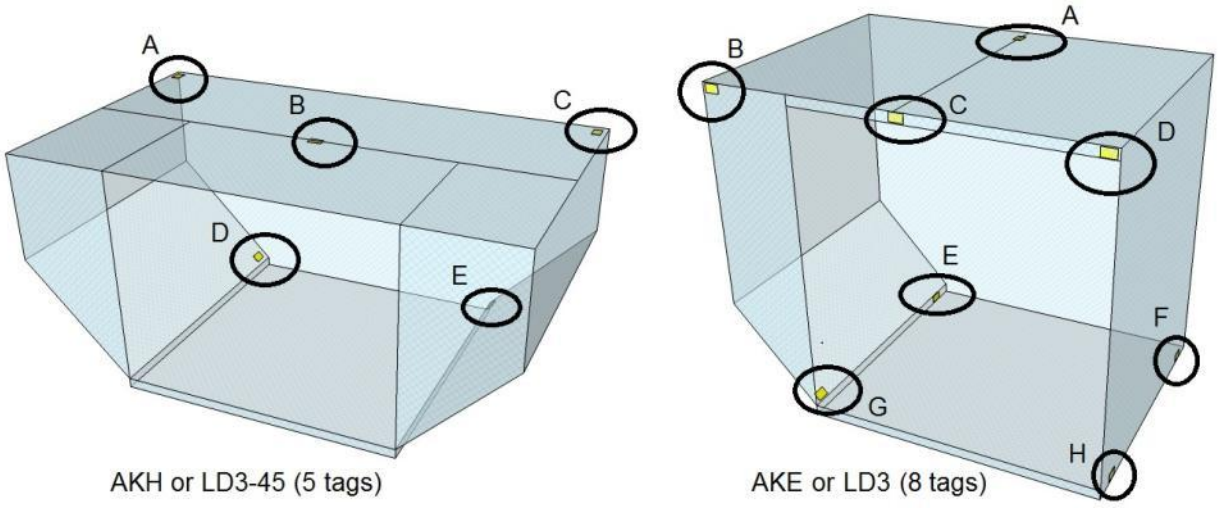

Figure 6-1. ULD types and their respective tag positions.

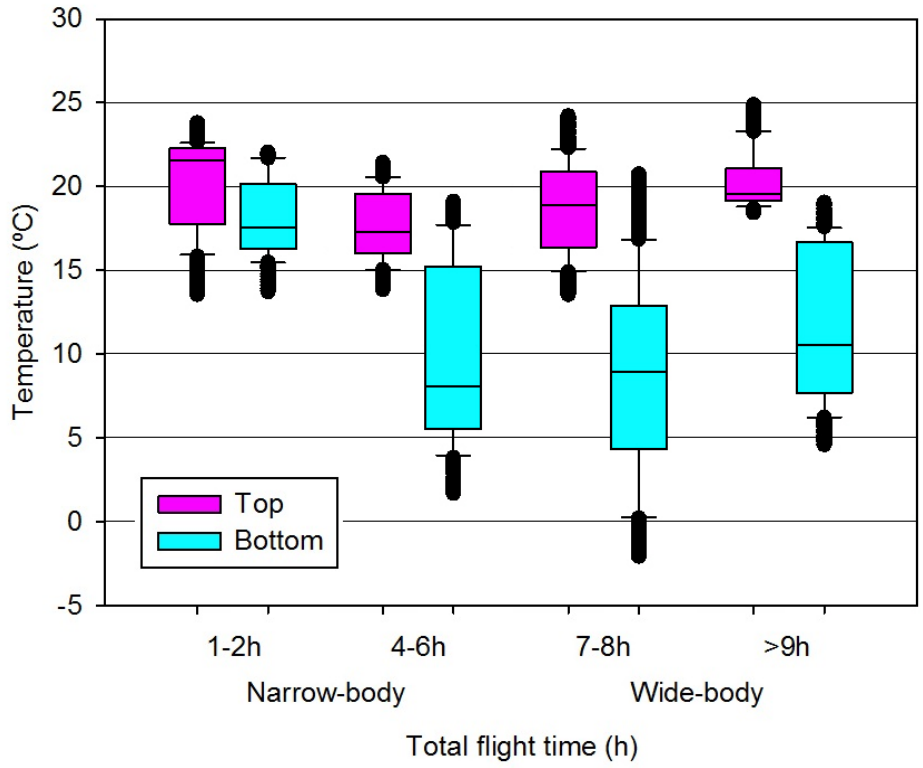

Figure 6-2. Temperatures recorded for top and bottom tags during flight (gate to gate). Data is congregated by total flight time and type of aircraft. The boundary of the box closest to zero indicates the 25th percentile, a line within the box marks the median, and the boundary of the box farthest from zero indicates the 75th percentile. Error bars above and below the box indicate the 90th and 10th percentiles.

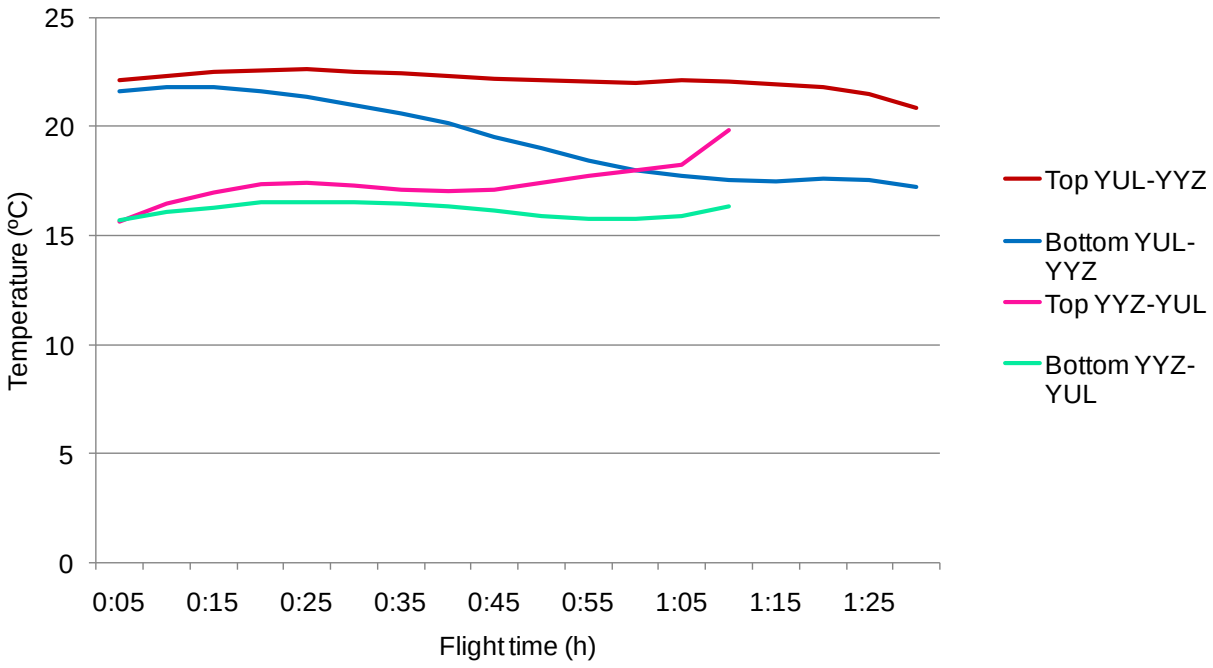

Figure 6-3. Graph of averaged top and bottom tag temperatures during flight (gate to gate) for both short flights (1-2h) to and from Montreal (YUL).

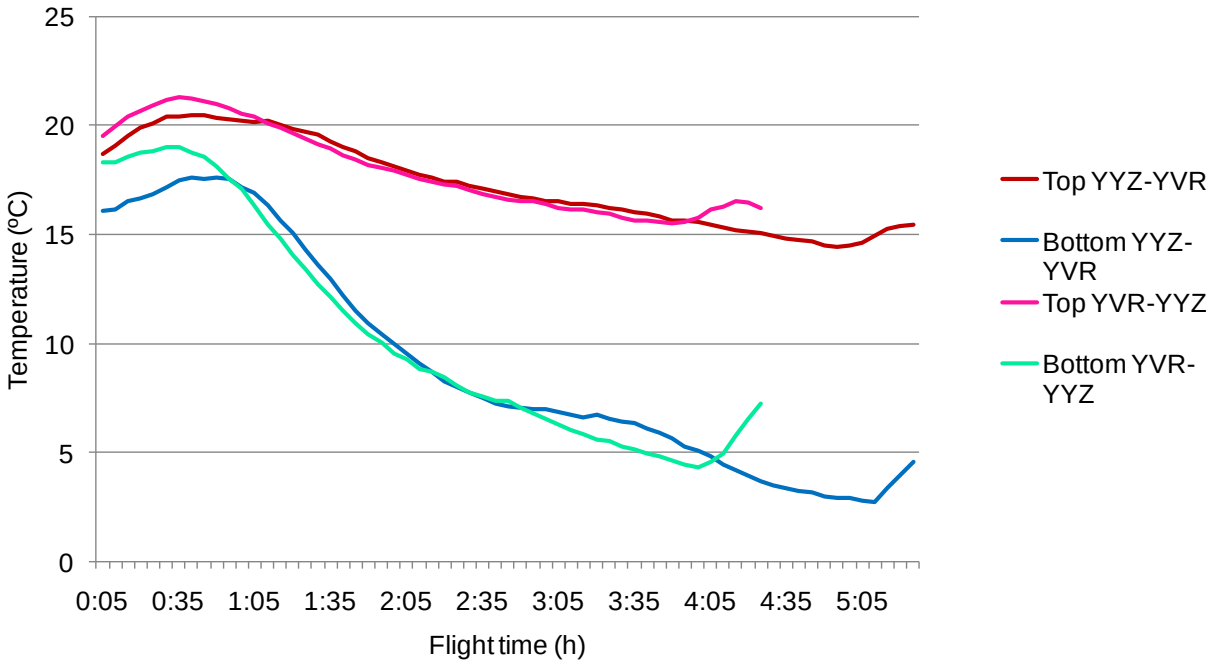

Figure 6-4. Graph of averaged top and bottom tag temperatures during flight (gate to gate) for both medium-short flights (4-6h) to and from Vancouver (YVR).

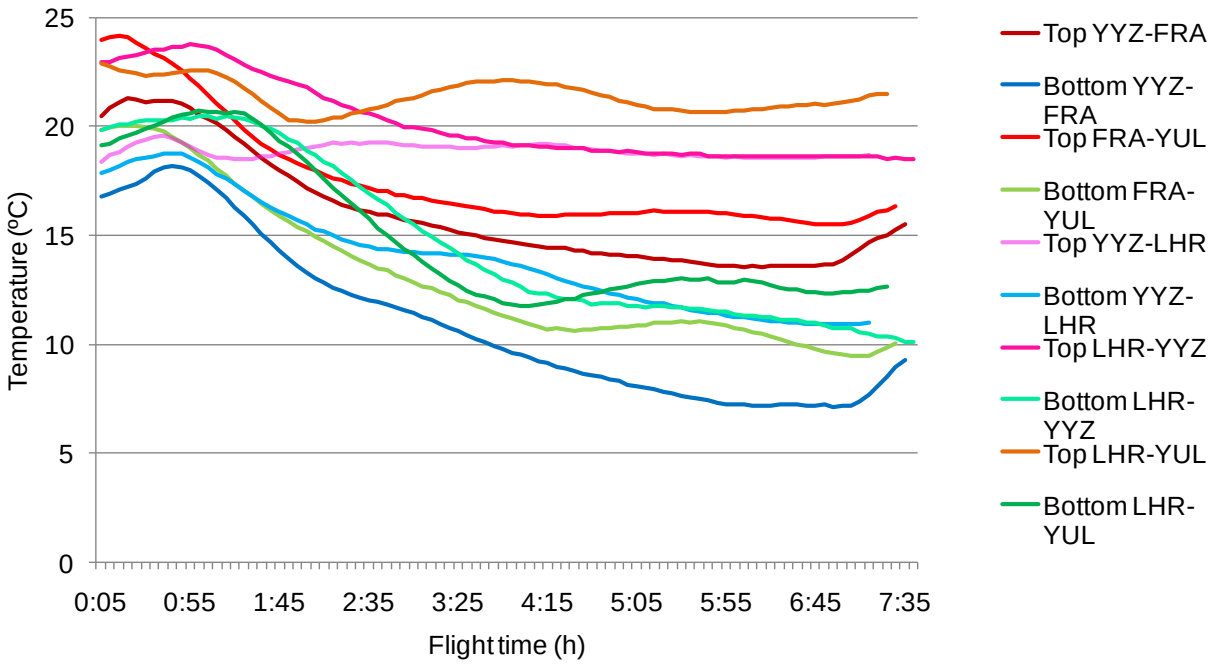

Figure 6-5. Graph of averaged top and bottom tag temperatures during flight (gate to gate) for all 7-8h flights to and from London (LHR) or Frankfurt (FRA). Red-pink colors are for top temperatures, and blue-green colors are for bottom temperatures.

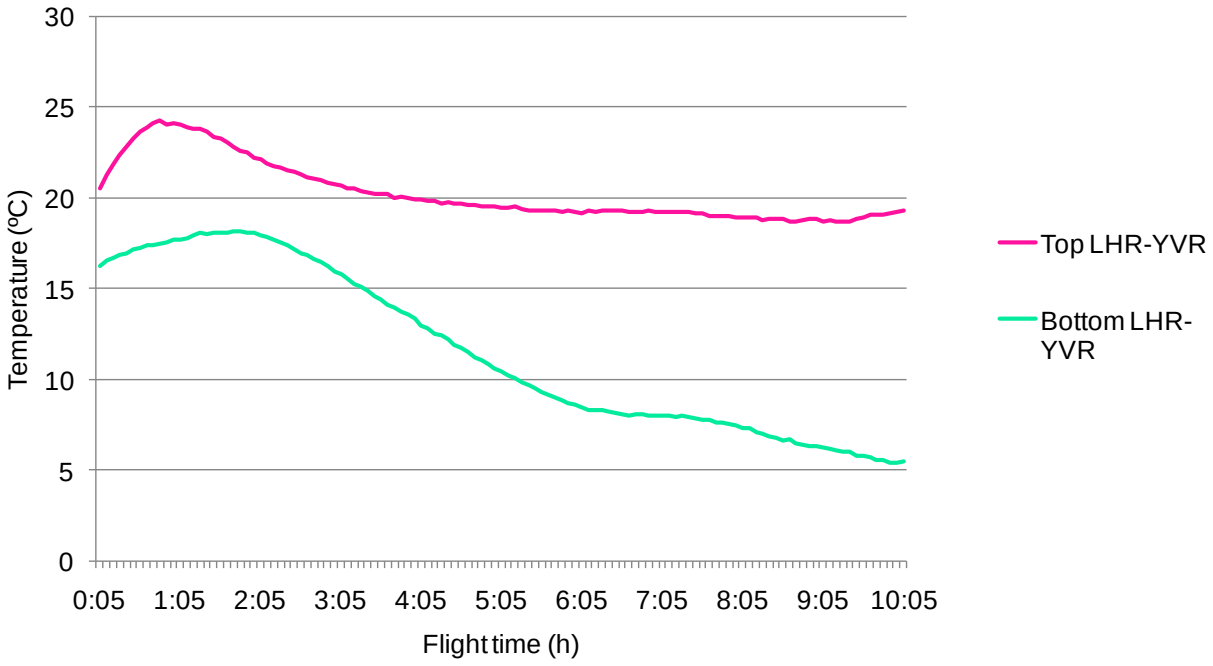

Figure 6-6. Graph of averaged top and bottom tag temperatures during flight (gate to gate) for the longest flight (above 9h) between London (LHR) and Vancouver (YVR).

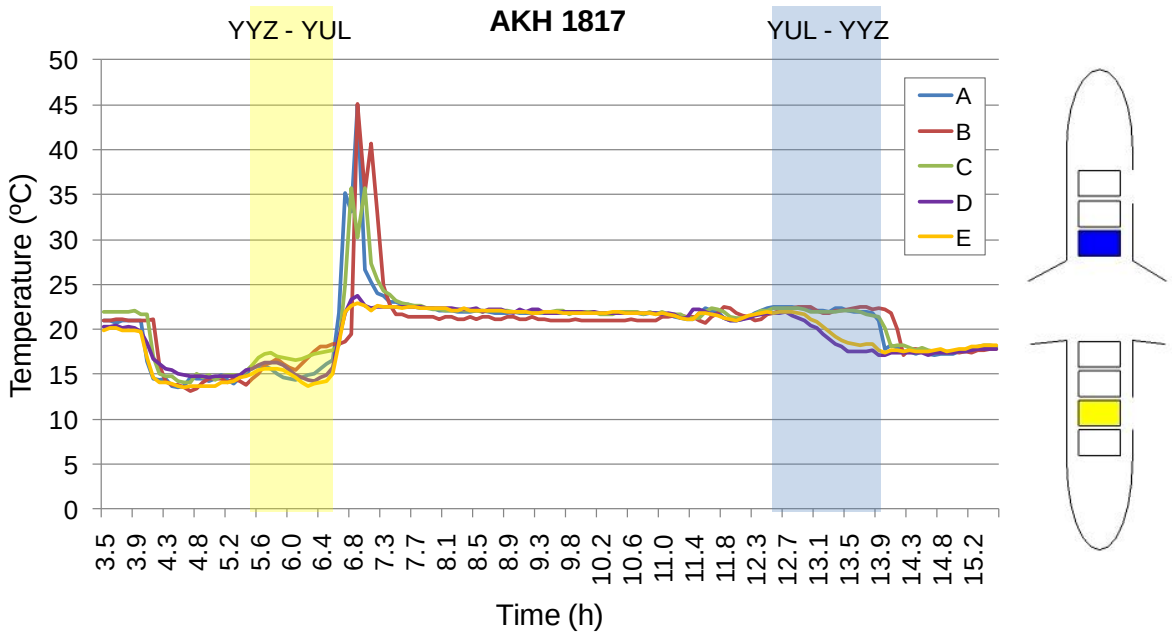

Figure 6-7. Temperature profiles of all tags for ULDs AKH 1817 to and from Montreal. First flight segment is highlighted in yellow and returning flight segment is highlighted in blue. Corresponding container positions are shown on the sketch to the right.

CHAPTER 7
GLOBAL TRACKING SYSTEM FOR AIR CARGO SUPPLY CHAIN

Introduction

Previous chapters have analyzed the use of radio frequency identification technology from the view point of air cargo transportation by exploring a wide variety of factors such as different materials, frequencies and implementations. The next logical step would be to describe the advantages radio frequency identification (RFID) brings to air cargo transportation and utilize these findings to recommend important parameters of a functional RFID prototype system to be used for air cargo tracking. Even though there are a few RFID applications in air-cargo business aside from some local solutions and smaller pilot projects for testing purposes, no major applications yet exist in this arena (Chang et al., in press).

According to the Merriam-Webster dictionary, a system is “a regularly interacting or interdependent group of items forming a unified whole” (Merriam Webster). In the case of general air cargo system, the items are the goods or freight, which can be grouped into unit load devices (ULDs) whereas the unified whole constitutes the entire distribution chain. The air cargo distribution chain starts in the cargo warehouse where the goods are accepted, after which they are loaded into ULDs, brought to the ramp, loaded onto the aircraft and flown to destination. The chain stops when the goods are picked-up at the other end. When implementing an RFID tracking system in the air cargo supply chain, it can be seen as a subsystem of the main transportation system. Therefore, for the air cargo RFID tracking system, the RFID tags are the items, the ULD tags represent the group of items and the readers and the infrastructure make the unified whole.

Goal of the system. The global air cargo RFID system should be able to gather and provide valuable information (items description, weight, dimension and location, time stamps of freight movement, alarms for temperature abuse, etc) along the transportation chain in an easy and effortless manner. The placement of RFID tags and readers should not be intrusive and should help improve operation efficiency and precision. The idea is to upgrade the quality of information without clogging or overflowing the databases with useless numbers.

The objective of this chapter is to identify the applicable points of RFID technology in the air cargo handling process. The main expected benefits would include:

- Ability to track shipments at the item level (shipment visibility)
- Improve operational performance and efficiency (simplify processes, manage recoveries and decrease processing time)
- Improved customer experience (shipment visibility online)
- Minimize reliance on manual input (reduce claims and performance failure)

However, for the implementation to give the best success it is necessary to evaluate carefully which technology is best in terms of frequency, type of tags, surrounding materials, etc. The findings in this dissertation will serve as a guideline when providing these recommendations. The following sections will describe the potential use case of RFID for each individual air cargo operation in greater detail.

Typical Air Cargo Warehouse Operations

The general process of freight handling as seen today in an air cargo warehouse is described in details in tables 7-1 to 7-5, while a brief overview is presented in Figure 7-1. The left columns of the tables describe the current process, whereas the right column explains how an RFID tracking system could improve the process. The actors

taking part are: cargo agent, station attendant, cargo planner, lead agent, booking coordinator, consignee and shipper.

The process ameliorations described in tables 7-1 to 7-5 can have more positive consequences than what they were originally designed for. In process #2 (Table 7-1), tagging every individual piece of a shipment with an RFID tag, instead of tagging every piece with the exact same label, allows unique identification of each piece as well as weight management. This is useful further down the road when they are loaded onto ULDs (process #7, Table 7-2). By knowing the weight of each single item it would be possible to estimate the ULD total weight more accurately, and therefore give a better precision to the “weight and balance” team who decides which container goes where in the cargo hold. In contrast, when a shipment of 10 boxes is accepted today, only the collective weight of all the boxes is recorded and every box has the same indentifying label (airway bill number, destination, client information, etc.), apart from showing “1 of 10”, “2 of 10”, “3 of 10”, etc. Moreover, knowing the dimension of each single item would be efficient for the planning agent (process #5, Table 7-2). For example, he could know ahead of time when an odd shaped package has to be planned onto a pallet because it would simply not fit inside a container.

ULD/item association is currently done manually and ineffectively by writing down which shipment is in which ULD (process #7, Table 7-2). Automatic association via RFID would minimize the risk of human error or hard to read messy hand writing. It could also be used to tell the station attendant if something is missing or if something should not be loaded right away. ULD tagging is not only useful for item/ULD association (process #7, Table 7-2) and ULD movement tracking in and out of the

warehouse (processes #11 and #12, Table 7-3), but also allows faster item locating and easier recovery if they were not placed in the right area. Each year, larger cargo airlines lose 5–6% of their ULD inventory – amounting to hundreds of millions of dollars in loss – due to breakdowns in their ULD tracking-facilities (Skorna and Richter, 2007).

Typical Air Cargo Ramp Operations

When ULDs and tub carts are brought to the ramp prior to loading of the aircrafts, some unpredictable and undesirable events can occur. For instance, the cargo could be dropped off at the wrong gate, or conversely, when the aircraft is being unloaded, the cargo could sit on the tarmac for a long time if the runner got the wrong message or forgot one of the ULDs at the ramp. Immediate knowledge of “which cargo is where and when” would contribute to minimization of such mistakes and optimization of the operations. Moreover, temperature tracking of perishable cargo on the tarmac could help prioritize the movement of goods by setting off alarms when sensitive products are being exposed to extreme conditions.

This study showed that even short periods of time on the tarmac could lead to high temperature elevations at the top of the ULDs (see chapter 6) for summer months. The opposite is probably true during winter, as the outside temperature is well below freezing, the freight can face highly damaging environment. Either way, cargo being exposed to outdoor conditions of all kinds is very vulnerable to temperature abuse and should be monitored to improve quality control.

Ramp operations are managed by airport employees, so when the air cargo company delivers the goods to the ramp the managing of the goods is out of their control until they are unloaded at destination. Goods can be delivered to the ramp up to 2h in advance of flight schedule. If the flight is delayed, the goods can stay on the

tarmac for long periods of time. When the weight and balance calculation is ready, the ground crew can start loading the cargo inside the plane according to the loading plan. The introduction of an RFID system would allow automatic time stamps and confirmation that cargo is on board (for operation efficiency and customer information update). Furthermore, in case a ULD is bumped (not flying on schedule) due to flight overweight for example, a message could be sent immediately to inform parties of this situation. Thus, using an RFID tracking system would help reduce the time that sensitive cargo may spend sitting on the tarmac under diverse weather conditions and sometime for long periods of time.

In addition, RFID instrumented cargo holds could permit temperature monitoring of sensitive goods. Or in a simpler application, it could notify the pilot of the recommended temperature to set the cargo hold at during flight based on the transported goods and the required temperature range information recorded on the tags. Currently, only aircrafts with temperature control capabilities are equipped with temperature sensors in their cargo hold (Howard, 2010, personal communication). Temperature monitoring would not only benefit perishables or live animals; it could also act as a back-up security system against adverse situations in the cargo hold such as fires.

Findings from this Study and Recommendations for RFID Tracking System Implementation

RFID implementation necessitates the incorporation of many factors and variables and the corresponding optimization based on the unique properties of the implementation environment. Even though the scope of the study discussed in this dissertation has not included all the aspects required for a successful commercial RFID implementation, it still provides invaluable information on some of the major variables

when implementing an RFID system such as choosing the right tag, the right frequency and the right ULD material. Following sections will describe these recommendations in greater detail.

Passive and Active RFID Tags

RFID systems can either be passive, which mean they communicate via signal backscattering and rely on RF energy transferred from the reader to the tag to power the tag; or they can be active or semi-active, meaning the tags have their own internal power source (typically a battery) to continuously power the tag and its RF communication circuitry, leading to longer read ranges than for passive tags. For the purpose of simplification, in this text, the word active will be used to represent both active and semi-active RFID tags.

RFID tags used for piece level identification are only being used once, and consequently have to be cheap. On the other hand, ULD tags can be permanently installed and reprogrammable, and therefore justifies a higher cost. From a practical point of view for air cargo, active tags are more appropriate for ULD identification because of their bigger size and longer read range. For similar reasons passive tags are better suited for piece level identification due to their smaller size and affordability. Moreover, active tags can easily support sensor applications such as temperature monitoring.

As was observed in chapter 6, cargo encounters wide temperature variations during transit, hence the need for a temperature monitoring solution. Temperature control inside the aircraft would be made possible with the use of active RFID temperature tags. RF propagation characteristics evaluated in this study (see chapter 4) would permit much better reader-tag communication for active systems than passive

systems. To achieve a RFID tag read, two communication links must be successful. First, the reader-to-tag link must not fail, and second, the tag-to-reader link has to be complete. In the case of passive systems, the success of the communication is often limited by the reader-to-tag link (Nikitin and Rao, 2006; Dobkin, 2008). The reader has a specific sensitivity in the order of -65dBm to -120dBm, whereas the passive tags have sensitivities of around -12dBm (Nikitin et al., 2009). Therefore, when the reader sends a signal into its surrounding – and the signal is attenuated with distance and interfering objects – if the tags receive enough energy to respond, their signal will most likely be received with enough energy at the reader end as well. In the case of active RFID systems, the tags do not need to collect a minimum amount of energy from the reader to broadcast. Having their own power source allows them to transmit their information autonomously. As a consequence, it is the "tag-to-reader" link that sets the limitation. In other words, it is the sensitivity of the reader that will determine the success of the communication, and therefore permit a much longer read range than for passive systems.

The signal levels observed in chapter 4 were from -16 to -27dBm for 433MHz, -6 to -17dBm for 915MHz, and -18 to -27dBm for 2.45GHz (Appendix D). If a typical passive RFID tag has a sensitivity or threshold of around -12dBm (Nikitin et al., 2009), even 915MHz would not offer enough coverage to read the tags anywhere in the cargo hold when using this test set-up (one reader antenna). Moreover, this test was performed inside an empty cargo compartment, which means the signal strengths would most likely be further reduced in the case of a fully loaded cargo hold. Further testing is required, but so far active RFID systems are thought to be a more feasible solution.

ULD Materials

Air cargo containers or ULDs can be made of different materials. Older ULDs were all made of aluminum, whereas newer ones are made of Kevlar® composite walls on an aluminum frame. Old containers are being replaced by this new style because of their much lighter weight (Howard, 2010, personal communication; Nordisk, 2010). This change is favorable to the findings of this study (see chapter 5), which state that Kevlar® is highly RF-lucent, whereas aluminum is RF-opaque. In other words, Kevlar® lets RF waves go through when aluminum totally reflects them. This result suggest that most RFID tags applied to the surface of Kevlar® UDLs would presumably lead to better readability than those applied on aluminum ULDs. Moreover, in the case of temperature monitoring, using Kevlar® ULD holds a strong advantage over aluminum since their content information could be read directly through the walls.

Frequency

Warehouse. The warehouse environment is susceptible to many external noises, such as 2-way radios, wireless networks, cell phones and automatic door entry systems, which could interfere with the RFID communication links as described in chapter 3. Based on this study, the frequencies of choice are 433MHz and 915MHz because of lower interference levels around these bands. Using 915MHz would give the flexibility of using active and/or passive RFID systems because of the higher power output allowance by FCC regulations in this band (FCC, 2008); whereas 433MHz is only suitable for active RFID systems. Using both active and passive systems could be a plausible solution as well given the use case requirements. As mentioned earlier, item tags have to be cheap because they are generally not being reused in the system, whereas container tags can be reprogrammable and permanently installed on the unit.

Taking into consideration the interference levels and the flexibility of the systems, 915MHz seems to be the best option for passive RFID, but both 433MHz and 915MHz could serve for the active. 2.4GHz displays a more significant interference due to wireless and GSM networks and thus not recommended for warehouse implementation.

Aircraft. The frequency of choice for cargo hold identification was shown to be 915MHz (see Chapter 4) because of an allowed maximum output power higher than at 433MHz (FCC, 2008) as well as a lower attenuation compared with 2.45GHz. As stated earlier, the higher signal level makes passive RFID systems a possible solution. On the other hand, when considering active systems, 433MHz might be a good alternative due to lower attenuation. However, before RFID implementation can take place inside an aircraft, many studies will have to be conducted to prove that RF signal would not be significantly interfering with other aircraft radio systems as per the Federal Aviation Administration document AC20-162 “Airworthiness approval and operational allowance of RFID systems” (FAA, 2008) which, in the end, could favor the use of passive tags.

International compatibility. ISM bands around 433MHz and 2.45GHz are available internationally. On the other hand, as much as 915MHz seems to be a good solution for many different applications, it is only allowed for use in the Americas (“region 2” according to the International Telecommunication Union). The rest of the world has different regulations for using similar frequencies, which can fall between 860-960MHz (standard ISO/IEC 18000-6). Therefore, a global air cargo tracking system would have to account for all those frequencies to be implementable everywhere. There exists tags that can function anywhere within that range, but the different regulations can imply different maximum output powers, different bandwidths, etc. Consequently, a

system that works in the United States would not necessarily work in an identical manner elsewhere. Such limitations would need to be taken into consideration in detail before a global system can be designed with assurance.

Conclusion

This chapter draws upon the results and conclusions of previous chapters to list the advantages and important parameters of a functioning RFID system from the view point of air cargo transportation. A detailed comparison of today's air cargo supply chain and an RFID enabled version is presented to show how greatly RFID would improve the visibility throughout the entire supply chain. In addition, the findings of previous chapters such as the interaction of air container materials with RFID, the advantages of different RFID frequencies in different situations, etc. are utilized to recommend parameters (such as the type of tag or the frequency band) based on the use case scenario. It is important to note that a fully functional implementation of RFID in air cargo supply chain would require full collaboration of many different parties involving private companies and government institutions. However, when the advantages presented in this chapter are taken into account, it is trivial to see such efforts would be beneficial for the entire air transportation industry.

Table 7-1. Current processes as well as proposed RFID solutions for the air cargo supply chain (cargo acceptance part).

	Cargo acceptance	
#	Today's process	Improvement with RFID system
1	Cargo agent determines origin and destination of requested service, determines compatibility of shipment with aircraft and station, and if acceptable, confirms booking with customer.	
2	Station attendant receives freight from customer and verifies size, weight and number of pieces at acceptance dock. Information is hand written on a piece of paper.	Product information is associated with the RFID tag ID which is applied to every piece of a shipment. Each piece has its own weight, dimension and special requirements (temperature, dangerous goods, live animal, priority, etc.) info associated with its RFID tag. Option: Weighing, dimensioning, tag programming and application could all be achieved automatically via a conveyor belt system.
3	Cargo agent verifies documents and accepts cargo if acceptable. He creates an airway bill (AWB), prints and places labels in a tray for station attendant.	Tag ID and AWB number are associated by reading the tag with a handheld RFID reader.
4	Station attendant attaches labels to shipment and delivers it to build-up area.	Labels have already been applied to shipment.

Table 7-2. Current processes as well as proposed RFID solutions for the air cargo supply chain (cargo build-up part).

	Cargo build-up	
#	Today's process	Improvement with RFID system
5	Cargo planner creates build-up plan.	
6	Booking coordinator pulls build-up plan.	
7	Station attendant loads shipment as per build-up plan and creates a planning load assembly (PLA) concurrently.	Container ULD: Each ULD has its own RFID tag, which is scanned simultaneously as the items are being loaded inside. This creates automatic association of the item level pieces and ULDs. This could be achieved with a wearable or handheld RFID reader. Pallet ULD: Build-up areas for pallet are predetermined by roller system on the floor. Therefore, item association could be done with a fixed RFID reader on the ceiling above the pallet build-up pit. Note: All ULD tags include their tare weight information so that shipment association gives a precise estimate of the ULD total weight after build-up.
8	Booking coordinator checks for additional shipments, adds to and finalizes build-up plan.	
9	Station attendant prepares final loads and PLAs and sends them to the planners 2h prior to the flight schedule.	The information is sent to the planner automatically from the database as the ULDs are created.
10	Planner enters information in the database and prints Runner's log.	This step is done automatically since all cargo information was updated in the database during build-up.

Table 7-3. Current processes as well as proposed RFID solutions for the air cargo supply chain (cargo to/from the ramp section).

	Cargo to/from the ramp	
#	Today's process	Improvement with RFID system
11	Station attendant stages and runs freight to aircraft 2h prior to flight schedule.	All ULD IDs are automatically read when crossing the warehouse export doors (portal RFID reader). Database is updated of the goods departure.
(Cargo delivered at the ramp is now in the hands of airport employees)		
12	Station attendant checks teletype for any special commodities messages (for inbound freight), retrieves time sensitive goods first and delivers to warehouse and informs Lead agent.	Station attendant receives an alarm when time sensitive goods are ready for pick-up. An additional message tells him the required temperature of the item for proper storage location in warehouse. All ULDs are automatically read at warehouse inbound door. Database is automatically updated of the goods arrival.
13	Station attendant retrieves and delivers non time-sensitive goods to import side of warehouse.	All ULDs were automatically read at warehouse inbound door. Database is automatically updated of the goods arrival.
14	Cargo agent (In-flight coordinator) begins database check-in, prints inbound manifest and verifies with physical goods.	Already done by automatic reading of the goods through inbound doorway entrance.

Table 7-4. Current processes as well as proposed RFID solutions for the air cargo supply chain (cargo break-down and storage section).

	Cargo break-down and storage	
#	Today's process	Improvement with RFID system
15	Station attendant sends copy of inbound manifest to lead agent, retrieves non shipper loaded units from storage, breaks down and sorts by AWB, moves to appropriate location, scans notes location on AWB and returns completed manifest to cargo agent.	During break-down, every piece is disassociated from the ULD, the same way it was associated previously. Pieces are read and associated with their storage location.
16	Station attendant moves shipper loaded units (SLUDs) and connecting shipments to proper location.	ULD tags should be read and associated with their waiting location.
17	Cargo agent checks-in SLUDs in database.	Automatic with scanning in previous step.
18	Cargo agent check-in goods not previously scanned, determines if pieces or entire shipments are missing, performs missing cargo transaction and completes check-in process.	Missing cargo should be triggered automatically since all goods were read at the inbound door.
19	Cargo agent identifies perishable, Live or hold for pick-up, contacts customer electronically or by phone, records conversation, completes paperwork and waits for customer to contact back. If no contact within 14 days warning is mailed to consignee. If no contact within 30 days, final warning is mailed to consignee and shipment is destroyed if destination is domestic or reported if not domestic.	Alarm is sent to cargo agent when time sensitive shipments have entered the warehouse. Customer receive an automatic email when their goods have arrived at the warehouse and are ready for pick-up.
20	Cargo agent determines if customer requires delivery. If "no" and goods are perishable, live or priority, cargo agent informs customer of 24h pick-up window, otherwise informs customer of 48h pick-up window. If "yes", arranges for ground transportation as per customer priority.	Automatic from database through email.

Table 7-5. Current processes as well as proposed RFID solutions for the air cargo supply chain (cargo delivery part).

	Cargo delivery	
#	Today's process	Improvement with RFID system
21	Cargo agent delivers documents to broker or consignee if delivery is requested and goods are not domestic, for Customs clearance. Once cleared, cargo agent checks AWB for Customs stamp.	
22	Cargo agent obtains consignee signature on AWB and collects outstanding charges for goods picked up, completes delivery process in database and identifies warehouse location on AWB, stamps "OK to release" on AWB and delivers AWB to consignee.	
23	Station attendant receives AWB from consignee, checks for "OK to release" stamp and retrieves shipment.	Before goods are released, an RFID read is required to update the database.
24	Station attendant ensures that consignee inspects shipment for damage before delivery and releases to if not damaged. If damaged, completes bad order report and attach to AWB.	Final database update, case closed.

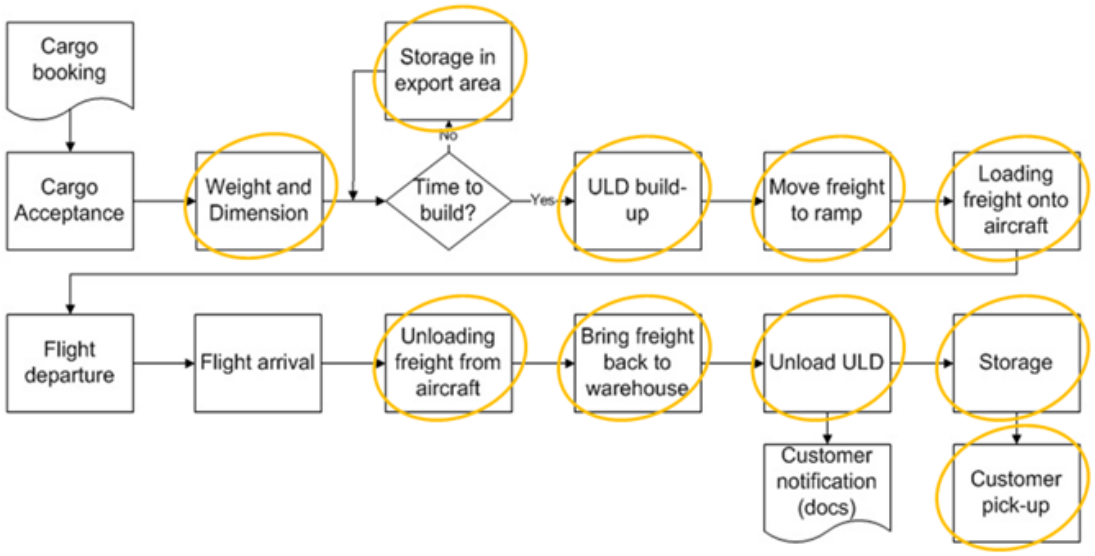

Figure 7-1. Overview of the air cargo operations where the circled steps represent suggested RFID reading points.

CHAPTER 8
GENERAL CONCLUSION

The goal of this dissertation was to explore the possibility of using radio frequency identification (RFID) to improve air cargo operations in terms of efficiency, safety and monitoring. This study showed interference levels at three ultra high frequencies (UHF) recorded in two air cargo warehouses. The interference levels from highest to lowest were at 2.45GHz, 433MHz and 915MHz respectively. There are ways to filter out interferences when designing an RFID system, and most of today's high end readers have that feature. However, the best way to avoid possible disturbing noises is surely to install the RFID system in an interference free environment. According to the results of these tests, which were performed inside two warehouses which may or may not give a realistic representation of all air cargo warehouses in the world, implementation of RFID systems at 915MHz in North America would bring the best results, interference-wise.

This study also demonstrated that frequencies have a major influence on signal propagation, especially inside a metal environment. Lower frequencies suffer less attenuation over distance, but have higher variation within the cargo hold. It was also demonstrated that antenna polarization can have a significant effect on signal propagation in some cases, and therefore should not be omitted when designing an RFID system for air cargo transportation. Moreover, FCC regulations restricts output powers at 433MHz more than at 915MHz and 2.45GHz, leading to the conclusion that more RF energy would be available in the cargo hold for reader/tag communication at 915MHz than at the other frequencies tested. Moreover, the study showed that the relationship between signal strength and tag reads is an important tool to take into account when implementing RFID systems.

This dissertation verified the effects of five commonly used air cargo container wall materials on RF propagation at the same three different frequencies. Three different tests were utilized to analyze the characteristics of RF propagation for each material and the results from all experiments showed a very strong effect of aluminum on RF transmission and minimal interaction for all other sample materials as expected. These finding suggest that the use of non-metallic containers for air transportation of perishable products should make real time temperature monitoring possible by allowing RF waves to transmit through the wall surface effortlessly.

This study demonstrated that a major temperature gradient can be found within the same ULD during ground operations as well as during flight, especially when the flight time exceeds 4h. Therefore, it is suggested that temperature sensitive shipments should be placed accordingly inside the ULD. This test was performed in the summer, for that reason, the increase of temperature during ground operations should be considered variable. However, the temperature distribution observed during flight should be consistent through the year since temperatures at high altitude do not vary widely.

This work presented a detailed comparison of today's air cargo supply chain and an RFID enabled version to show how greatly RFID would improve the visibility throughout the entire supply chain. It is important to note that a fully functional implementation of RFID in air cargo supply chain would require full collaboration of many different parties involving private companies and government institutions. However, when the advantages presented in this dissertation are taken into account, it is trivial to see such efforts would be beneficial for the entire air transportation industry.

APPENDIX A
DC-10 CARGO HOLD AND CARGO DOOR SPECS

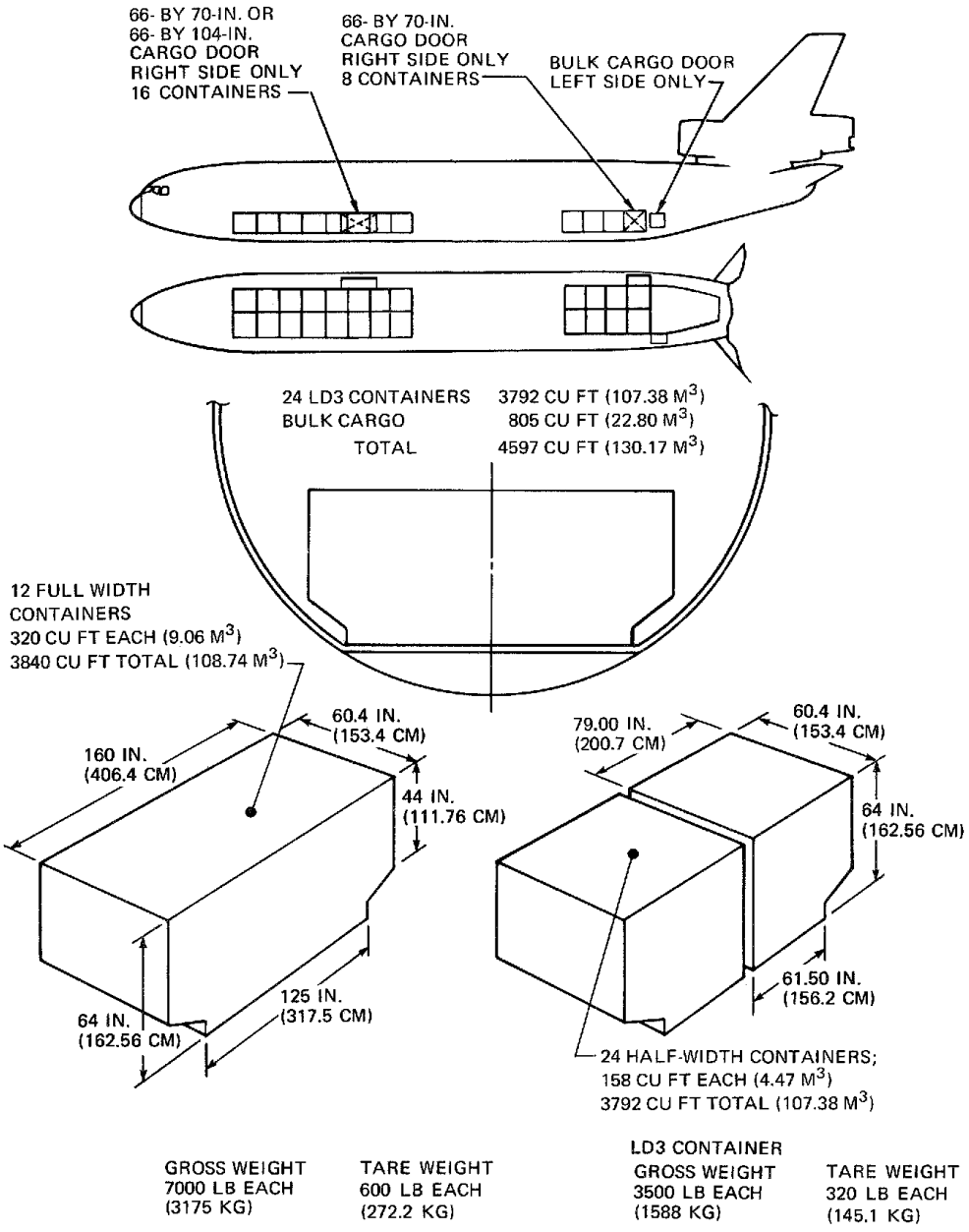

Figure A-1. Standard cargo compartment and containers for model DC-10 series 10, 10CF, 30, 30CF, 40 and 40CF (Boeing, 2010c).

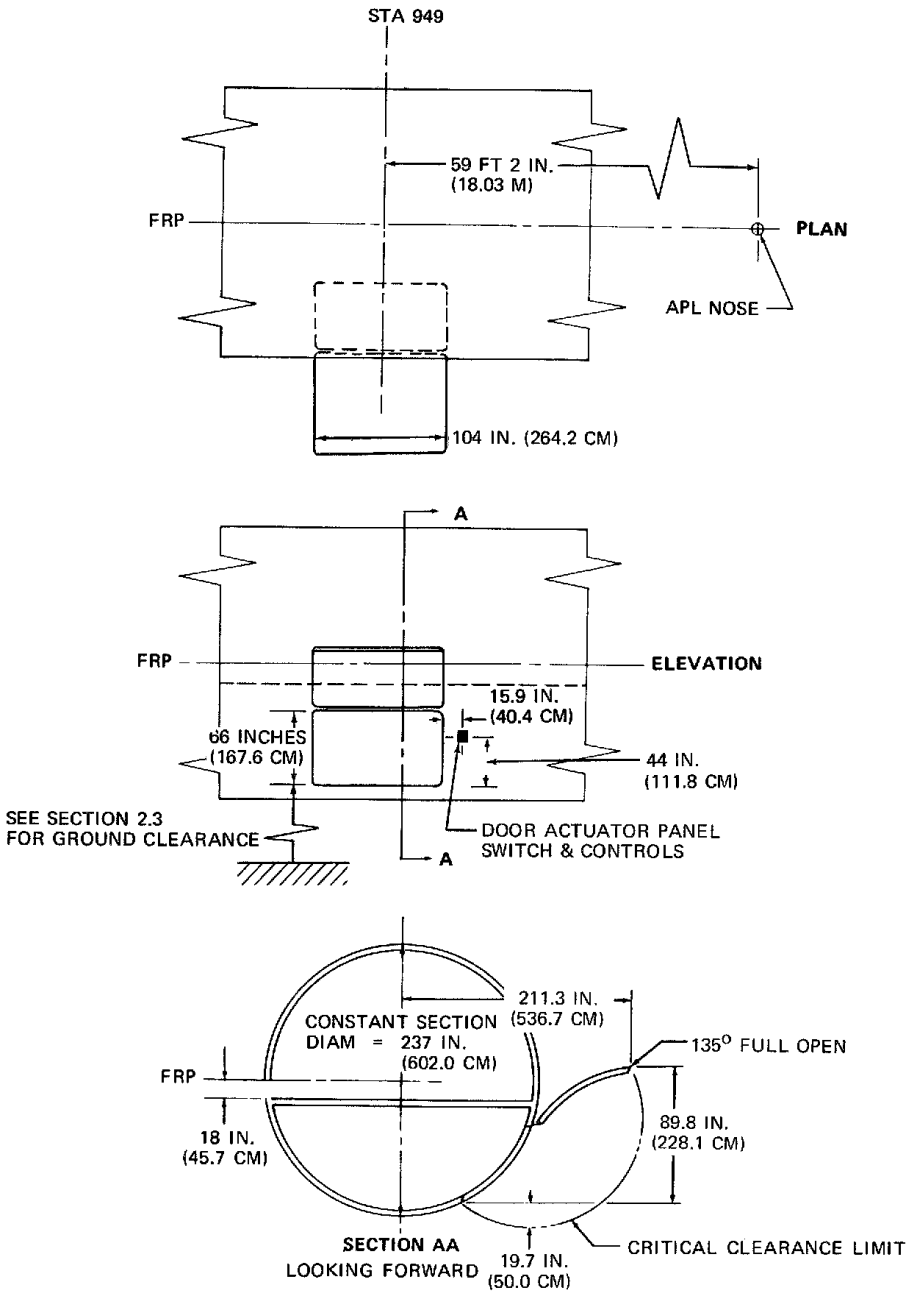

Figure A-2. Forward cargo loading door, model DC-10 series 10, 10CF, 30, 30CF, 40 and 40CF (Boeing, 2010c).

APPENDIX B
RADIO FREQUENCY ATTENUATION SURFACE PLOTS

All plots are following the color coded spectrum where red is high attenuation, or 70dBm (weak signal) and purple is low attenuation, or 30dBm (strong signal) as indicated in the example graph below. Slices are numbered from 1 to 12 which represent the distance from the front of the cargo hold in meters. Surface plots are shown as if you were standing at the back of the aircraft, looking forward. Therefore, the right side of the plot is the starboard side of the vessel and the left is port, as also indicated in the example plot below.

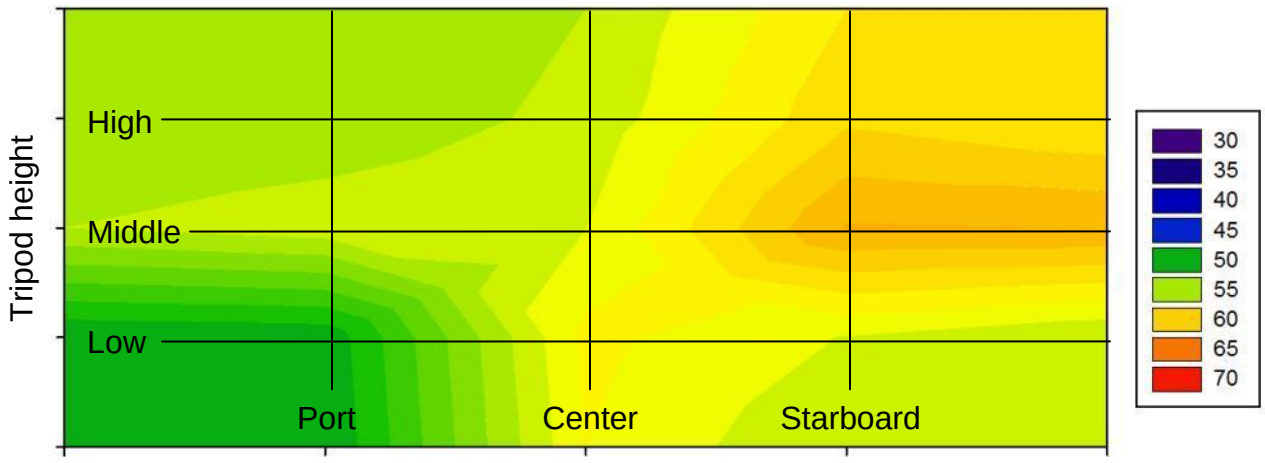

Figure B-1. Attenuation surface plot example – one slice of data (dBm)

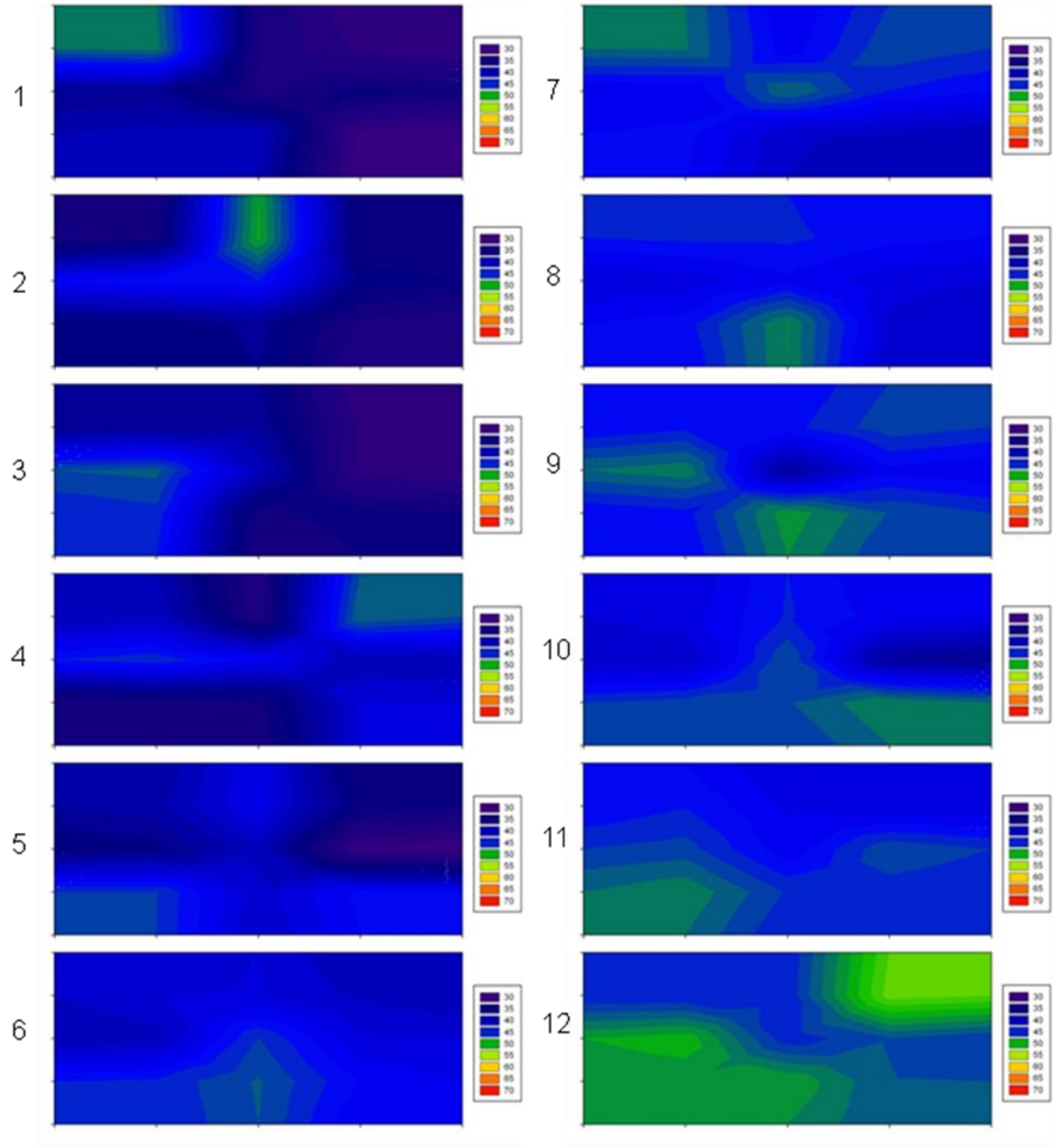

Figure B-2. Attenuation surface plot for 433MHz, top end antenna position and circular polarization.

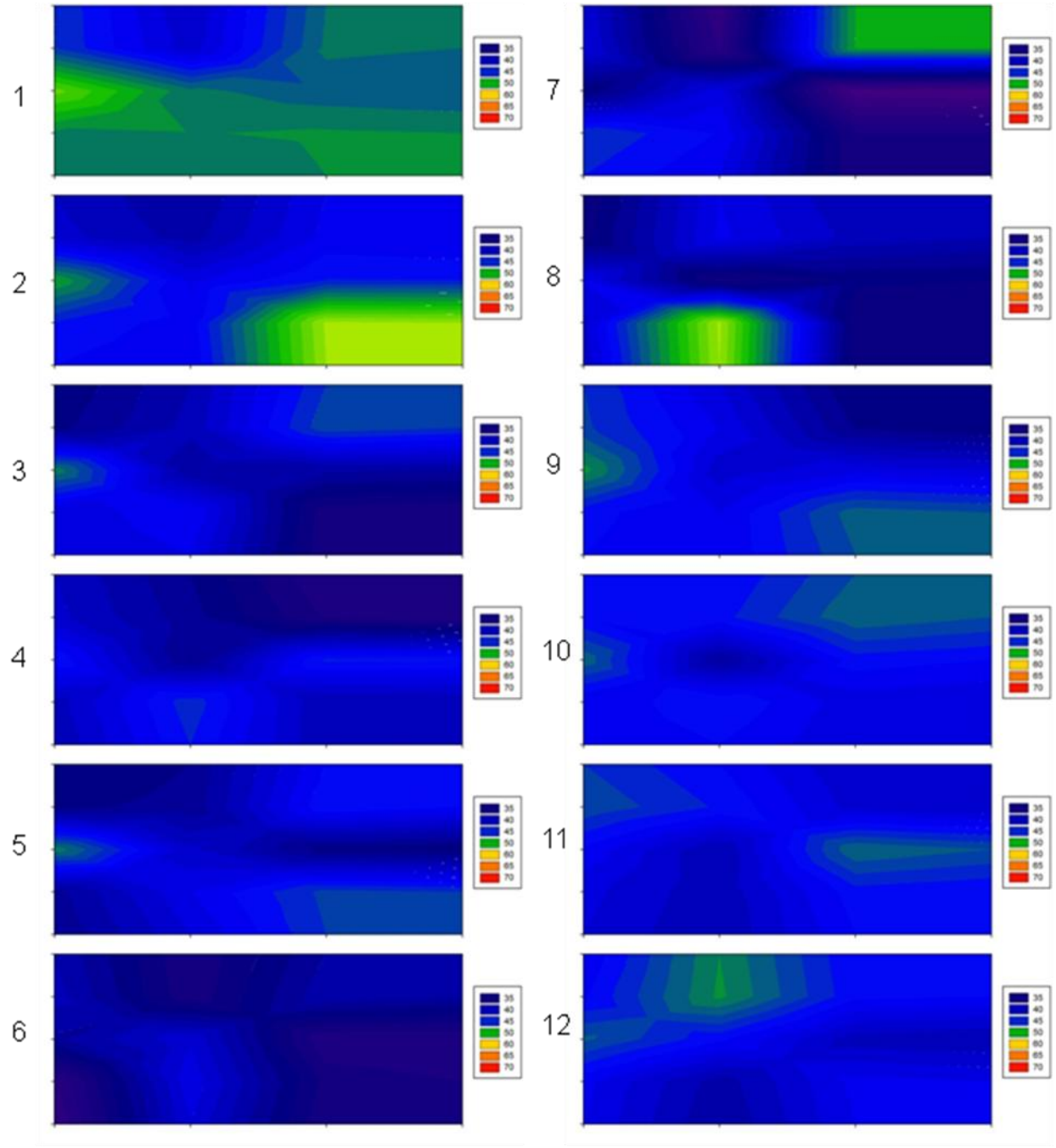

Figure B-3. Attenuation surface plot for 433MHz, center ceiling antenna position and circular polarization.

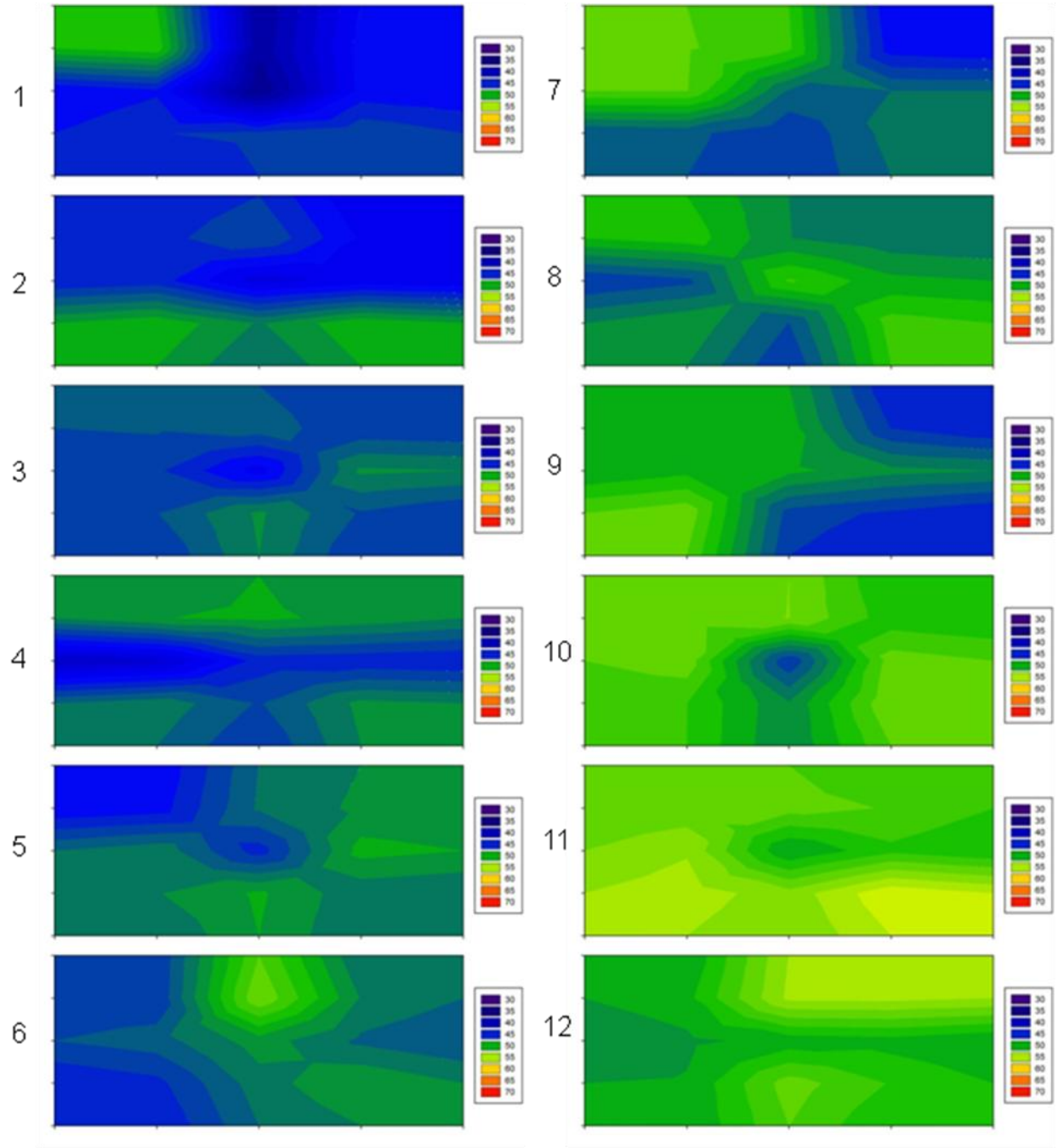

Figure B-4. Attenuation surface plot for 915MHz, top end antenna position and circular polarization.

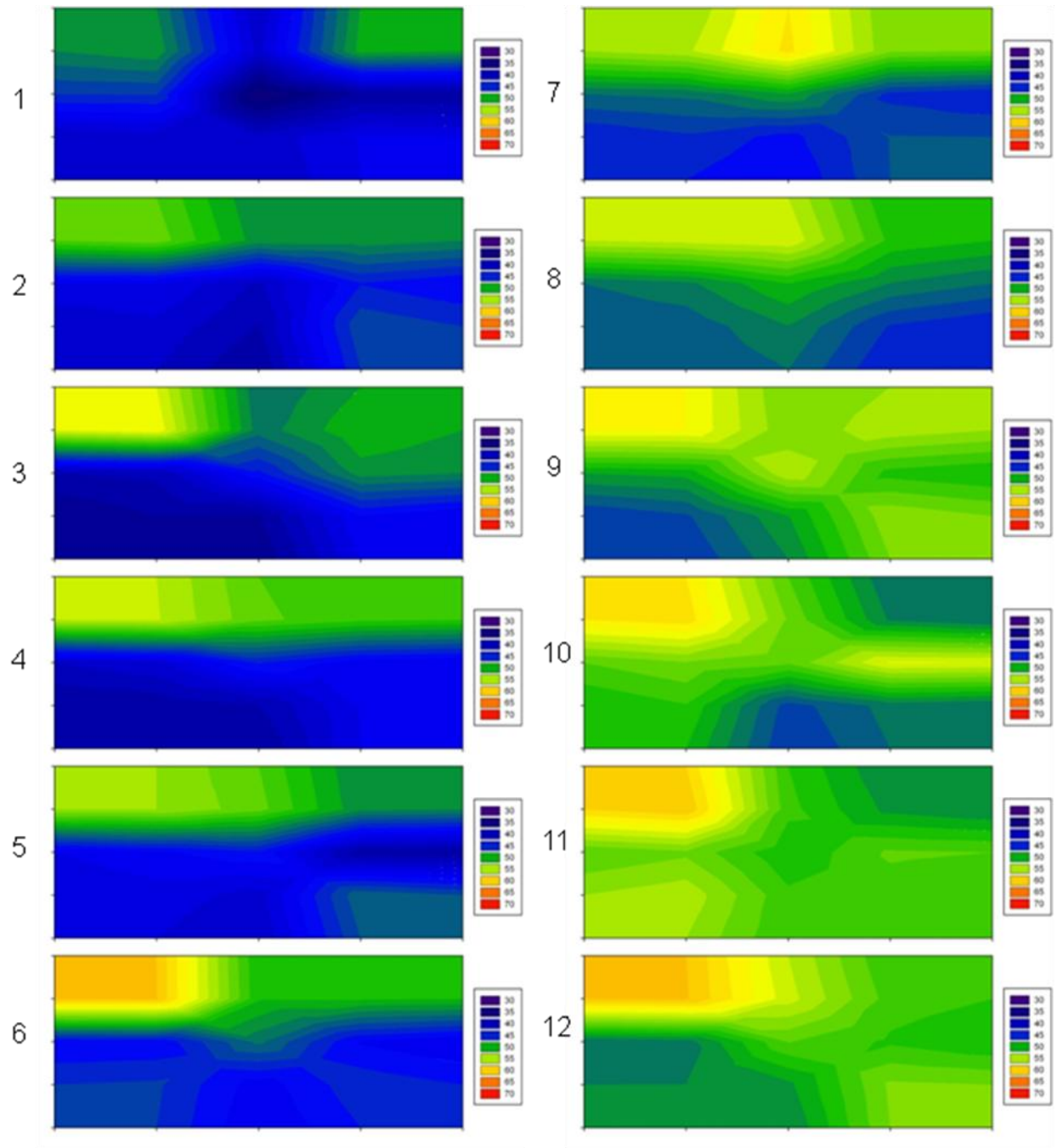

Figure B-5. Attenuation surface plot for 915MHz, top end antenna position and linear polarization.

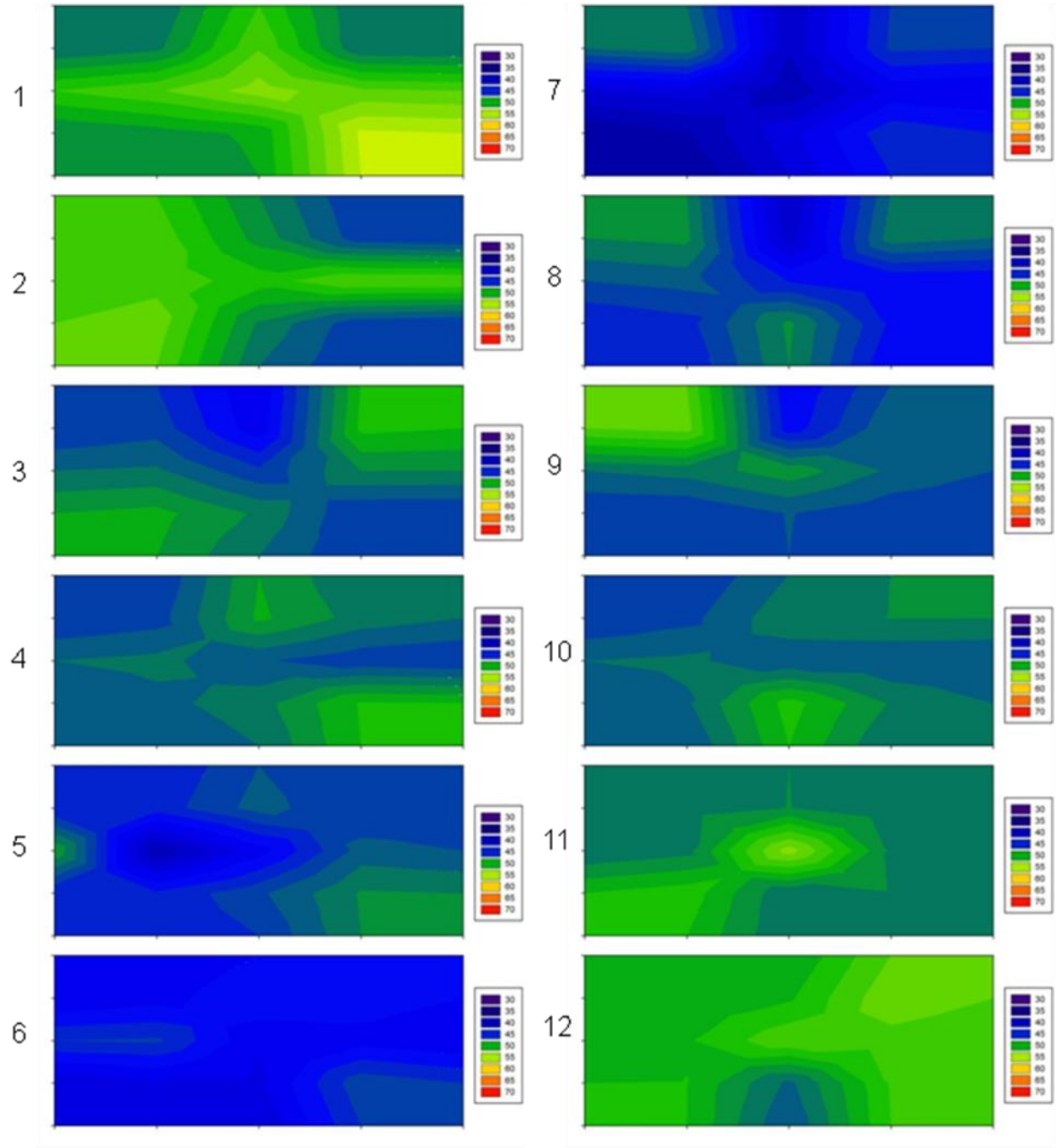

Figure B-6. Attenuation surface plot for 915MHz, center ceiling antenna position and circular polarization.

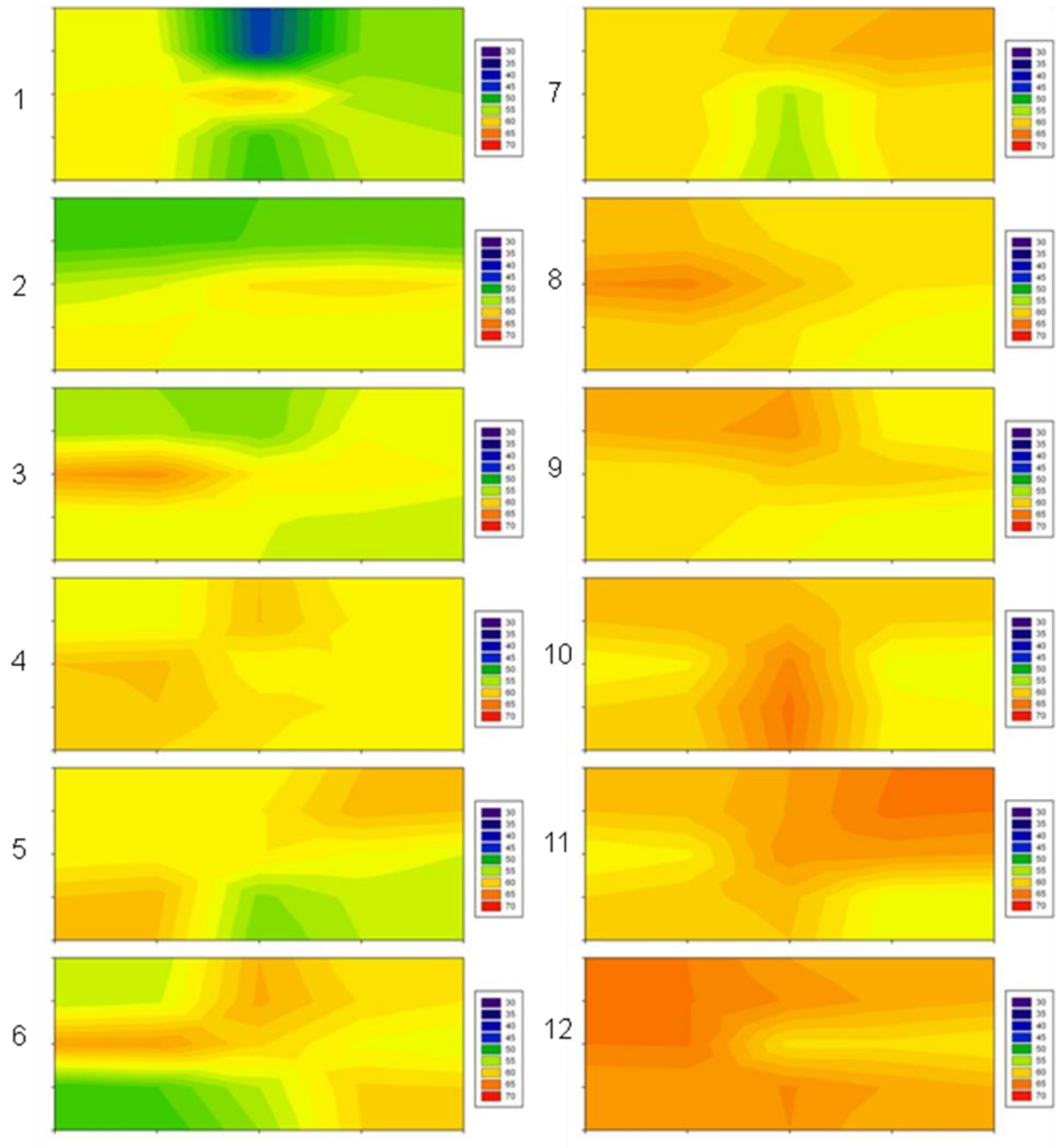

Figure B-7. Attenuation surface plot for 2.45GHz, top end antenna position and circular polarization.

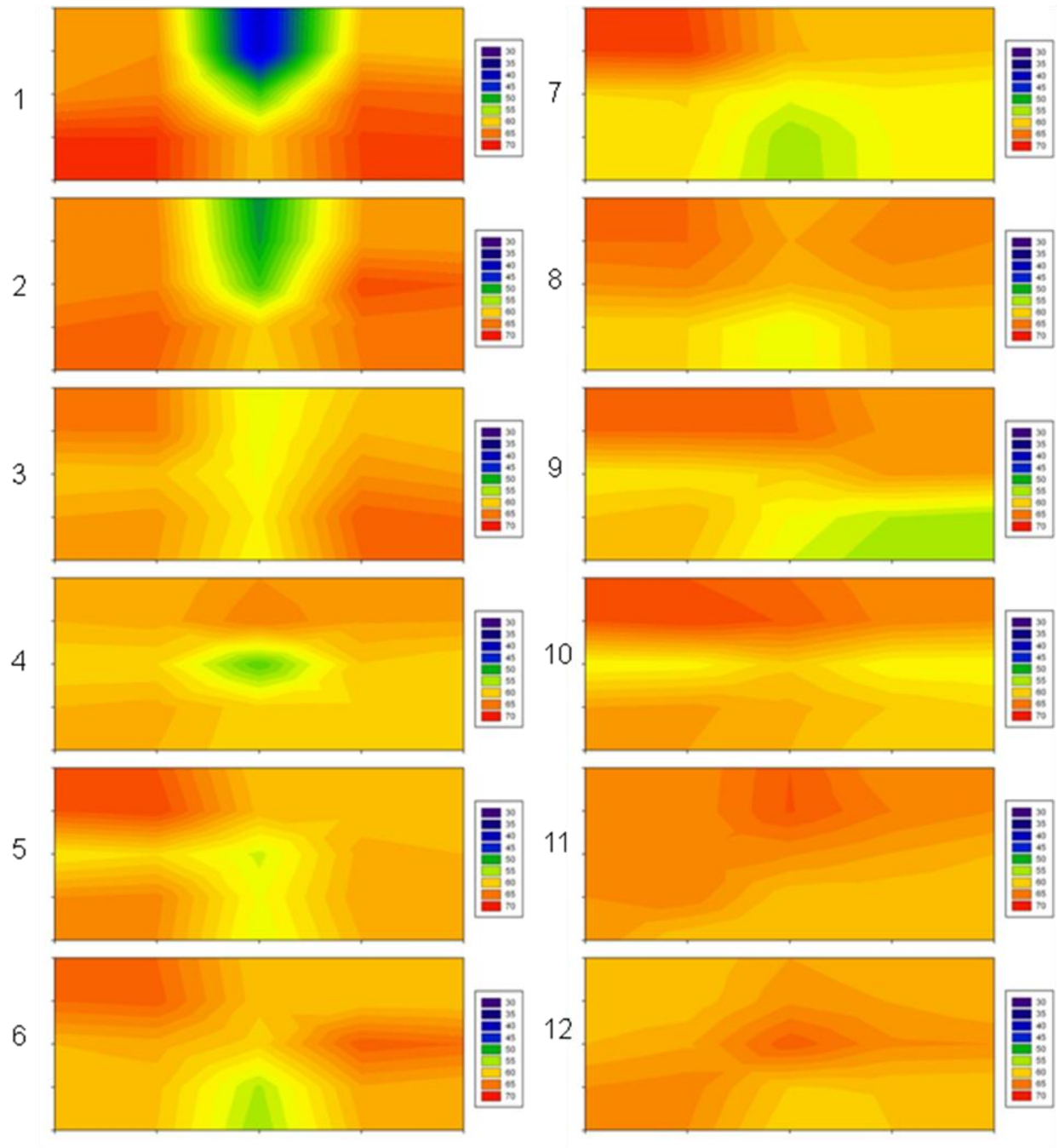

Figure B-8. Attenuation surface plot for 2.45GHz, top end antenna position and linear polarization.

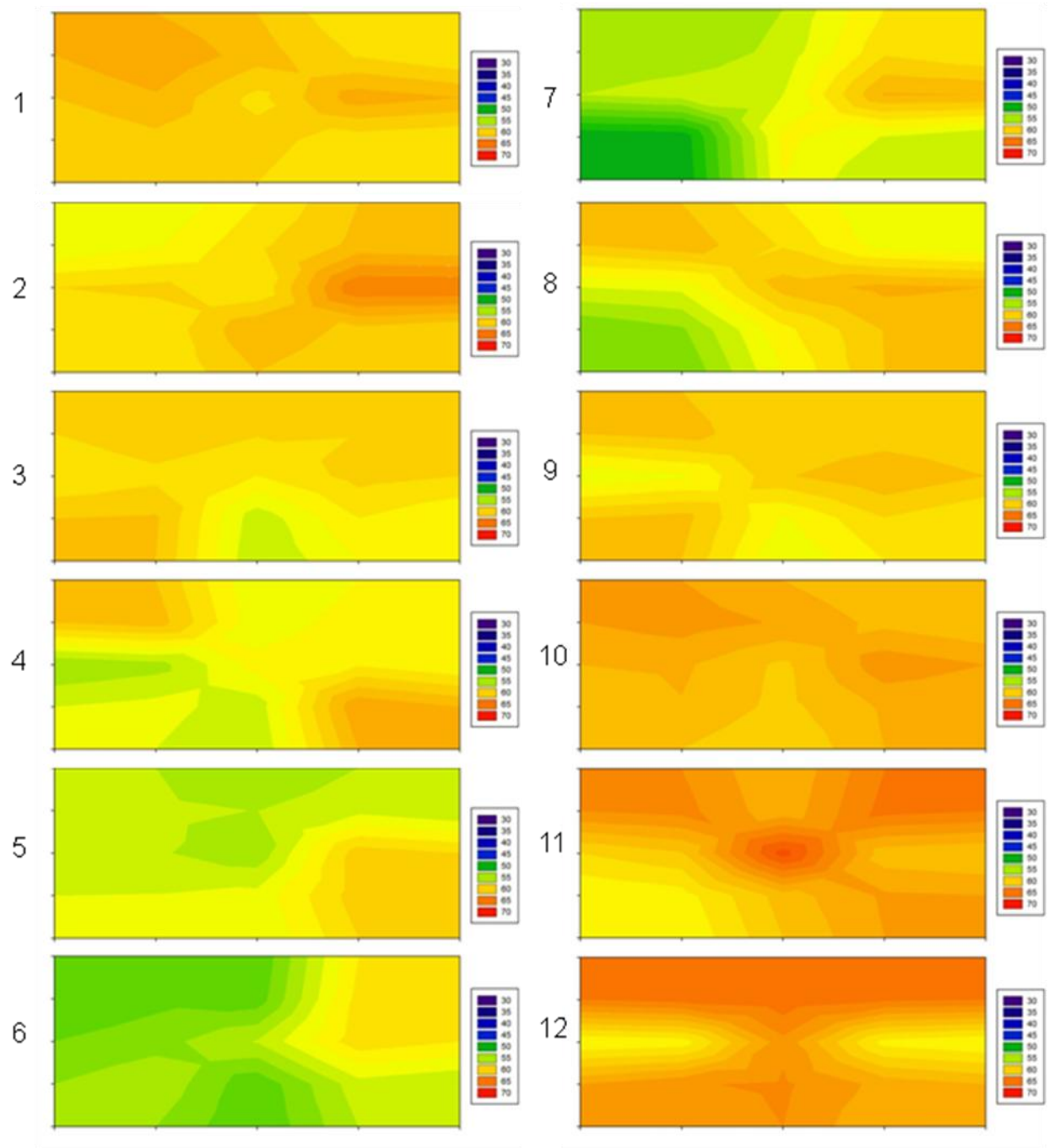

Figure B-9. Attenuation surface plot for 2.45GHz, center ceiling antenna position and circular polarization.

APPENDIX C
STATISTICAL ANALYSIS RESULTS FOR DC-10 RADIO FREQUENCY PROPAGATION

All statistical analyses were computed using SAS 9.1 (SAS Institute Inc., Cary NC) and significance was accepted at level $\alpha = 0.01$.

Table C-1. Effects of frequency, antenna location and antenna polarization on attenuation levels of the complete dataset.

Effects	mean	F value	p-value
Frequency			
433MHz	41.69		
915MHz	47.64	1258.26	< 0.0001
2.45GHz	59.34		
Location			
Top End	51.39	15.19	< 0.0001
Ceiling	49.12		
Polarization			
Circular	49.23	68.81	< 0.0001
Linear	54.47		

Table C-2. Effect of width on attenuation levels for each frequency, antenna location and polarization.

Constants			Effects	mean	F value	p-value
Frequency	Location	Polarization	Width			
433	Top End	Circular	Port	42.63	2.06	0.1328
			Center	42.03		
			Starboard	40.45		
		Linear	Port	N/A	N/A	N/A
			Center	N/A		
			Starboard	N/A		
	Ceiling	Circular	Port	42.51	0.84	0.4343
			Center	41.22		
			Starboard	41.30		
915	Top End	Circular	Port	48.36	0.46	0.6331
			Center	47.57		
			Starboard	48.06		
		Linear	Port	48.85	0.62	0.5417
			Center	47.38		
			Starboard	47.84		
	Ceiling	Circular	Port	46.94	0.39	0.6760
			Center	46.55		
			Starboard	47.26		
2450	Top End	Circular	Port	58.77	0.7	0.4992
			Center	58.32		
			Starboard	57.87		
		Linear	Port	62.60	12.5	< 0.0001
			Center	58.39		
			Starboard	61.75		
	Ceiling	Circular	Port	58.11	3.04	0.0522
			Center	58.47		
			Starboard	59.77		

Table C-3. Effect of height on attenuation levels for each frequency, antenna location and polarization.

Constants			Effects	mean	F value	p-value
Frequency	Location	Polarization	Height			
433	Top End	Circular	High	41.51	0.25	0.7770
			Middle	41.43		
			Low	42.16		
	Top End	Linear	High	N/A	N/A	N/A
			Middle	N/A		
			Low	N/A		
	Ceiling	Circular	High	41.11	0.46	0.6353
			Middle	41.74		
			Low	42.18		
915	Top End	Circular	High	48.43	2.16	0.1210
			Middle	47.01		
			Low	48.54		
	Top End	Linear	High	52.66	27.13	< 0.0001
			Middle	46.37		
			Low	45.03		
	Ceiling	Circular	High	46.86	0.01	0.9936
			Middle	46.94		
			Low	46.94		
2450	Top End	Circular	High	58.25	0.94	0.3943
			Middle	58.87		
			Low	57.85		
	Top End	Linear	High	61.91	1.61	0.2054
			Middle	60.28		
			Low	60.54		
	Ceiling	Circular	High	59.16	0.8	0.4524
			Middle	58.92		
			Low	58.28		

Table C-4. Effect of depth on attenuation levels for each frequency, antenna location and polarization.

Constants			Effects	mean	F value	p-value
Frequency	Location	Polarization	Depth	(dBm)		
433MHz	Top End	Circular	1	36.61	6.28	< 0.0001
			2	38.97		
			3	37.73		
			4	39.65		
			5	39.15		
			6	42.32		
			7	43.51		
			8	43.30		
			9	44.41		
			10	43.47		
			11	44.21		
			12	47.11		
	Top End	Linear	1	N/A	N/A	N/A
			2	N/A		
			3	N/A		
			4	N/A		
			5	N/A		
			6	N/A		
			7	N/A		
			8	N/A		
			9	N/A		
			10	N/A		
			11	N/A		
			12	N/A		
	Ceiling	Circular	1	46.96	3.61	0.0003
			2	44.10		
			3	40.47		
			4	39.97		
			5	40.82		
			6	36.92		
			7	39.03		
			8	40.08		
			9	42.96		
			10	43.24		
			11	42.58		
			12	42.93		

Table C-4. Continued

Constants			Effect	Mean	F value	p-value
Frequency	Location	Polarization	Depth	(dBm)		
915MHz	Top End	Circular	1	43.63	8.33	< 0.0001
			2	45.48		
			3	45.99		
			4	46.45		
			5	47.21		
			6	47.67		
			7	47.94		
			8	48.72		
			9	48.28		
			10	50.95		
			11	52.67		
			12	50.94		
	Top End	Linear	1	42.22	4.88	< 0.0001
			2	44.54		
			3	44.94		
			4	45.02		
			5	45.40		
			6	47.32		
			7	49.07		
			8	49.64		
			9	52.04		
			10	51.61		
			11	52.48		
			12	51.94		
	Ceiling	Circular	1	50.81	11.82	< 0.0001
			2	49.51		
			3	46.75		
			4	47.27		
			5	44.68		
			6	43.25		
			7	42.37		
			8	45.15		
			9	46.86		
			10	47.35		
			11	43.59		
			12	50.32		

Table C-4. Continued

Constants			Effect	Mean	F value	p-value
Frequency	Location	Polarization	Depth	(dBm)		
2.45GHz	Top End	Circular	1	54.57	5.83	< 0.0001
			2	55.44		
			3	56.77		
			4	58.37		
			5	57.55		
			6	57.78		
			7	58.29		
			8	59.38		
			9	59.09		
			10	59.96		
			11	60.69		
			12	61.90		
		Linear	1	60.05	0.53	0.8819
			2	60.70		
			3	60.81		
			4	59.82		
			5	60.65		
			6	61.07		
			7	59.12		
			8	61.41		
			9	60.61		
			10	61.57		
			11	62.92		
			12	62.17		
	Ceiling	Circular	1	59.99	9.95	< 0.0001
			2	59.55		
			3	58.61		
			4	57.56		
			5	56.31		
			6	54.82		
			7	55.94		
			8	58.40		
			9	59.19		
			10	61.16		
			11	61.77		
			12	62.08		

APPENDIX D
RADIO FREQUENCY SIGNAL STRENGTH PROPAGATION SURFACE PLOTS

All plots are following the color coded spectrum where purple is high signal strength, or 0dBm and red is low signal strength, or -40dBm as indicated in the example graph below. Slices are numbered from 1 to 12 which represent the distance from the front of the cargo hold in meters. Surface plots are shown as if you were standing at the back of the aircraft, looking forward. Therefore, the right side of the plot is the starboard side of the vessel and the left is port, as also indicated in the example plot below.

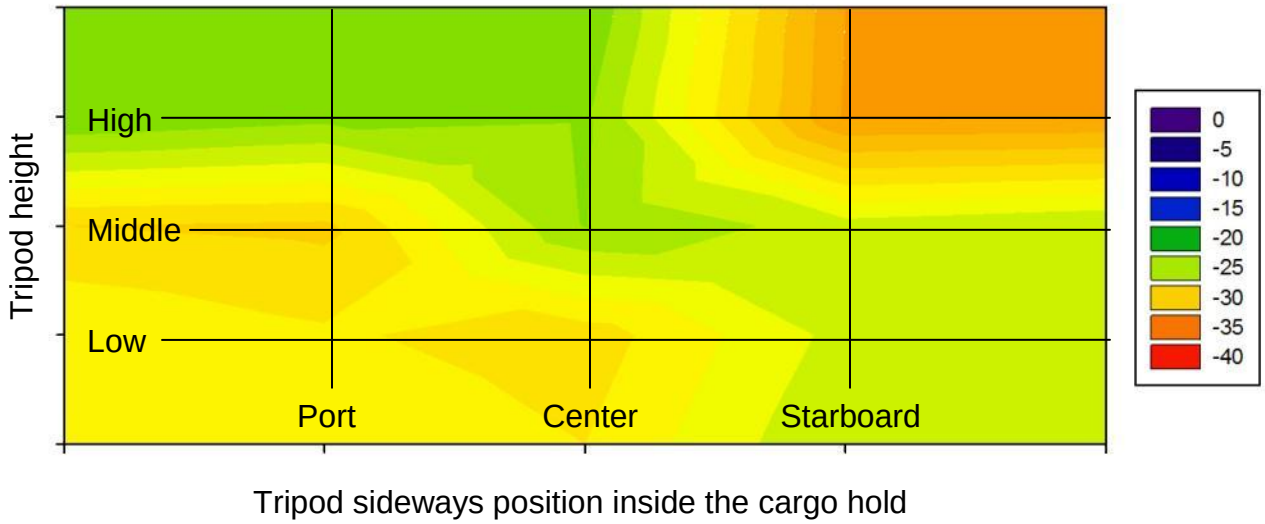

Figure D-1. Signal strength surface plot example – one slice of data (dBm)

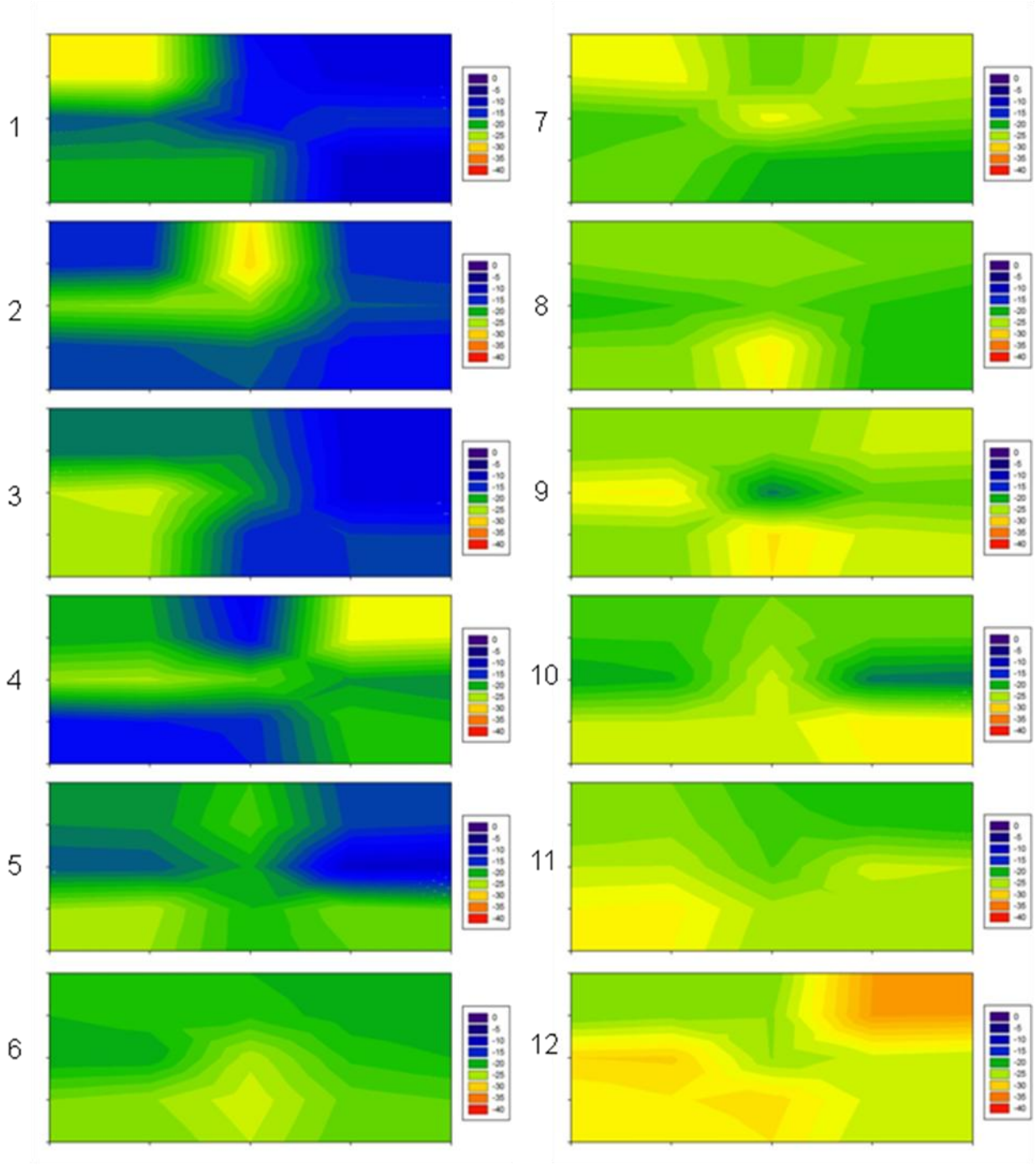

Figure D-2. Signal strength surface plot for 433MHz, top end antenna position and circular polarization.

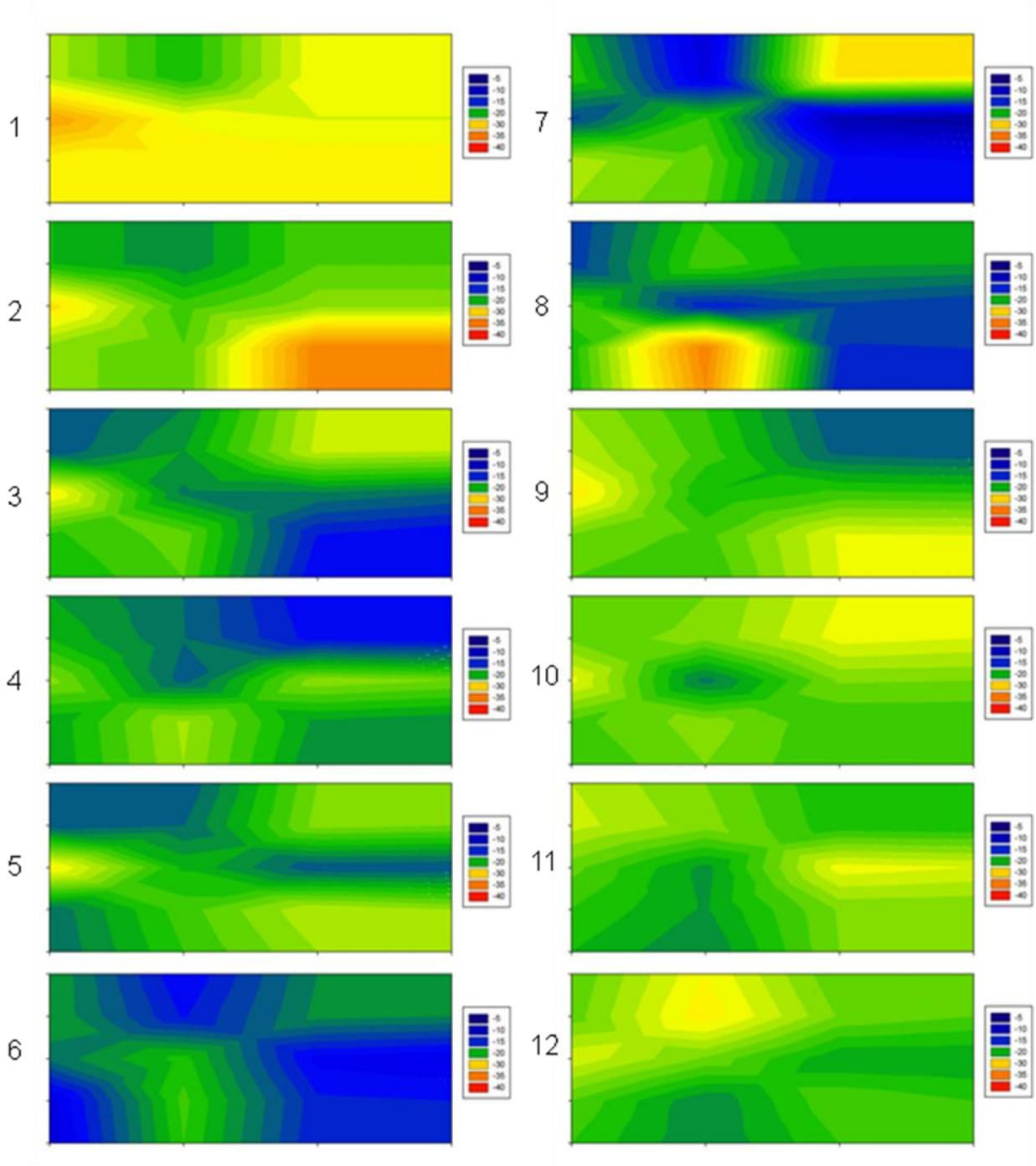

Figure D-3. Signal strength surface plot for 433MHz, center ceiling antenna position and circular polarization.

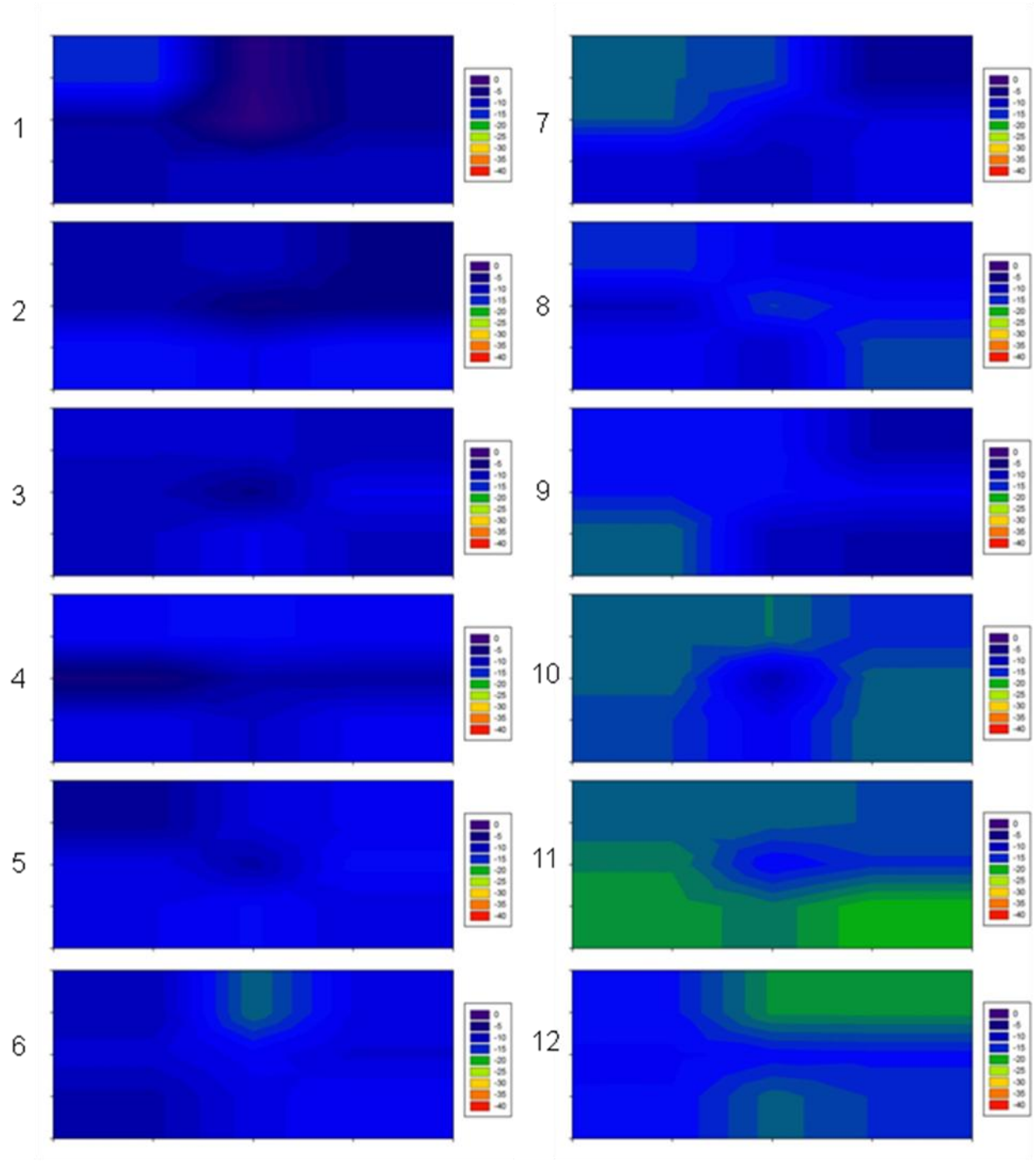

Figure D-4. Signal strength surface plot for 915MHz, top end antenna position and circular polarization.

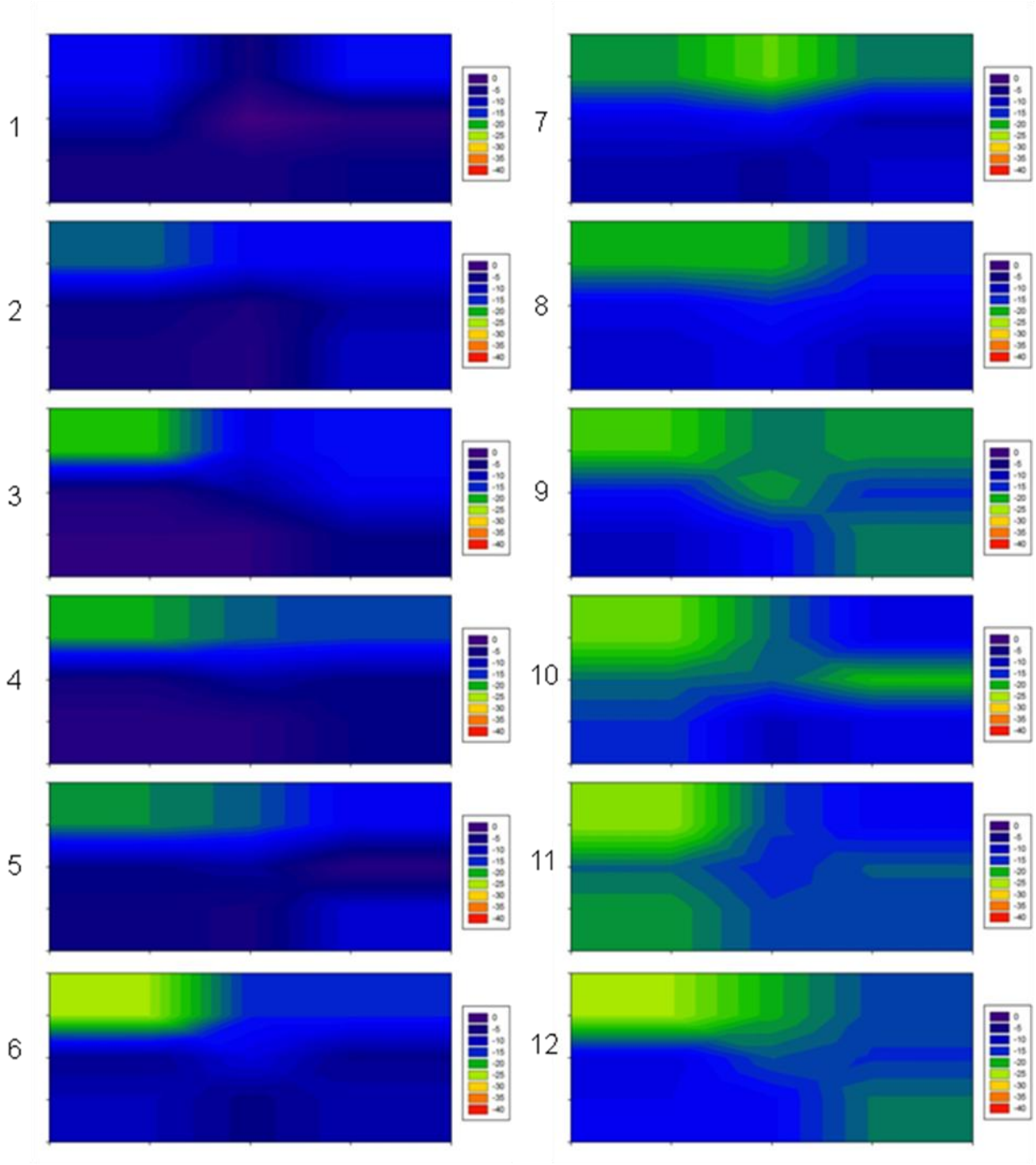

Figure D-5. Signal strength surface plot for 915MHz, top end antenna position and linear polarization.

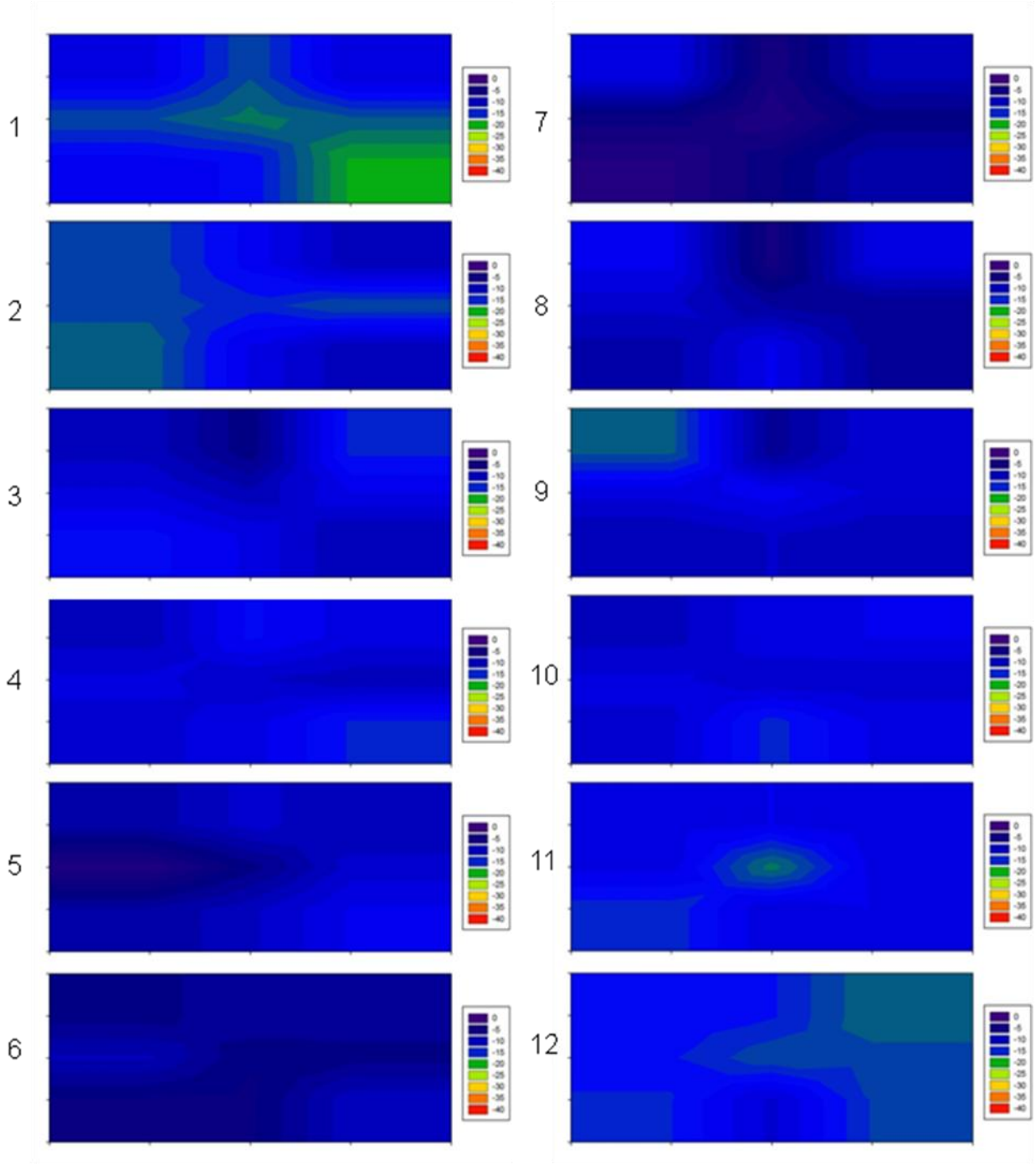

Figure D-6. Signal strength surface plot for 915MHz, center ceiling antenna position and circular polarization.

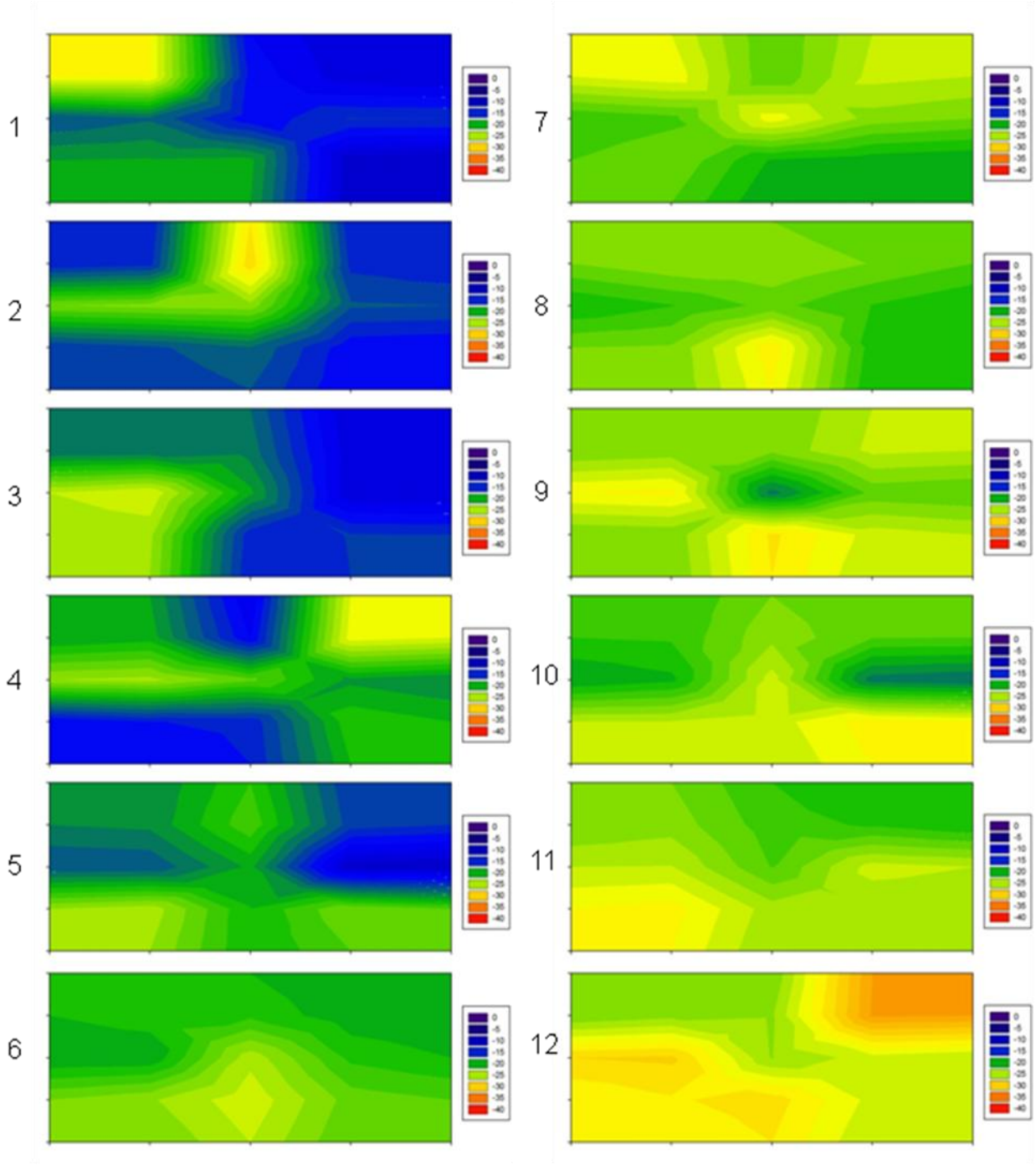

Figure D-7. Signal strength surface plot for 2.45GHz, top end antenna position and circular polarization.

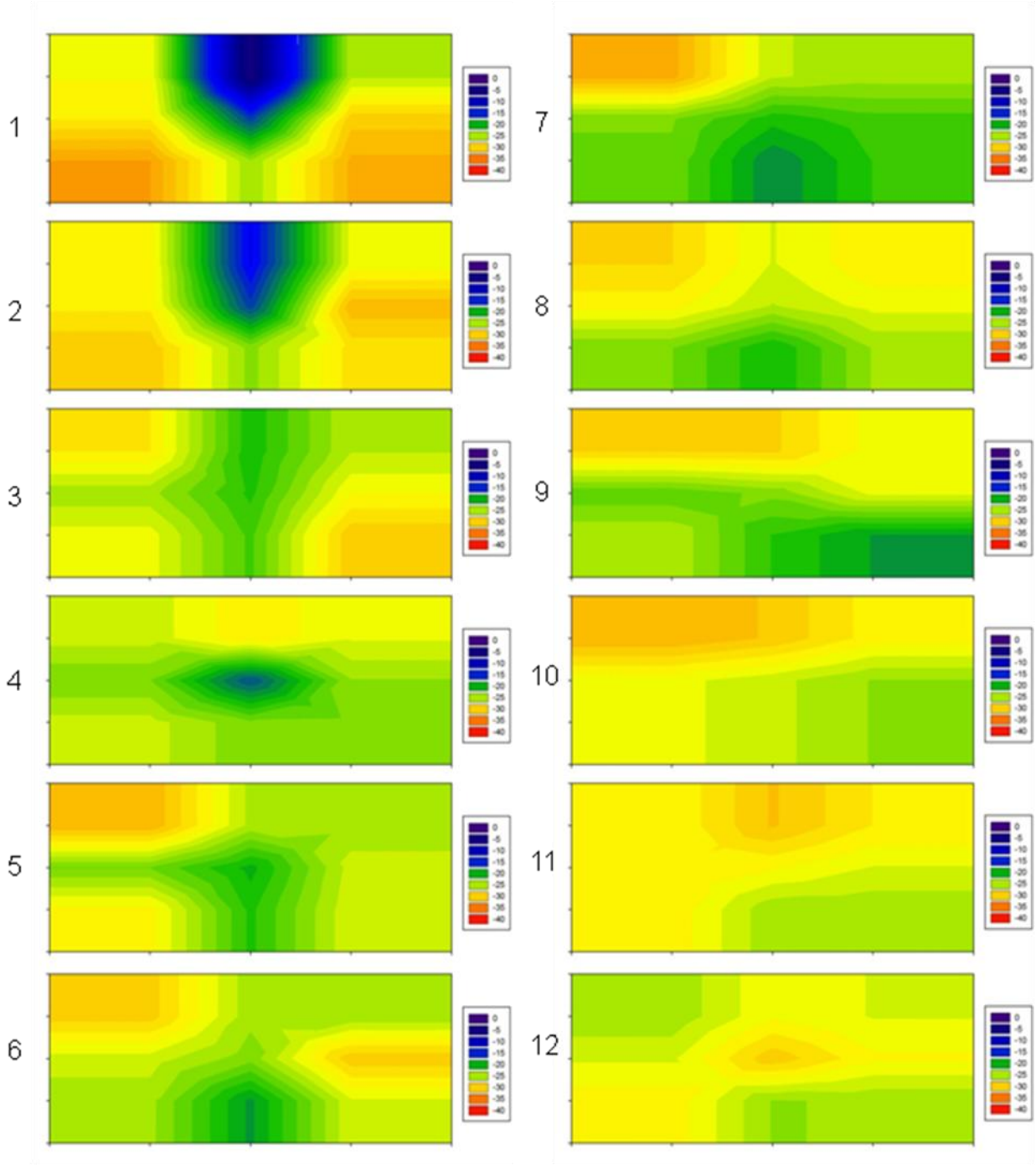

Figure D-8. Signal strength surface plot for 2.45GHz, top end antenna position and linear polarization.

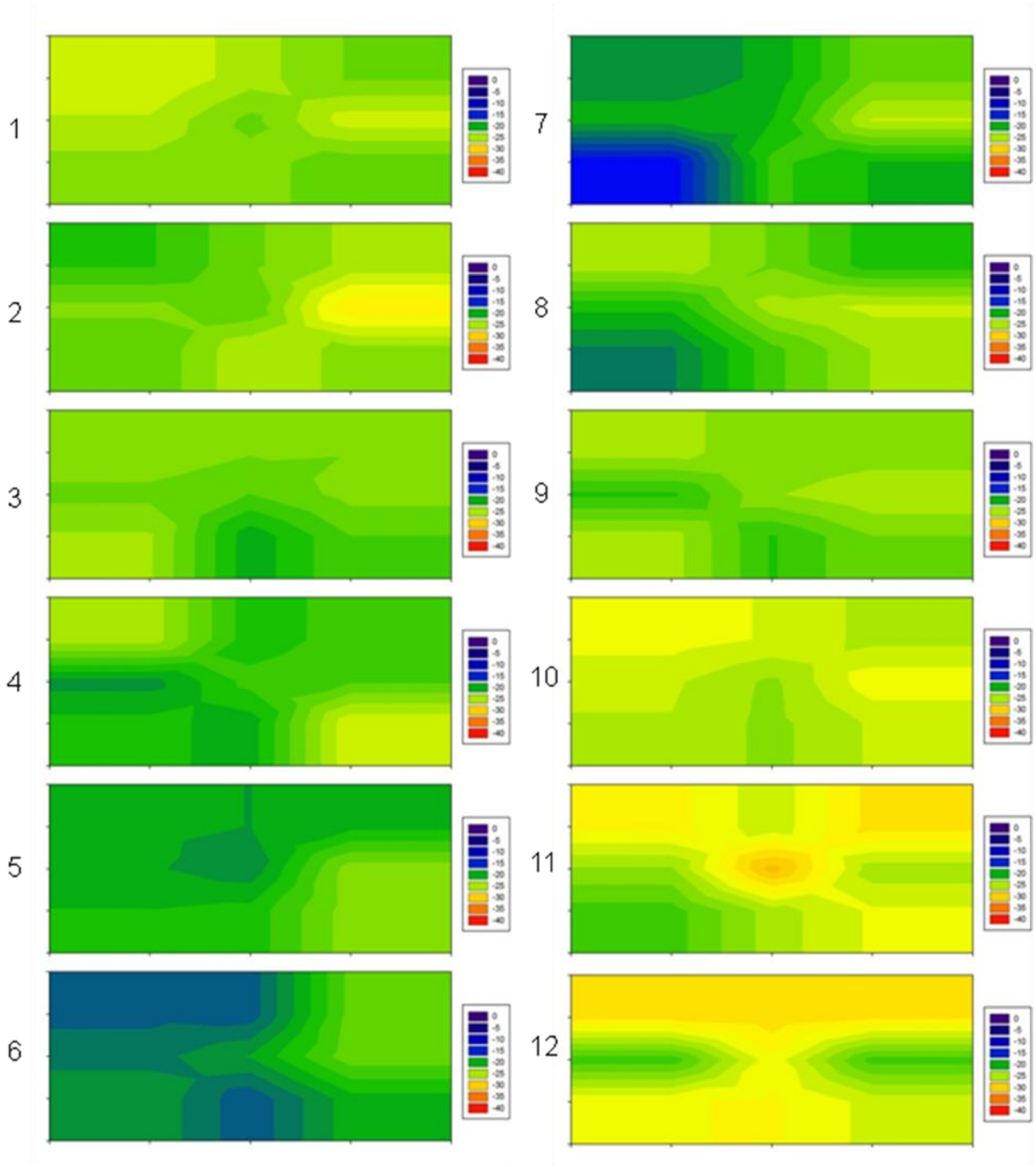

Figure D-9. Signal strength surface plot for 2.45GHz, center ceiling antenna position and circular polarization.

APPENDIX E
UNIT LOAD DEVICES, TEMPERATURE GRAPHS AND POSITIONS

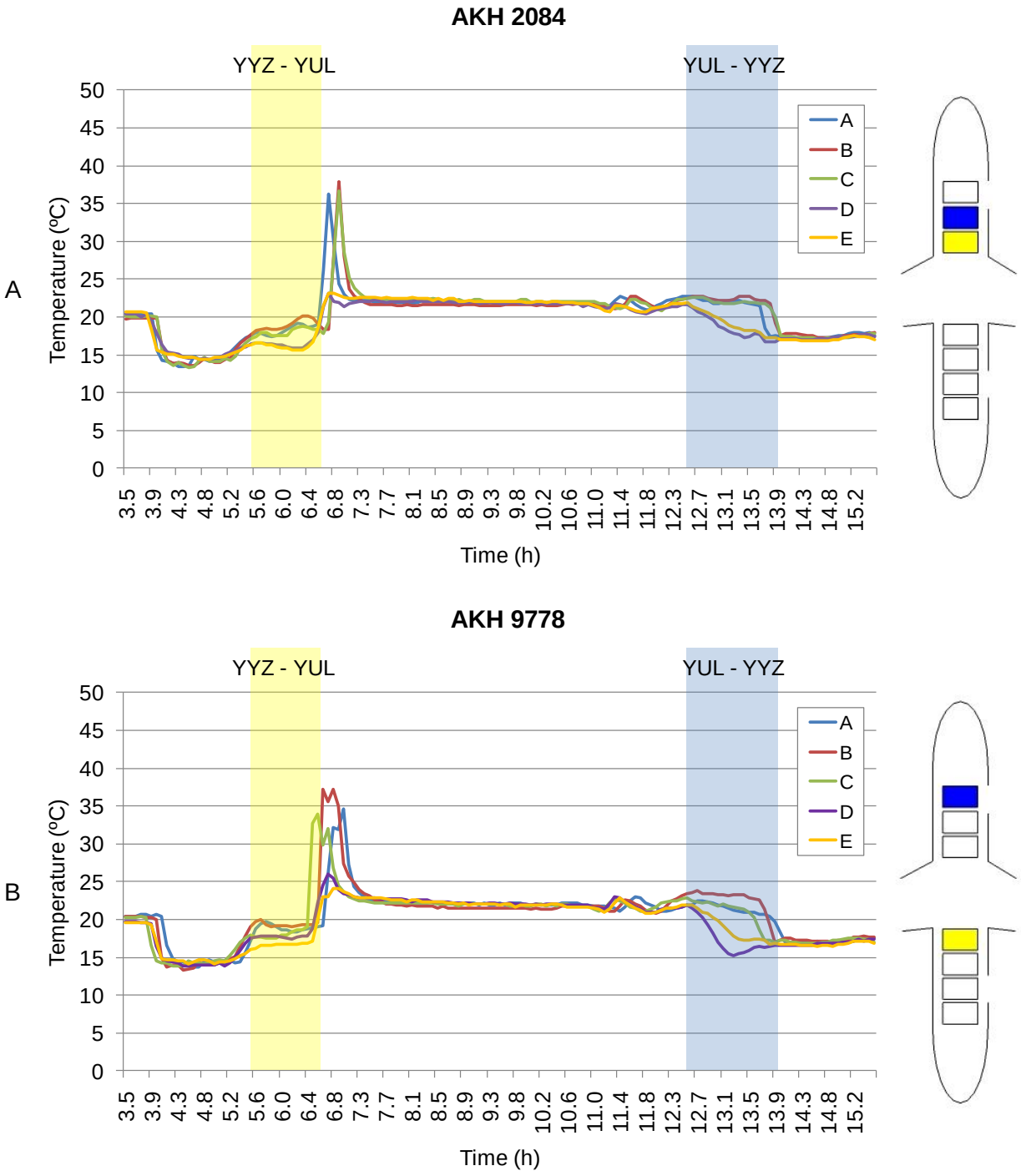

Figure E-1. Temperature profiles of all tags for ULDs (A) AKH 2084 and (B) AKH 9778 to and from Montreal (YUL). First flight segments are highlighted in yellow and returning flight segments are highlighted in blue. Corresponding container positions are shown on the A320 sketch to the right.

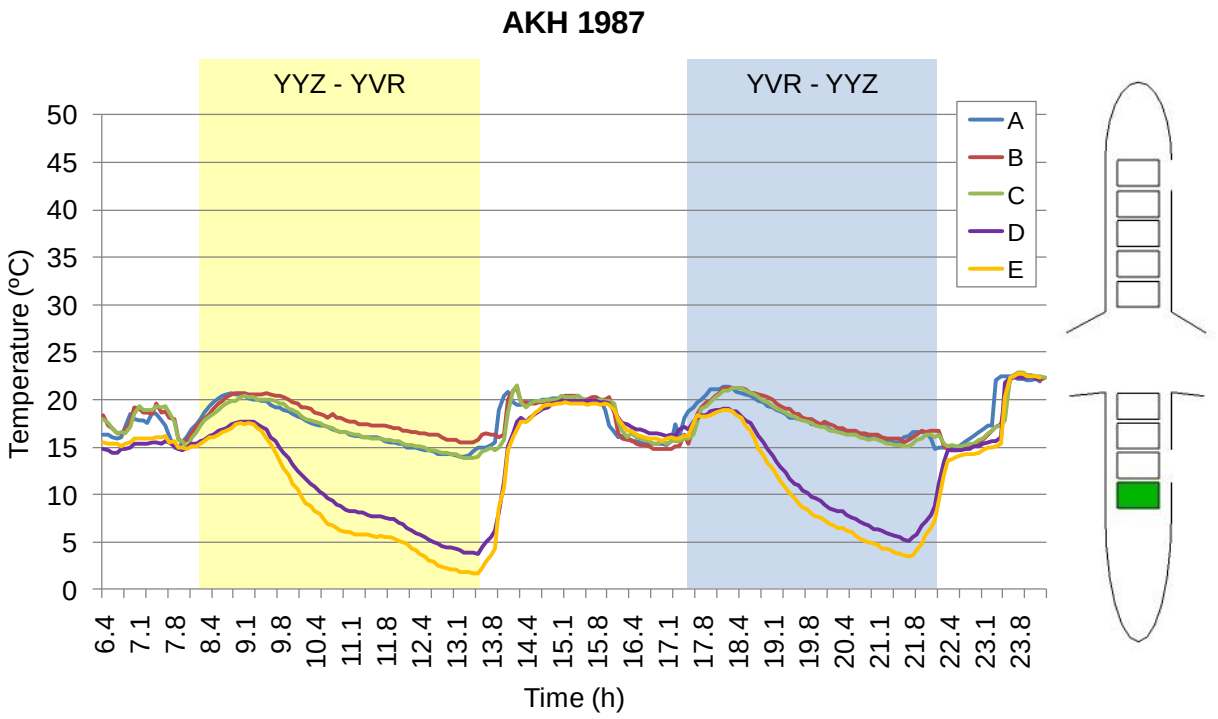

Figure E-2. Temperature profiles of all tags for ULDs AKH 1987 to and from Vancouver (YVR). First flight segment is highlighted in yellow and returning flight segment is highlighted in blue. Container position was the same for both flight and is consequently shown in green on the A321 sketch to the right.

A

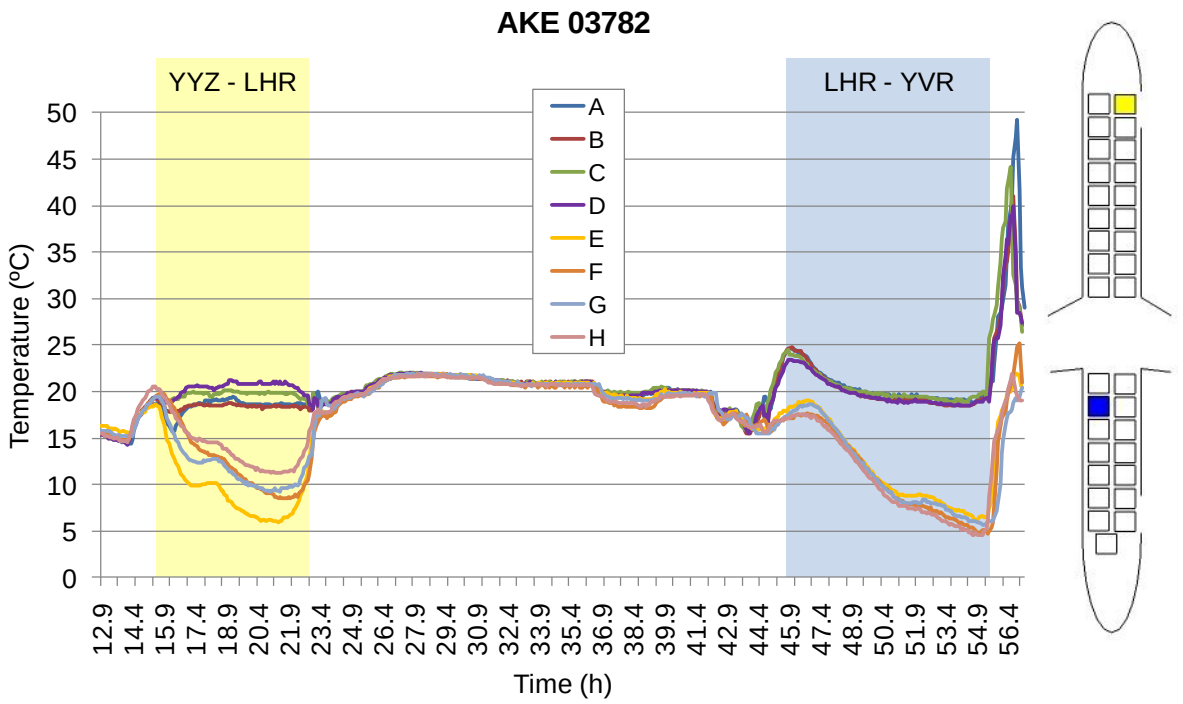

B

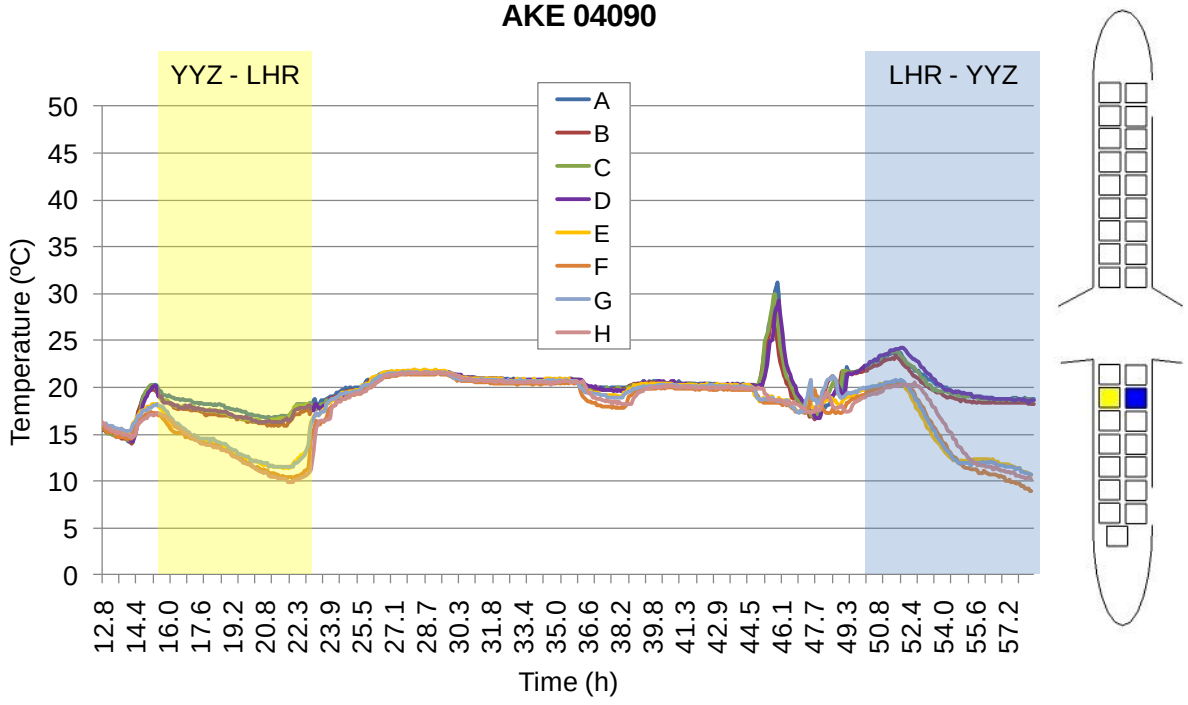

Figure E-3. Temperature profiles of all tags for ULDs (A) AKE 03782, (B) AKE 04090, (C) AKE 04969, and (D) AKE 05335 to and from London (LHR). First flight segments are highlighted in yellow and returning flight segments are highlighted in blue. Corresponding container positions are shown on the A330 sketch to the right.

C

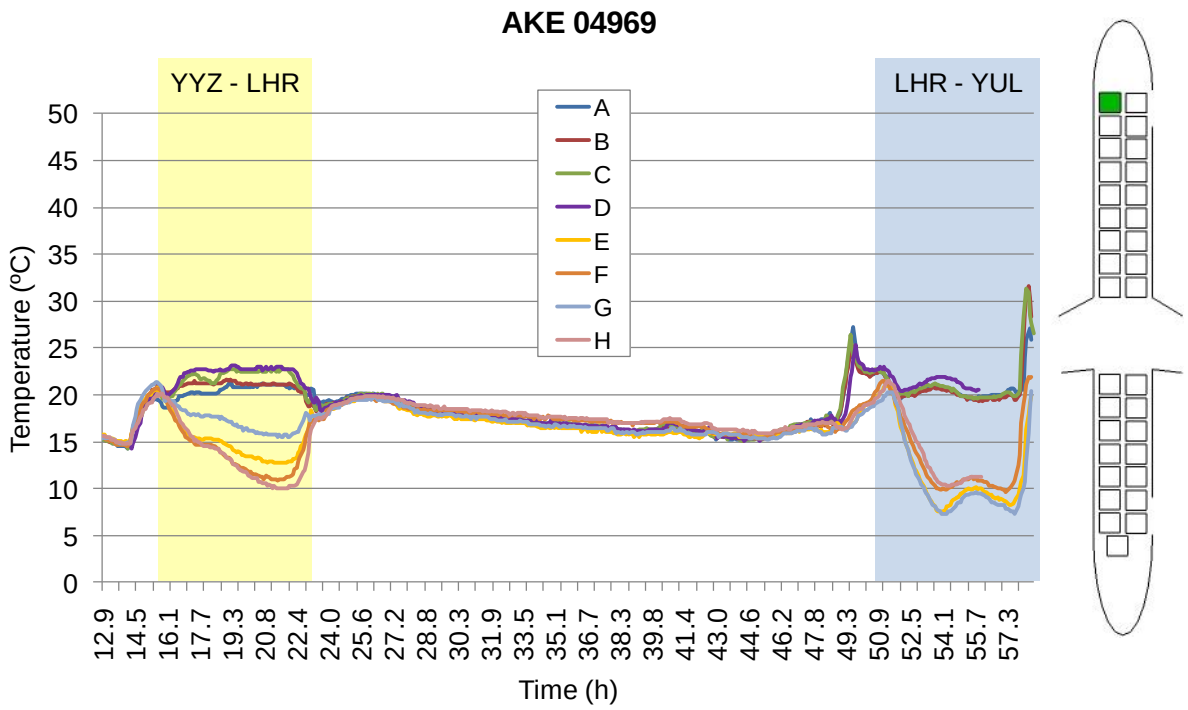

D

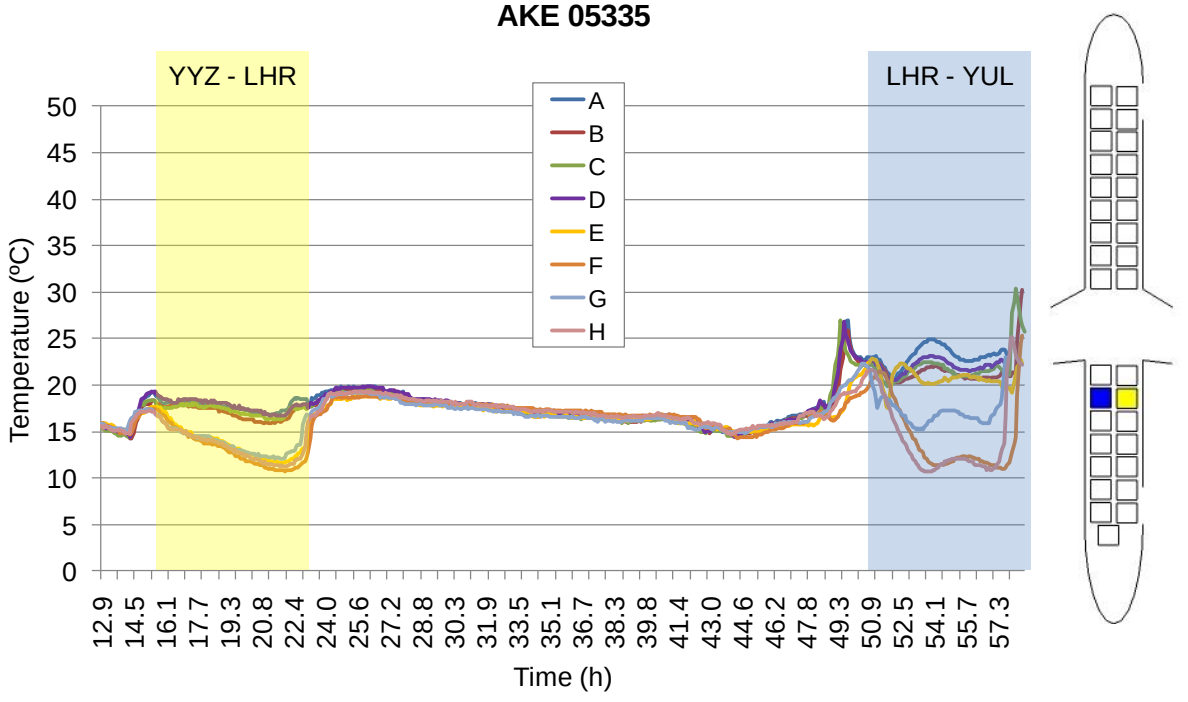

Figure E-3. Continued.

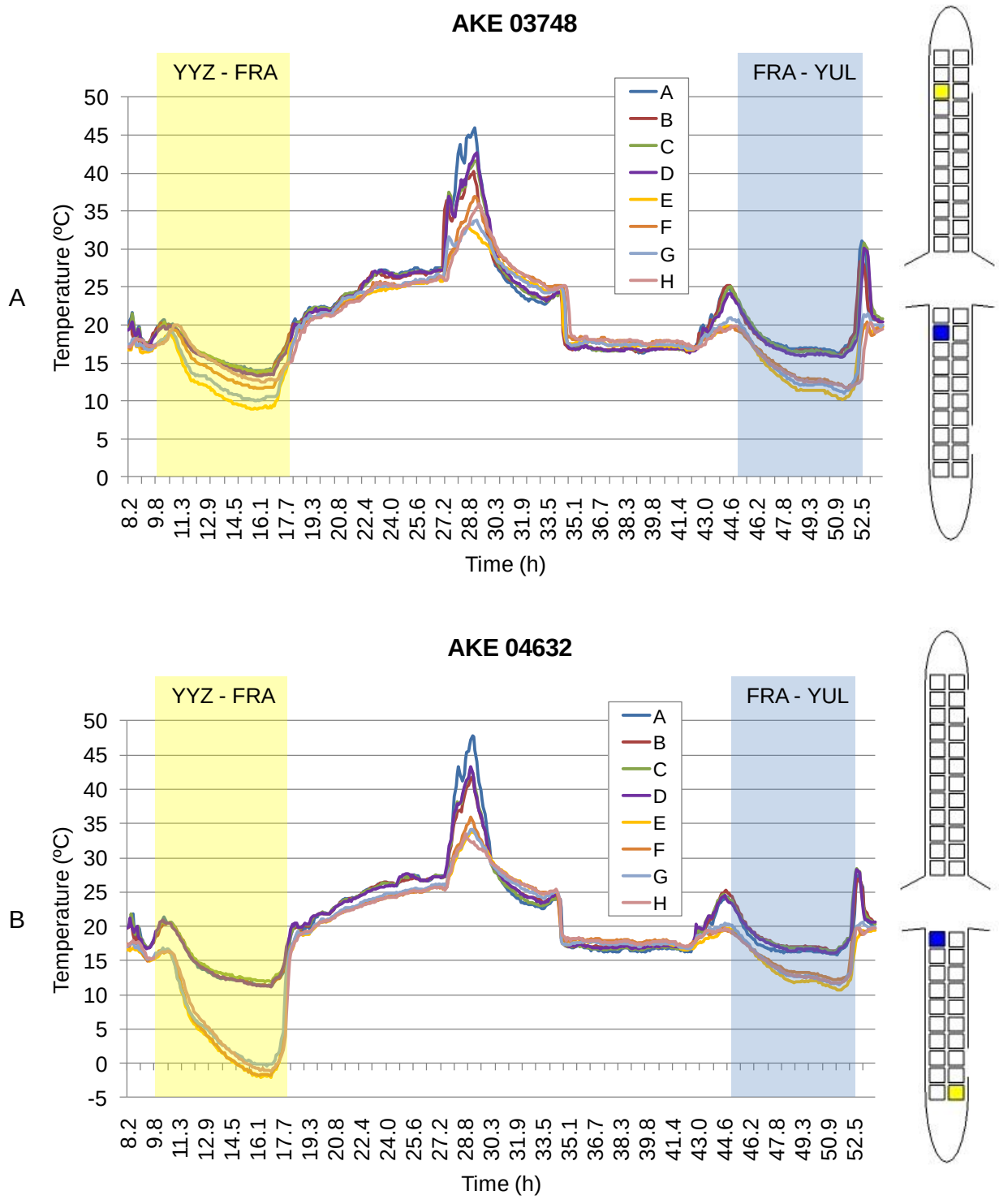

Figure E-4. Temperature profiles of all tags for ULDs (A) AKE 03748, (B) AKE 04632, (C) AKE 05168, and (D) AKE 05255 to and from Frankfurt (FRA). First flight segments are highlighted in yellow and returning flight segments are highlighted in blue. Corresponding container positions are shown on the B777 sketch to the right.

C

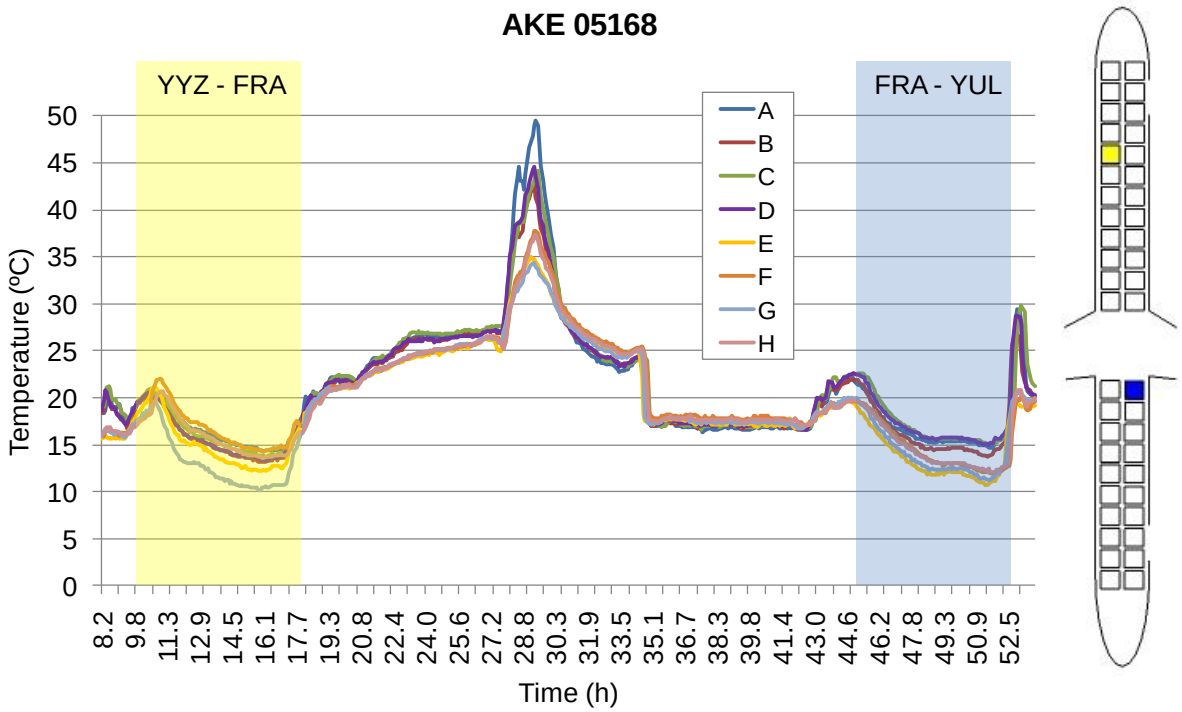

D

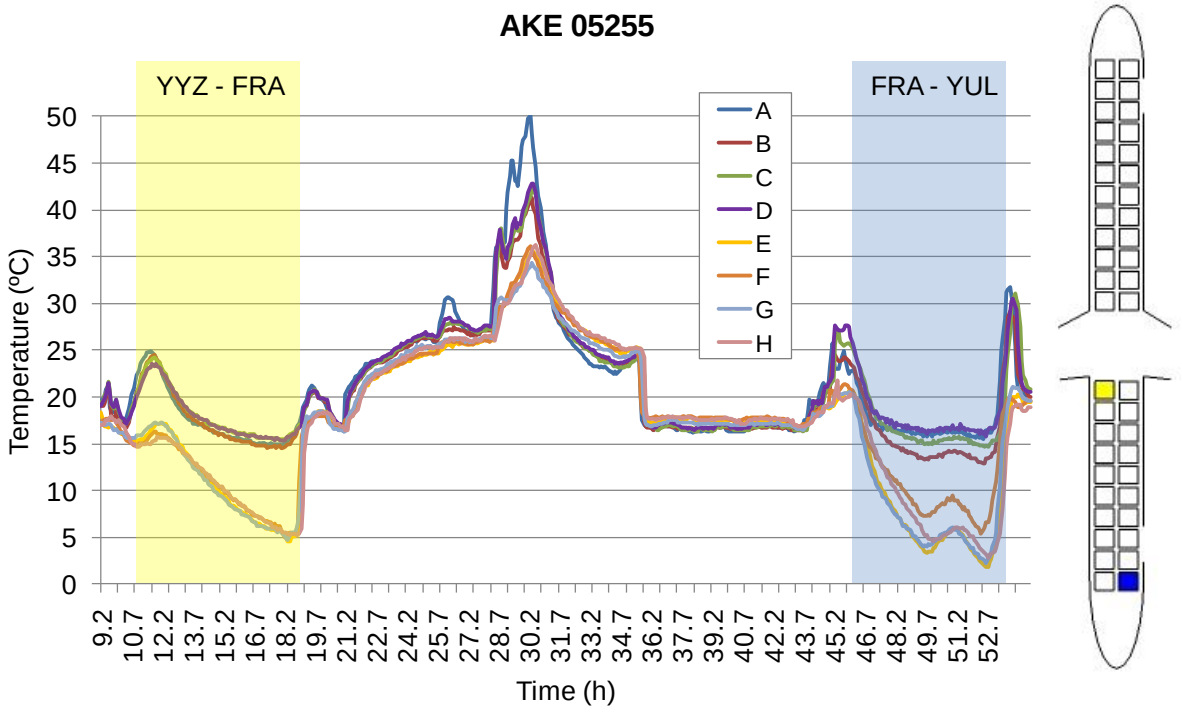

Figure E-4. Continued.

LIST OF REFERENCES

Abad, E., F. Palacio, M. Nuin, A. Zárate, D.E. Gonzáles, A. Juarros, J. M. Gómez and S. Marco. 2009. RFID smart tag for traceability and cold chain monitoring of foods: Demonstration in an intercontinental fresh fish logistic chain. *Journal of Food Engineering* 93(4): 394-399.

Air Canada. 2007. Publication 167 - B777 - Load planning. 5.

Air Canada. 2006. Publication 163 - A330 - Load planning. 5.

Air Canada. 2005. Publication 169 - A320 - Load planning. 6.

Air Canada. 2005. Publication 172 - A321 - Load planning. 5.

Airbus. 2009. Airbus continues to play major role in composites revolution. Airbus - 40Y of Innovation. Available at: http://www.airbus.com/en/corporate/innovation/40years-innovation/40-years-innovation-items/?tx_ttnews%5Btt_news%5D=233&tx_ttnews%5BbackPid%5D=782&cHash=e0bce8b6c7. Accessed 05/23 2010.

Altunbas, A. E. 2010. *Wearable RFID reader and compact fractal patch antenna design.* Gainesville, Fla.: University of Florida.

Anonym. 2007. Composite materials in aviation. The Airplanes Channel. Available at: http://www.airplanes.com/blog/composite-materials-in-aviation/. Accessed 04/09 2010.

Anritsu. 2009. Fundamentals of interference in wireless networks. 11410-005361-16.

Anritsu. 2008. Guide to Spectrum Analyzers.

Ashford, N., C. A. Moore and H. P. M. Stanton. 1984. *Airport operations.* New York: Wiley.

Bilstein, R. E. 1994. *Flight in America: from the Wrights to the astronauts.* Rev. ed. Baltimore: Johns Hopkins University Press.

Blaunstein, N. and C. G. Christodoulou. 2007. *Radio propagation and adaptive antennas for wireless communication links: terrestrial, atmospheric and ionospheric.* Hoboken, N.J.: Wiley-Interscience.

Boeing. 2010a. Boeing 787 dreamliner will provide new solutions for airlines, passengers. Boeing. Available at: http://www.boeing.com/commercial/787family/background.html. Accessed 04/09 2010.

Boeing. 2010b. Commercial airplanes. Boeing. Available at: http://www.boeing.com/commercial/safety/index.html. Accessed 04/09 2010.

Boeing. 2010c. Commercial airplanes - DC-10 family. Boeing. Available at: http://www.boeing.com/commercial/dc-10/index.html. Accessed 04/25 2010.

Boeing. 2008. World air cargo forecast 2008-2009. Accessed 09/02 2009.

Bollen, A. F., D. W. Brash and B. L. Bycroft. 1998. Air-freight coolchain improvements using insulation and supplemental cooling. *Applied Engineering in Agriculture* 14(1): 49-53.

Catto-Smith, C. 2006. Thermal protection of perishable air cargo during ground handling. In *International symposium on fresh produce supply chain management.*

Cerino, A. and W. P. Walsh. 2000. Research and application of radio frequency identification (RFID) technology to enhance aviation security. In *Proceedings of the IEEE 2000 National Aerospace and Electronics Conference. NAECON 2000,* 127-135.

Cerino, A., G. L. Fuller and R. W. Devereux. 1997. EMI from sources in the cargo bay. In *Digital Avionics Systems Conference, 1997. 16th DASC., AIAA/IEEE,* 4.1-9-16 vol.1.

Chang, Y. S., C. H. Oh, Y. S. Whang, J. J. Lee, J. A. Kwon, M. S. Kang, J. S. Park and Y. P. Ung. 2006. Development of RFID enabled aircraft maintenance system. In *2006 IEEE International Conference on Industrial Informatics,* 224-229.

Chang, Y. S., M. G. Son and C. H. Oh. Design and implementation of RFID based air-cargo monitoring system. *Advanced Engineering Informatics.* In Press, Corrected Proof.

Chen, S. C. Q. and V. Thomas. 2001. Optimization of inductive RFID technology. In *Proceedings of the 2001 IEEE International Symposium on Electronics and the Environment,* 82-87.

Cheng, D. K. 1993. *Fundamentals of engineering electromagnetics.* Prentice Hall.

Chow, H. K. H., K. L. Choy, W. B. Lee and K. C. Lau. 2006. Design of a RFID case-based resource management system for warehouse operations. *Expert Systems with Applications* 30(4): 561-576.

Clampitt, H. G. 2006. *RFID certification textbook.* 2nd ed. Houston, TX: PWD Group, Inc.

Day, D. A. 2009. Composites and advanced materials. U.S. Centennial of flight commission. Available at: http://www.centennialofflight.gov/essay/Evolution_of_Technology/composites/Tech40.htm. Accessed 01/26 2010.

Devereux, R. W., G. L. Fuller and R. Schillinger. 1997. Further analysis of the CV-580 and B-727 aircraft RF coupling experiment data. In *Digital Avionics Systems Conference, 1997. 16th DASC., AIAA/IEEE,* 4.1-1-8 vol.1.

Devereux, R. W., G. L. Fuller and R. Schillinger. 1997. Electromagnetic susceptibility of installed avionics. In *Digital Avionics Systems Conference, 1997. 16th DASC., AIAA/IEEE,* 4.1-17-24 vol.1.

Dobkin, D. M. and S. M. Weigand. 2005. Environmental effects on RFID tag antennas. *Microwave Symposium Digest, 2005 IEEE MTT-S International*.

Dobkin, D. M. 2008. *The RF in RFID: passive UHF RFID in practice.* Amsterdam; Boston: Elsevier / Newnes.

Domdouzis, K., B. Kumar and C. Anumba. 2007. Radio-Frequency Identification (RFID) applications: A brief introduction. *Advanced Engineering Informatics* 21(4): 350-355.

Elias, B. 2007. CRS report for congress - Air cargo security. RL32022.

Ely, J. J., T. X. Nguyen, S. V. koppen, M. T. Salud and J. H. Beggs. 2003. Wireless phone threat assessment and new wireless technology concerns for aircraft navigation radios. NASA/TP-2003-212446.

Émond, J. P. 2008. The cold chain. In *RFID Technology and Applications,* 144. ed. S. B. MilesSarma, S. E. and Williams, J. R., New York, NY, USA: Cambridge University press.

Émond, J. P. 2007. Quantifying RFID's cold chain benefits. In *RFID Journal LIVE! 2007 Conference*.

Émond, J. P., F. Mercier and M. C. N. Nunes. 1999. In-flight temperature conditions in the holds of a widebody aircraft. In *Proceedings of the 20th InternationalCongress of Refrigeration,* Paper No. 281.

ETSI. 2007. Electromagnetic compatibility and Radio spectrum Matters (ERM); Technical characteristics of RFID in the UHF Band; System Reference Document for Radio Frequency Identification (RFID) equipment; Part 1: RFID equipment operating in the range from 865 MHz to 868 MHz. ETSI TR 102 649-1.

FAA. 2008. Airworthiness approval and operational allowance of RFID systems. AC20-1621.

FAA. 2006. FAA aerospace forecast fiscal years 2006-2017. 1-90.

FCC. 2008. Part 15 - Radio frequency devices. 1-157.

Finkenzeller, K. 2003. *RFID handbook: fundamentals and applications in contactless smart cards and identification.* New York, NY, USA: John Wiley & Sons, Inc.

Flightglobal. 2009. Aircraft profile: Airbus A320. Available at: http://www.flightglobal.com/articles/2008/01/01/221129/airbus-a320-aircraft-profile.html. Accessed 09/02 2009.

Forster, P. W. and A. C. Regan. 2001. Electronic integration in the air cargo industry: an information processing model of on-time performance. *Transportation Journal* 40(4): 46-61.

Foster, P. R. and R. A. Burberry. 1999. Antenna problems in RFID systems. *IEE Colloquium on RFID Technology* 3/1-3/5.

Friis, H. T. 1946. A note on a simple transmission formula. *Proceedings of the I.R.E.* 34(5): 254.

Fuschini, F., C. Piersanti, F. Paolazzi and G. Falciasecca. 2008. Analytical approach to the backscattering from UHF RFID transponder. *Antennas and Wireless Propagation Letters, IEEE* 733-35.

Griffin, J. D., G. D. Durgin, A. Haldi and B. Kippelen. 2006. RF tag antenna performance on various materials using radio link budgets. *Antennas and Wireless Propagation Letters, IEEE* 5(1): 247-250.

Hallowell, S. F. and P. Z. Jankowski. 2005. Transportation security technologies research and development. In *IEEE Military Communications Conference, 2005. MILCOM 2005.* 1753-1756 Vol. 3.

Henderson, T. 2010. Static electricity - Lesson 3. The Physics Classroom. Available at: http://www.physicsclassroom.com/class/estatics/u8l3c.cfm. Accessed 07/03 2010.

IATA. 2002. *ULD technical manual, 17th edition.* Montreal, Canada: International Air Transport Association.

Impinj. 2007. UHF Gen 2 RFID readers - Five factors for success.

Intelleflex. 2010. The Intelleflex XC3 technology platform: An implementation of the new ISO Class 3 standard.

Jacinto, C., M. Romano, A. Montes, P. Sousa and M. S. Nunes. 2009. RFID tuning methodology applied on airport baggage tracking. In *IEEE Conference on Emerging Technologies & Factory Automation, 2009. ETFA 2009.* 1-4.

Jedermann, R. and W. Lang. 2007. Semi-passive RFID and beyond: steps towards automated quality tracing in the food chain. *Int. J. Radio Frequency Identification* 1(3): 247-259.

Jedermann, R., J. P. Émond and W. Lang. 2007. Shelf life prediction by intelligent RFID technical limits of model accuracy. In *International Conference on Dynamics in Logistics*.

Jedermann, R., L. Ruiz-Garcia and W. Lang. 2009. Spatial temperature profiling by semi-passive RFID loggers for perishable food transportation. *Computers and Electronics in Agriculture* 65(2): 145-154.

Keskilammi, M., L. Sydänheimo and M. Kivikoski. 2003. Radio frequency technology for automated manufacturing and logistics control. Part 1: Passive RFID systems and the effects of antenna parameters on operational distance. *The International Journal of Advanced Manufacturing Technology* 21(10): 769-774.

Ketzenberg, M. E. and J. M. Bloemhof-Ruwaard. 2009. The value of RFID technology enabled information to manage perishables. ERIM Report Series Reference No. ERS-2009-020-LIS.

Khan, M. A., M. Sharma and P. R. Brahmanandha. 2009. A survey of RFID tags. *International Journal of Recent Trends in Engineering* 1(4).

Kim, D. Y., H. G. Yoon, B. J. Jang and J. G. Yook. 2008. Interference analysis of UHF RFID systems. *Progress in Electromagnetics Research B* 4115-126.

Kumar, R., S. K. Kaura, A. K. Sharma, D. P. Chhachhia and A. K. Aggarwal. 2007. Knife-edge diffraction pattern as an interference phenomenon: An experimental reality. *Optics & Laser Technology* 39(2): 256-261.

LaBerge, E. F. C. 2007. An analysis of the effects of RFID tags on narrowband navigation and communication receivers.

Lahiri, S. 2006. *RFID sourcebook.* Upper Saddle River, NJ, USA: IBM Press.

Landt, J. 2005. The history of RFID. *Potentials, IEEE* 24(4): 8-11.

Laniel, M., J. P. Émond and A. E. Altunbas. 2009. RFID behavior study in enclosed marine container for real time temperature tracking. *Sensing and Instrumentation for Food Quality and Safety* 3(1): 34-40.

Liang, B., A. Hu and Z. Qin. 2006. Trends and brief comments on anti-collision techniques in radio frequency identification system. In *2006 6th International Conference on ITS Telecommunications Proceedings,* 241-245.

Littell, R. C., G. A. Milliken, W. W. Stroup, R. D. Wolfinger and O. Schabenberber. 2006. *SAS for mixed models.* 2nd ed. Cary, NC, USA: SAS Publishing.

Longhurst, R. S. 1967. *Geometrical and physical optics.* 2nd ed. London: Longman.

Mac Carthy, U. M. 2009. Assesment of UHF RFID as an automatic ID data carrier for item level food supply chain traceability. PhD diss. Dublin: University College Dublin.

Mayer, L. W., M. Wrulich and S. Caban. 2006. Measurements and channel modeling for short range indoor UHF applications. In *First European Conference on Antennas and Propagation. EuCAP 2006.* 1-5.

McCarthy, T. M. 2003. Conducting a market opportunity analysis for air cargo operations. *Transportation Journal*: May 18, 2010.

McCoy, T., R. J. Bullock and P. V. Brennan. 2005. RFID for airport security and efficiency. In *The IEE Seminar on Signal Processing Solutions for Homeland Security, 2005. (Ref. No. 2005/11108),* 9 pp.

Merriam Webster, I. *Merriam-Webster's open dictionary [electronic resource].* Springfield, MA: Merriam-Webster.

Meyers, M., M. Brown, S. Patadia and S. Dua. 2007. *Mike Meyers' comptia RFID+ certification passport.* New York: McGraw-Hill.

Mo, L. and H. J. Zhang. 2007. RFID antenna near the surface of metal. In *2007 International Symposium on Microwave, Antenna, Propagation and EMC Technologies for Wireless Communications,* 803-806.

Moir, I. and A. G. Seabridge. 2001. *Aircraft systems: mechanical, electrical, and avionics subsystems integration.* Reston, VA; Bury St. Edmunds, U.K.: American Institute of Aeronautics and Astronautics; Professional Engineering Pub.

NFPG. 2008. United Kingdom frequency allocation table.

Nguyen, T. X. and J. J. Mielnik. 2008. Radio frequency compatibility of an RFID tag on glideslope navigation receivers. In *IEEE International Symposium on Electromagnetic Compatibility. EMC 2008,* 1-6.

Nguyen, T. X., J. J. Ely, S. V. Koppen and M. S. Fersch. 2008. RFID transponders' RF emissions in aircraft communication and navigation radio bands. In *2008 International Symposium on Electromagnetic Compatibility - EMC Europe,* 1-6.

Nguyen, T. X., S. V. Koppen, L. J. Smit, R. A. Williams and M. T. Salud. 2005. Wireless phone threat assessment for aircraft communication and navigation radios. In *2005 International Symposium on Electromagnetic Compatibility. EMC 2005,* 135-140 Vol. 1.

Nguyen, T. X., S. V. Koppen, J. J. Ely, G. N. Szatkowski, J. J. Mielnik and M. T. P. Salud. 2007. Small aircraft RF interference path loss. In *IEEE International Symposium on Electromagnetic Compatibility. EMC 2007,* 1-6.

Nguyen, T. X., J. J. Ely, K. L. Dudley, S. A. Scearce, M. O. Hatfield and R. E. Ri. 2006. Passenger transmitters as a possible cause of aircraft fuel ignition - in support of an aircraft accident investigation. In *IEEE International Symposium on Electromagnetic Compatibility. EMC 2006,* 228-233.

Nguyen, T. X., S. V. Koppen, J. J. Ely, R. A. Williams, L. J. Smith and M. T. P. Salud. 2004. Portable wireless device threat assessment for aircraft navigation radios.

Nikitin, P. V. and K. V. S. Rao. 2009. LabVIEW-based UHF RFID tag test and measurement system. *IEEE Transactions on Industrial Electronics,* 56(7): 2374-2381.

Nikitin, P. V. and K. V. S. Rao. 2008. Antennas and propagation in UHF RFID systems. *2008 IEEE International Conference on RFID,* 277-288.

Nikitin, P. V. and K. V. S. Rao. 2006. Performance limitations of passive UHF RFID systems. In *2006 IEEE Antennas and Propagation Society International Symposium,* 1011-1014.

Nikitin, P. V., K. V. S. Rao, R. Martinez and S. F. Lam. 2009. Sensitivity and impedance measurements of UHF RFID chips. *IEEE Transactions on Microwave Theory and Techniques,* 57(5): 1297-1302.

Nikitin, P. V., D. D. Arumugam, M. J. Chabalko, B. E. Henty and D. D. Stancil. 2010. Long range passive UHF RFID system using HVAC ducts. *Proceedings of the IEEE* PP(99): 1-7.

Nordisk. 2010. Air cargo containers. Teleflex Incorporated. Available at: http://www.nordisk-aviation.com/default.aspx?Cat=2&Id=11. Accessed 02/02 2010.

NTIA. 2010. Federal spectrum use summary, 30 MHz - 3000 GHz.

NTIA. 2003. United States frequency allocations - the radio spectrum.

NTSB. 2010. NTSB - Aviation - Accident database & synopses. National Transportation Safety Board. Available at: http://www.ntsb.gov/ntsb/query.asp. Accessed 05/21 2010.

Nunes, M. C. N., J. P. Émond and J. K. Brecht. 2003. Quality of strawberries as affected by temperature abuse during ground, in-flight and retail handling operations. In 239-246. Acta Hort. (ISHS).

Nunes, M. C. N., J. P. Émond, K. V. Chau, M. Rauth, S. Dea and W. Pelletier. 2006. Effects of in-store conditions on the quality of freshfruits and vegetables. 262.

O'Connor, M. C. 2005. IATA approves UHF for bag tags.

Ott, R. L. and M. T. Longnecker. 2004. *A first course in statistical methods.* Belmont, CA, USA: Brooks/Cole – Thomson Learning.

Penttilä, K., M. Keskilammi, L. Sydänheimo and M. Kivikoski. 2006. Radio frequency technology for automated manufacturing and logistics control. Part 2: RFID antenna utilisation in industrial applications. *The International Journal of Advanced Manufacturing Technology* 31(1): 116-124.

Poon, T. C., K. L. Choy, H. K. H. Chow, H. C. W. Lau, F. T. S. Chan and K. C. Ho. 2009. A RFID case-based logistics resource management system for managing order-picking operations in warehouses. *Expert Systems with Applications* 36(4): 8277-8301.

Prothro, J. T., G. D. Durgin and J. D. Griffin. 2006. The effects of a metal ground plane on RFID tag antennas. In *IEEE Antennas and Propagation Society International Symposium 2006,* 3241-3244.

Rao, K. V. S. 1999. An overview of backscattered radio frequency identification system (RFID). In *1999 Asia Pacific Microwave Conference,* 746-749 vol.3.

Rappaport, T. S. 2002. *Wireless communications : principles and practice.* 2nd ed. Upper Saddle River, N.J.: Prentice Hall PTR.

Rappaport, T. S. and C. D. McGillem. 1989. UHF fading in factories. *IEEE Journal on Selected Areas in Communications,* 7(1): 40-48.

Raumonen, P., L. Sydanheimo, L. Ukkonen, M. Keskilammi and M. Kivikoski. 2003. Folded dipole antenna near metal plate. *IEEE Antennas and Propagation Society International Symposium,* 1848-851 vol.1.

Reed, R. 2009. Refraction of light. Interactagram.com. Available at: http://interactagram.com/physics/optics/refraction/. Accessed 06/30 2010.

Reitz, J. R., R. W. Christy and F. J. Milford. 1993. Monochromatic waves in bounded regions. In *Foundations of electromagnetic theory,* 441-469. ed. Anonymous , Reading, Mass.: Addison-Wesley.

Roussos, G. and V. Kostakos. 2009. RFID in pervasive computing: State-of-the-art and outlook. *Pervasive and Mobile Computing* 5(1): 110-131.

Ruiz-Garcia, L., P. Barreiro and J. I. Robla. 2008. Performance of ZigBee-Based wireless sensor nodes for real-time monitoring of fruit logistics. *Journal of Food Engineering* 87(3): 405-415.

SAS Institute. *SAS/STAT 9.1 user's guide.* Cary, N.C.: SAS Institute, Norwood, Mass.

Saunders, B. 2003. Award-winning blast resistant cargo container at Dubai air show spotlight.

Schmoetzer, K. 2005. Enhanced cargo monitoring - container communication interface. In *International Aircraft Systems Fire Protection Working Group,* Airbus, dept. BCECS4.

Schmoetzer, K. 2001. Aircraft fire detection: Requirements, qualification and certification aspects. In *12th international conference on automatic fire detection,* National Institute of Standards and Technology.

Shahidi, R. 1995. *Link budget analysis: student manual.* Arlington, VA: LLC.

Skorna, A. C. H. and A. Richter. 2007. RFID and air cargo. RFID Jounal. Available at: www.rfidjournal.com/article/articleview/3482/. 2008.

Sydänheimo, L., L. Ukkonen and M. Kivikoski. 2006. Effects of size and shape of metallic objects on performance of passive radio frequency identification. *The International Journal of Advanced Manufacturing Technology* 30(9): 897-905.

Syversen, E., F. J. Pineda and J. Watson. 2008. Temperature variations recorded during interinstitutional air shipments of laboratory mice. *Journal of the American Association for Laboratory Animal Science* 47(1): 31-36.

Taylor, M. J. H. 1989. *The aerospace chronology.* London: Tri-Service Press.

The Aluminum Association. 2008. Aluminum in aircraft. The Aluminum Association. Available at: http://www.aluminum.org/Content/NavigationMenu/TheIndustry/TransportationMarket/Aircraft/default.htm. Accessed 01/26 2010.

Valenzuela, R. A., O. Landron and D. L. Jacobs. 1997. Estimating local mean signal strength of indoor multipath propagation. *IEEE Transactions on Vehicular Technology,* 46(1): 203-212.

van de Voort, M. and A. Ligtvoet. 2006. Towards an RFID policy for Europe. DRR-4046-EC.

Vega, H. 2008. Air cargo, trade and transportation costs of perishables and exotics from South America. *Journal of Air Transport Management* 14(6, Sp. Iss. SI): 324-328.

Véronneau, S. and J. Roy. 2009. RFID benefits, costs, and possibilities: The economical analysis of RFID deployment in a cruise corporation global service supply chain. *International Journal of Production Economics* 122(2): 692-702.

Villeneuve, S., M. O. Nagdi and J. P. Émond. 2001. Heat transfer in air cargo unit load devices. *International Society for Horticultural Science Acta Hortuculturae* 566245-250.

Villeneuve, S., F. Mercier, W. Pelletier, M. O. Nagdi and J. P. Émond. 2000. Effect of environmental conditions in air shipment of perishables during ground operations. In *ASAE Annual International Meeting,* ASAE.

Villeneuve, S. 2006.
Étude des phénomènes d'échange thermique et des conditions environmentales ayant un impact sur la conservation des denrées périssables lors des opérations aéroportuaires. PhD diss. Québec: Université Laval.

Visich, J. K., S. Li, B. M. Khumawala and P. M. Reyes. 2009. Empirical evidence of RFID impacts on supply chain performance. *International Journal of Operations & Production Management* 29(11-12): 1290-1315.

Wang, H., S. Chen and Y. Xie. 2010. An RFID-based digital warehouse management system in the tobacco industry: a case study. *Internation Journal of Production Research* 48(9): 2513-2548.

Wegener, P. P. 1997. *What makes airplanes fly?: history, science, and applications of aerodynamics.* 2nd ed. New York: Springer.

Wilmes, H., B. Kolesnikov, A. Fink and C. Kindervater. 2002. New design concepts for a CFRP fuselage.

Winder, S. and J. J. Carr. 2002. *Radio and RF engineering pocket book. 3rd* ed. Oxford: Newnes.

Wright, T. 2008. Temperature sensitive pharmaceutical transportation - a changing picture.

Wu, N. C., M. A. Nystrom, T. R. Lin and H. C. Yu. 2006. Challenges to global RFID adoption. *Technovation* 26(12): 1317-1323.

Yonemoto, N., K. Yamamoto, K. Yamada and T. Hirata. 2007. RF emission measurement of 433 MHZ RFID tags for EMI evaluation to onboard instruments of aircrafts. In *7th International Symposium on Electromagnetic Compatibility and Electromagnetic Ecology,* 232-235.

Yuanxin, O., H. Yao, P. Ling, W. Dongwei and X. Zhang. 2008. An intelligent RFID reader and its application in airport baggage handling system. In *4th International Conference on Wireless Communications, Networking and Mobile Computing, 2008. WiCOM '08.* 1-4.

Zhang Q., G. Cheng, Z. Wang, J. Wei and D. Yan. 2009. Development of RFID application system in cargo inbound and outbound. In *TENCON 2009 - 2009 IEEE Region 10 Conference,* 1-6.

Zweig, S. E. 2006. Advances in vaccine stability monitoring technology. *Vaccine* 24(33-34): 5977-5985.

BIOGRAPHICAL SKETCH

Magalie Laniel was born in Montreal, Quebec, Canada. She attended Laval University in Québec city where she received, in 2004, a Bachelor of Engineering in food engineering. In the following fall, she began a master's under the direction of Dr Émond in the Department of Agricultural and Biological Engineering at the University of Florida. Her masters' work opened the path to continue her studies towards the PhD. Along the years, she has been working on several projects involving radio frequency identification (RFID) technology, packaging and transportation of perishables.